E-ISSN: 2148-6247

Turkish Journal of PHARMACEUTICAL SCIENCES

An Official Journal of the Turkish Pharmacists' Association, Academy of Pharmacy

Volume: 20 Issue: 2 April 2023

www.turkjps.org

PubMed Central PubMed Scopus TRDİZİN

galenos

Turkish Journal of
PHARMACEUTICAL SCIENCES

OWNER

Onur Arman ÜNEY on behalf of the Turkish Pharmacists' Association

Editor-in-Chief

Prof. İlkay Erdoğan Orhan, Ph.D.
ORCID: https://orcid.org/0000-0002-7379-5436
Gazi University, Faculty of Pharmacy, Department of Pharmacognosy, Ankara, TÜRKİYE
iorhan@gazi.edu.tr

Associate Editors

Prof. Bensu Karahalil, Ph.D.
ORCID: https://orcid.org/0000-0003-1625-6337
Gazi University, Faculty of Pharmacy, Department of Pharmaceutical Toxicology, Ankara, TÜRKİYE
bensu@gazi.edu.tr

Assoc. Prof. Sinem Aslan Erdem, Ph.D.
ORCID: https://orcid.org/0000-0003-1504-1916
Ankara University, Faculty of Pharmacy, Department of Pharmacognosy, Ankara, TÜRKİYE
saslan@pharmacy.ankara.edu.tr

Editorial Board

Prof. Afonso Miguel CAVACO, Ph.D.
ORCID: orcid.org/0000-0001-8466-0484
Lisbon University, Faculty of Pharmacy, Department of Pharmacy, Pharmacology and Health Technologies, Lisboa, PORTUGAL
acavaco@campus.ul.pt

Prof. Bezhan CHANKVETADZE, Ph.D.
ORCID: orcid.org/0000-0003-2379-9815
Ivane Javakhishvili Tbilisi State University, Institute of Physical and Analytical Chemistry, Tbilisi, GEORGIA
jpba_bezhan@yahoo.com

Prof. Blanca LAFFON, Ph.D.
ORCID: orcid.org/0000-0001-7649-2599
DICOMOSA group, Advanced Scientific Research Center (CICA), Department of Psychology, Area Psychobiology, University of A Coruña, Central Services of Research Building (ESCI), Campus Elviña s/n, A Coruña, SPAIN
blanca.laffon@udc.es

Prof. Christine LAFFORGUE, Ph.D.
ORCID: orcid.org/0000-0001-7798-2565
Paris Saclay University, Faculty of Pharmacy, Department of Dermopharmacology and Cosmetology, Paris, FRANCE
christine.lafforgue@universite-paris-saclay.fr

Prof. Dietmar FUCHS, Ph.D.
ORCID: orcid.org/0000-0003-1627-9563
Innsbruck Medical University, Center for Chemistry and Biomedicine, Institute of Biological Chemistry, Biocenter, Innsbruck, AUSTRIA
dietmar.fuchs@i-med.ac.at

Prof. Francesco EPIFANO, Ph.D.
ORCID: 0000-0002-0381-7812
Università degli Studi G. d'Annunzio Chieti e Pescara, Chieti CH, ITALY
francesco.epifano@unich.it

Prof. Fernanda BORGES, Ph.D.
ORCID: orcid.org/0000-0003-1050-2402
Porto University, Faculty of Sciences, Department of Chemistry and Biochemistry, Porto, PORTUGAL
fborges@fc.up.pt

Prof. Göksel ŞENER, Ph.D.
ORCID: orcid.org/0000-0001-7444-6193
Fenerbahçe University, Faculty of Pharmacy, Department of Pharmacology, İstanbul, TÜRKİYE
gsener@marmara.edu.tr

Prof. Gülbin ÖZÇELİKAY, Ph.D.
ORCID: orcid.org/0000-0002-1580-5050
Ankara University, Faculty of Pharmacy, Department of Pharmacy Management, Ankara, TÜRKİYE
gozcelikay@ankara.edu.tr

Prof. Hermann BOLT, Ph.D.
ORCID: orcid.org/0000-0002-5271-5871
Dortmund University, Leibniz Research Centre, Institute of Occupational Physiology, Dortmund, GERMANY
bolt@ifado.de

Prof. Hildebert WAGNER, Ph.D.
Ludwig-Maximilians University, Center for Pharmaceutical Research, Institute of Pharmacy, Munich, GERMANY
H.Wagner@cup.uni-muenchen.de

Prof. İ. İrem ÇANKAYA, Ph.D.
ORCID: orcid.org/0000-0001-8531-9130
Hacettepe University, Faculty of Pharmacy, Department of Pharmaceutical Botany, Ankara, TÜRKİYE
itatli@hacettepe.edu.tr

Prof. K. Arzum ERDEM GÜRSAN, Ph.D.
ORCID: orcid.org/0000-0002-4375-8386
Ege University, Faculty of Pharmacy, Department of Analytical Chemistry, İzmir, TÜRKİYE
arzum.erdem@ege.edu.tr

Prof. Bambang KUSWANDI, Ph.D.
ORCID: 0000-0002-1983-6110
Chemo and Biosensors Group, Faculty of Pharmacy University of Jember, East Java, INDONESIA
b_kuswandi.farmasi@unej.ac.id

Prof. Luciano SASO, Ph.D.
ORCID: orcid.org/0000-0003-4530-8706
Sapienze University, Faculty of Pharmacy and Medicine, Department of Physiology and Pharmacology "Vittorio Erspamer", Rome, ITALY
luciano.saso@uniroma1.it

Prof. Maarten J. POSTMA, Ph.D.
ORCID: orcid.org/0000-0002-6306-3653
University of Groningen (Netherlands), Department of Pharmacy, Unit of Pharmacoepidemiology & Pharmacoeconomics, Groningen, HOLLAND
m.j.postma@rug.nl

Prof. Meriç KÖKSAL AKKOÇ, Ph.D.
ORCID: orcid.org/0000-0001-7662-9364
Yeditepe University, Faculty of Pharmacy, Department of Pharmaceutical Chemistry, İstanbul, TÜRKİYE
merickoksal@yeditepe.edu.tr

Prof. Mesut SANCAR, Ph.D.
ORCID: orcid.org/0000-0002-7445-3235
Marmara University, Faculty of Pharmacy, Department of Clinical Pharmacy, İstanbul, TÜRKİYE
mesut.sancar@marmara.edu.tr

Assoc. Prof. Nadja Cristhina de SOUZA PINTO, Ph.D.
ORCID: orcid.org/0000-0003-4206-964X
University of São Paulo, Institute of Chemistry, São Paulo, BRAZIL
nadja@iq.usp.br

Turkish Journal of
PHARMACEUTICAL SCIENCES

Assoc. Prof. Neslihan AYGÜN KOCABAŞ, Ph.D. E.R.T.
ORCID: orcid.org/0000-0000-0000-0000
Total Research & Technology Feluy Zone Industrielle Feluy, Refining & Chemicals, Strategy – Development - Research, Toxicology Manager, Seneffe, BELGIUM
neslihan.aygun.kocabas@total.com

Prof. Rob VERPOORTE, Ph.D.
ORCID: orcid.org/0000-0001-6180-1424
Leiden University, Natural Products Laboratory, Leiden, NETHERLANDS
verpoort@chem.leidenuniv.nl

Prof. Robert RAPOPORT, Ph.D.
ORCID: orcid.org/0000-0001-8554-1014
Cincinati University, Faculty of Pharmacy, Department of Pharmacology and Cell Biophysics, Cincinati, USA
robertrapoport@gmail.com

Prof. Tayfun UZBAY, Ph.D.
ORCID: orcid.org/0000-0002-9784-5637
Üsküdar University, Faculty of Medicine, Department of Medical Pharmacology, Istanbul, TÜRKİYE
tayfun.uzbay@uskudar.edu.tr

Prof. Wolfgang SADEE, Ph.D.
ORCID: orcid.org/0000-0003-1894-6374Ohio State University, Center for Pharmacogenomics, Ohio, USA
wolfgang.sadee@osumc.edu

Advisory Board

Prof. Yusuf ÖZTÜRK, Ph.D.
Anadolu University, Faculty of Pharmacy, Department of Pharmacology, Eskişehir, TÜRKİYE
ORCID: 0000-0002-9488-0891

Prof. Tayfun UZBAY, Ph.D.
Üsküdar University, Faculty of Medicine, Department of Medical Pharmacology, İstanbul, TÜRKİYE
ORCID: orcid.org/0000-0002-9784-5637

Prof. K. Hüsnü Can BAŞER, Ph.D.
Anadolu University, Faculty of Pharmacy, Department of Pharmacognosy, Eskişehir, TÜRKİYE
ORCID: 0000-0003-2710-0231

Prof. Erdem YEŞİLADA, Ph.D.
Yeditepe University, Faculty of Pharmacy, Department of Pharmacognosy, İstanbul, TÜRKİYE
ORCID: 0000-0002-1348-6033

Prof. Yılmaz ÇAPAN, Ph.D.
Hacettepe University, Faculty of Pharmacy, Department of Pharmaceutical Technology, Ankara, TÜRKİYE
ORCID: 0000-0003-1234-9018

Prof. Sibel A. ÖZKAN, Ph.D.
Ankara University, Faculty of Pharmacy, Department of Analytical Chemistry, Ankara, TÜRKİYE
ORCID: 0000-0001-7494-3077

Prof. Ekrem SEZİK, Ph.D.
İstanbul Health and Technology University, Faculty of Pharmacy, Department of Pharmacognosy, İstanbul, TÜRKİYE
ORCID: 0000-0002-8284-0948

Prof. Gönül ŞAHİN, Ph.D.
Eastern Mediterranean University, Faculty of Pharmacy, Department of Pharmaceutical Toxicology, Famagusta, CYPRUS
ORCID: 0000-0003-3742-6841

Prof. Sevda ŞENEL, Ph.D.
Hacettepe University, Faculty of Pharmacy, Department of Pharmaceutical Technology, Ankara, TÜRKİYE
ORCID: 0000-0002-1467-3471

Prof. Sevim ROLLAS, Ph.D.
Marmara University, Faculty of Pharmacy, Department of Pharmaceutical Chemistry, İstanbul, TÜRKİYE
ORCID: 0000-0002-4144-6952

Prof. Göksel ŞENER, Ph.D.
Fenerbahçe University, Faculty of Pharmacy, Department of Pharmacology, İstanbul, TÜRKİYE
ORCID: 0000-0001-7444-6193

Prof. Erdal BEDİR, Ph.D.
İzmir Institute of Technology, Department of Bioengineering, İzmir, TÜRKİYE
ORCID: 0000-0003-1262-063X

Prof. Nurşen BAŞARAN, Ph.D.
Hacettepe University, Faculty of Pharmacy, Department of Pharmaceutical Toxicology, Ankara, TÜRKİYE
ORCID: 0000-0001-8581-8933

Prof. Bensu KARAHALİL, Ph.D.
Gazi University, Faculty of Pharmacy, Department of Pharmaceutical Toxicology, Ankara, TÜRKİYE
ORCID: 0000-0003-1625-6337

Prof. Betül DEMİRCİ, Ph.D.
Anadolu University, Faculty of Pharmacy, Department of Pharmacognosy, Eskişehir, TÜRKİYE
ORCID: 0000-0003-2343-746X

Prof. Bengi USLU, Ph.D.
Ankara University, Faculty of Pharmacy, Department of Analytical Chemistry, Ankara, TÜRKİYE
ORCID: 0000-0002-7327-4913

Prof. Ahmet AYDIN, Ph.D.
Yeditepe University, Faculty of Pharmacy, Department of Pharmaceutical Toxicology, İstanbul, TÜRKİYE
ORCID: 0000-0003-3499-6435

Prof. İlkay ERDOĞAN ORHAN, Ph.D.
Gazi University, Faculty of Pharmacy, Department of Pharmacognosy, Ankara, TÜRKİYE
ORCID: 0000-0002-7379-5436

Prof. Ş. Güniz KÜÇÜKGÜZEL, Ph.D.
Fenerbahçe University Faculty of Pharmacy, Department of Pharmaceutical Chemistry, İstanbul, TÜRKİYE
ORCID: 0000-0001-9405-8905

Prof. Engin Umut AKKAYA, Ph.D.
Dalian University of Technology, Department of Chemistry, Dalian, CHINA
ORCID: 0000-0003-4720-7554

Prof. Esra AKKOL, Ph.D.
Gazi University, Faculty of Pharmacy, Department of Pharmacognosy, Ankara, TÜRKİYE
ORCID: 0000-0002-5829-7869

Prof. Erem BİLENSOY, Ph.D.
Hacettepe University, Faculty of Pharmacy, Department of Pharmaceutical Technology, Ankara, TÜRKİYE
ORCID: 0000-0003-3911-6388

Prof. Uğur TAMER, Ph.D.
Gazi University, Faculty of Pharmacy, Department of Analytical Chemistry, Ankara, TÜRKİYE
ORCID: 0000-0001-9989-6123

Prof. Gülaçtı TOPÇU, Ph.D.
Bezmialem Vakıf University, Faculty of Pharmacy, Department of Pharmacognosy, İstanbul, TÜRKİYE
ORCID: 0000-0002-7946-6545

Prof. Hasan KIRMIZIBEKMEZ, Ph.D.
Yeditepe University, Faculty of Pharmacy, Department of Pharmacognosy, İstanbul, TÜRKİYE
ORCID: 0000-0002-6118-8225

Douglas Siqueira de Almeida Chaves, Ph.D.
Federal Rural University of Rio de Janeiro, Department of Pharmaceutical Sciences, Rio de Janeiro, BRAZIL
ORCID: 0000-0002-0571-9538

**Members of the Advisory Board consist of the scientists who received Science Award presented by TEB Academy of Pharmacy in chronological order.*

Turkish Journal of
PHARMACEUTICAL SCIENCES

AIMS AND SCOPE

The Turkish Journal of Pharmaceutical Sciences is the only scientific periodical publication of the Turkish Pharmacists' Association and has been published since April 2004.
Turkish Journal of Pharmaceutical Sciences journal is regularly published 6 times in a year (February, April, June, August, October, December). The issuing body of the journal is Galenos Yayinevi/Publishing House level. The aim of Turkish Journal of Pharmaceutical Sciences is to publish original research papers of the highest scientific and clinical value at an international level.
The target audience includes specialists and professionals in all fields of pharmaceutical sciences.
The editorial policies are based on the "Recommendations for the Conduct, Reporting, Editing, and Publication of Scholarly Work in Medical Journals (ICMJE Recommendations)" by the International Committee of Medical Journal Editors (20, archived at http://www.icmje.org/) rules.

Editorial Independence

Turkish Journal of Pharmaceutical Sciences is an independent journal with independent editors and principles and has no commerical relationship with the commercial product, drug or pharmaceutical company regarding decisions and review processes upon articles.

ABSTRACTED/INDEXED IN

PubMed
PubMed Central
Web of Science-Emerging Sources Citation Index (ESCI)
SCOPUS SJR
TÜBİTAK/ULAKBİM TR Dizin
ProQuest
Chemical Abstracts Service (CAS)
EBSCO
EMBASE
GALE
Index Copernicus
Analytical Abstracts
International Pharmaceutical Abstracts (IPA)
Medicinal & Aromatic Plants Abstracts (MAPA)
British Library
CSIR INDIA
GOALI
Hinari
OARE
ARDI
AGORA
Türkiye Atıf Dizini
Türk Medline
UDL-EDGE
J- Gate
Idealonline
CABI

OPEN ACCESS POLICY

This journal provides immediate open access to its content on the principle that making research freely available to the public supports a greater global exchange of knowledge.
Open Access Policy is based on the rules of the Budapest Open Access Initiative (BOAI) http://www.budapestopenaccessinitiative.org/. By "open access" to peer-reviewed research literature, we mean its free availability on the public internet, permitting any users to read, download, copy, distribute, print, search, or link to the full texts of these articles, crawl them for indexing, pass them as data to software, or use them for any other lawful purpose, without financial, legal, or technical barriers other than those inseparable from gaining access to the internet itself. The only constraint on reproduction and distribution, and the only role for copyright in this domain, should be to give authors control over the integrity of their work and the right to be properly acknowledged and cited.

CORRESPONDENCE ADDRESS

All correspondence should be directed to the Turkish Journal of Pharmaceutical Sciences Editorial Board

Post Address: Turkish Pharmacists' Association, Mustafa Kemal Mah 2147.Sok No:3 06510 Çankaya/Ankara, TÜRKİYE
Phone: +90 (312) 409 81 00
Fax: +90 (312) 409 81 09
Web Page: http://turkjps.org
E-mail: turkjps@gmail.com

PERMISSIONS

Requests for permission to reproduce published material should be sent to the publisher.
Publisher: Erkan Mor
Adress: Molla Gürani Mah. Kaçamak Sok. 21/1 Fındıkzade, Fatih, Istanbul, Türkiye
Telephone: +90 212 621 99 25
Fax: +90 212 621 99 27
Web page: http://www.galenos.com.tr/en
E-mail: info@galenos.com.tr

ISSUING BODY CORRESPONDING ADDRESS

Issuing Body : Galenos Yayınevi
Address: Molla Gürani Mah. Kaçamak Sk. No: 21/, 34093 İstanbul, Türkiye
Phone: +90 212 621 99 25 Fax: +90 212 621 99 27
E-mail: info@galenos.com.tr

MATERIAL DISCLAIMER

The author(s) is (are) responsible for the articles published in the JOURNAL.
The editors, editorial board and publisher do not accept any responsibility for the articles.
This work is licensed under a Creative Commons Attribution-NonCommercial-NoDerivatives 4.0 International License.

galenos yayınevi

Publisher Contact
Address: Molla Gürani Mah. Kaçamak Sk. No: 21/1
34093 İstanbul, Türkiye
Phone: +90 (530) 177 30 97
E-mail: info@galenos.com.tr/yayin@galenos.com.tr
Web: www.galenos.com.tr | **Publisher Certificate Number:** 14521

Publication Date: May 2023
E-ISSN: 2148-6247
International scientific journal published bimonthly.

Turkish Journal of
PHARMACEUTICAL SCIENCES

INSTRUCTIONS TO AUTHORS

Turkish Journal of Pharmaceutical Sciences journal is published 6 times (February, April, June, August, October, December) per year and publishes the following articles:

- Research articles
- Reviews (only upon the request or consent of the Editorial Board)
- Preliminary results/Short communications/Technical notes/Letters to the Editor in every field of pharmaceutical sciences.

The publication language of the journal is English.

The Turkish Journal of Pharmaceutical Sciences does not charge any article submission or processing charges.

A manuscript will be considered only with the understanding that it is an original contribution that has not been published elsewhere.

The Journal should be abbreviated as "Turk J Pharm Sci" when referenced.

The scientific and ethical liability of the manuscripts belongs to the authors and the copyright of the manuscripts belongs to the Journal. Authors are responsible for the contents of the manuscript and accuracy of the references. All manuscripts submitted for publication must be accompanied by the Copyright Transfer Form [copyright transfer]. Once this form, signed by all the authors, has been submitted, it is understood that neither the manuscript nor the data it contains have been submitted elsewhere or previously published and authors declare the statement of scientific contributions and responsibilities of all authors.

Experimental, clinical and drug studies requiring approval by an ethics committee must be submitted to the JOURNAL with an ethics committee approval report including approval number confirming that the study was conducted in accordance with international agreements and the Declaration of Helsinki (revised 2013) (http://www.wma.net/en/30publications/10policies/b3/). The approval of the ethics committee and the fact that informed consent was given by the patients should be indicated in the Materials and Methods section. In experimental animal studies, the authors should indicate that the procedures followed were in accordance with animal rights as per the Guide for the Care and Use of Laboratory Animals (http://oacu.od.nih.gov/regs/guide/guide.pdf) and they should obtain animal ethics committee approval.

Authors must provide disclosure/acknowledgment of financial or material support, if any was received, for the current study.

If the article includes any direct or indirect commercial links or if any institution provided material support to the study, authors must state in the cover letter that they have no relationship with the commercial product, drug, pharmaceutical company, etc. concerned; or specify the type of relationship (consultant, other agreements), if any.

Authors must provide a statement on the absence of conflicts of interest among the authors and provide authorship contributions.

All manuscripts submitted to the journal are screened for plagiarism using the 'iThenticate' software. Results indicating plagiarism may result in manuscripts being returned or rejected.

The Review Process

This is an independent international journal based on double-blind peer-review principles. The manuscript is assigned to the Editor-in-Chief, who reviews the manuscript and makes an initial decision based on manuscript quality and editorial priorities. Manuscripts that pass initial evaluation are sent for external peer review, and the Editor-in-Chief assigns an Associate Editor. The Associate Editor sends the manuscript to at least two reviewers (internal and/or external reviewers). The Associate Editor recommends a decision based on the reviewers' recommendations and returns the manuscript to the Editor-in-Chief. The Editor-in-Chief makes a final decision based on editorial priorities, manuscript quality, and reviewer recommendations. If there are any conflicting recommendations from reviewers, the Editor-in-Chief can assign a new reviewer.

The scientific board guiding the selection of the papers to be published in the Journal consists of elected experts of the Journal and if necessary, selected from national and international authorities. The Editor-in-Chief, Associate Editors may make minor corrections to accepted manuscripts that do not change the main text of the paper.

In case of any suspicion or claim regarding scientific shortcomings or ethical infringement, the Journal reserves the right to submit the manuscript to the supporting institutions or other authorities for investigation. The Journal accepts the responsibility of initiating action but does not undertake any responsibility for an actual investigation or any power of decision.

The Editorial Policies and General Guidelines for manuscript preparation specified below are based on "Recommendations for the Conduct, Reporting, Editing, and Publication of Scholarly Work in Medical Journals (ICMJE Recommendations)" by the International Committee of Medical Journal Editors (20, archived at http://www.icmje.org/).

Preparation of research articles, systematic reviews and meta-analyses must comply with study design guidelines:

CONSORT statement for randomized controlled trials (Moher D, Schultz KF, Altman D, for the CONSORT Group. The CONSORT statement revised recommendations for improving the quality of reports of parallel group randomized trials. JAMA 2001; 285: 1987-91) (http://www.consort-statement.org/);

PRISMA statement of preferred reporting items for systematic reviews and meta-analyses (Moher D, Liberati A, Tetzlaff J, Altman DG, The PRISMA Group. Preferred Reporting Items for Systematic Reviews and Meta-Analyses: The PRISMA Statement. PLoS Med 2009; 6(7): e1000097.) (http://www.prisma-statement.org/);

STARD checklist for the reporting of studies of diagnostic accuracy (Bossuyt PM, Reitsma JB, Bruns DE, Gatsonis CA, Glasziou PP, Irwig LM, et al., for the STARD Group. Towards complete and accurate reporting of studies of diagnostic accuracy: the STARD initiative. Ann Intern Med 2003;138:40-4.) (http://www.stard-statement.org/);

STROBE statement, a checklist of items that should be included in reports of observational studies (http://www.strobe-statement.org/);

MOOSE guidelines for meta-analysis and systemic reviews of observational studies (Stroup DF, Berlin JA, Morton SC, et al. Meta-analysis of observational studies in epidemiology: a proposal for reporting Meta-analysis of observational Studies in Epidemiology (MOOSE) group. JAMA 2000; 283: 2008-12).

Turkish Journal of
PHARMACEUTICAL SCIENCES

INSTRUCTIONS TO AUTHORS

GENERAL GUIDELINES

Manuscripts can only be submitted electronically through the Journal Agent website (http://journalagent.com/tjps/) after creating an account. This system allows online submission and review.

Format: Manuscripts should be prepared using Microsoft Word, size A4 with 2.5 cm margins on all sides, 12 pt Arial font and 1.5 line spacing.

Abbreviations: Abbreviations should be defined at first mention and used consistently thereafter. Internationally accepted abbreviations should be used; refer to scientific writing guides as necessary.

Cover letter: The cover letter should include statements about manuscript type, single-Journal submission affirmation, conflict of interest statement, sources of outside funding, equipment (if applicable), for original research articles.

ETHICS COMMITTEE APPROVAL

The editorial board and our reviewers systematically ask for ethics committee approval from every research manuscript submitted to the Turkish Journal of Pharmaceutical Sciences. If a submitted manuscript does not have ethical approval, which is necessary for every human or animal experiment as stated in international ethical guidelines, it must be rejected on the first evaluation.

Research involving animals should be conducted with the same rigor as research in humans; the Turkish Journal of Pharmaceutical Sciences asks original approval document to show implements the 3Rs principles. If a study does not have ethics committee approval or authors claim that their study does not need approval, the study is consulted to and evaluated by the editorial board for approval.

SIMILARITY

The Turkish Journal of Pharmaceutical Sciences is routinely looking for similarity index score from every manuscript submitted before evaluation by the editorial board and reviewers. The journal uses iThenticate plagiarism checker software to verify the originality of written work. There is no acceptable similarity index; but, exceptions are made for similarities less than 15 %.

REFERENCES

Authors are solely responsible for the accuracy of all references.

In-text citations: References should be indicated as a superscript immediately after the period/full stop of the relevant sentence. If the author(s) of a reference is/are indicated at the beginning of the sentence, this reference should be written as a superscript immediately after the author's name. If relevant research has been conducted in Türkiye or by Turkish investigators, these studies should be given priority while citing the literature.

Presentations presented in congresses, unpublished manuscripts, theses, Internet addresses, and personal interviews or experiences should not be indicated as references. If such references are used, they should be indicated in parentheses at the end of the relevant sentence in the text, without reference number and written in full, in order to clarify their nature.

References section: References should be numbered consecutively in the order in which they are first mentioned in the text. All authors should be listed regardless of number. The titles of Journals should be abbreviated according to the style used in the Index Medicus.

Reference Format

Journal: Last name(s) of the author(s) and initials, article title, publication title and its original abbreviation, publication date, volume, the inclusive page numbers. Example: Collin JR, Rathbun JE. Involutional entropion: a review with evaluation of a procedure. Arch Ophthalmol. 1978;96:1058-1064.

Book: Last name(s) of the author(s) and initials, book title, edition, place of publication, date of publication and inclusive page numbers of the extract cited.

Example: Herbert L. The Infectious Diseases (1st ed). Philadelphia; Mosby Harcourt; 1999:11;1-8.

Book Chapter: Last name(s) of the author(s) and initials, chapter title, book editors, book title, edition, place of publication, date of publication and inclusive page numbers of the cited piece.

Example: O'Brien TP, Green WR. Periocular Infections. In: Feigin RD, Cherry JD, eds. Textbook of Pediatric Infectious Diseases (4th ed). Philadelphia; W.B. Saunders Company;1998:1273-1278.

Books in which the editor and author are the same person: Last name(s) of the author(s) and initials, chapter title, book editors, book title, edition, place of publication, date of publication and inclusive page numbers of the cited piece. Example: Solcia E, Capella C, Kloppel G. Tumors of the exocrine pancreas. In: Solcia E, Capella C, Kloppel G, eds. Tumors of the Pancreas. 2nd ed. Washington: Armed Forces Institute of Pathology; 1997:145-210.

TABLES, GRAPHICS, FIGURES, AND IMAGES

All visual materials together with their legends should be located on separate pages that follow the main text.

Images: Images (pictures) should be numbered and include a brief title. Permission to reproduce pictures that were published elsewhere must be included. All pictures should be of the highest quality possible, in

JPEG format, and at a minimum resolution of 300 dpi.

Tables, Graphics, Figures: All tables, graphics or figures should be enumerated according to their sequence within the text and a brief descriptive caption should be written. Any abbreviations used should be defined in the accompanying legend. Tables in particular should be explanatory and facilitate readers' understanding of the manuscript, and should not repeat data presented in the main text.

MANUSCRIPT TYPES

Original Articles

Clinical research should comprise clinical observation, new techniques or laboratories studies. Original research articles should include title, structured abstract, key words relevant to the content of the article, introduction, materials and methods, results, discussion, study limitations, conclusion references, tables/figures/images and

Turkish Journal of
PHARMACEUTICAL SCIENCES

INSTRUCTIONS TO AUTHORS

acknowledgement sections. Title, abstract and key words should be written in both Turkish and English. The manuscript should be formatted in accordance with the above-mentioned guidelines and should not exceed 16 A4 pages.

Title Page: This page should include the title of the manuscript, short title, name(s) of the authors and author information. The following descriptions should be stated in the given order:

1. Title of the manuscript (Turkish and English), as concise and explanatory as possible, including no abbreviations, up to 135 characters

2. Short title (Turkish and English), up to 60 characters

3. Name(s) and surname(s) of the author(s) (without abbreviations and academic titles) and affiliations

4. Name, address, e-mail, phone and fax number of the corresponding author

5. The place and date of scientific meeting in which the manuscript was presented and its abstract published in the abstract book, if applicable

Abstract: A summary of the manuscript should be written in both Turkish and English. References should not be cited in the abstract. Use of abbreviations should be avoided as much as possible; if any abbreviations are used, they must be taken into consideration independently of the abbreviations used in the text. For original articles, the structured abstract should include the following sub-headings:

Objectives: The aim of the study should be clearly stated.

Materials and Methods: The study and standard criteria used should be defined; it should also be indicated whether the study is randomized or not, whether it is retrospective or prospective, and the statistical methods applied should be indicated, if applicable.

Results: The detailed results of the study should be given and the statistical significance level should be indicated.

Conclusion: Should summarize the results of the study, the clinical applicability of the results should be defined, and the favorable and unfavorable aspects should be declared.

Keywords: A list of minimum , but no more than 5 key words must follow the abstract. Key words in English should be consistent with "Medical Subject Headings (MESH)" (www.nlm.nih.gov/mesh/MBrowser.html). Turkish key words should be direct translations of the terms in MESH.

Original research articles should have the following sections:

Introduction: Should consist of a brief explanation of the topic and indicate the objective of the study, supported by information from the literature.

Materials and Methods: The study plan should be clearly described, indicating whether the study is randomized or not, whether it is retrospective or prospective, the number of trials, the characteristics, and the statistical methods used.

Results: The results of the study should be stated, with tables/figures given in numerical order; the results should be evaluated according to the statistical analysis methods applied. See General Guidelines for details about the preparation of visual material.

Discussion: The study results should be discussed in terms of their favorable and unfavorable aspects and they should be compared with the literature. The conclusion of the study should be highlighted.

Study Limitations: Limitations of the study should be discussed. In addition, an evaluation of the implications of the obtained findings/results for future research should be outlined.

Conclusion: The conclusion of the study should be highlighted.

Acknowledgements: Any technical or financial support or editorial contributions (statistical analysis, English/Turkish evaluation) towards the study should appear at the end of the article.

References: Authors are responsible for the accuracy of the references. See General Guidelines for details about the usage and formatting required.

Review Articles

Review articles can address any aspect of clinical or laboratory pharmaceuticals. Review articles must provide critical analyses of contemporary evidence and provide directions of or future research. Most review articles are commissioned, but other review submissions are also welcome. Before sending a review, discussion with the editor is recommended.

Reviews articles analyze topics in depth, independently and objectively. The first chapter should include the title in Turkish and English, an unstructured summary and key words. Source of all citations should be indicated. The entire text should not exceed 25 pages (A, formatted as specified above).

Turkish Journal of
PHARMACEUTICAL SCIENCES

CONTENTS

Turk J Pharm Sci 2023;20(2):68-77
DOI: 10.4274/tjps.galenos.2022.57639

ORIGINAL ARTICLE

Olea europaea L. Leaf Extract Attenuates Temozolomide-Induced Senescence-Associated Secretion Phenotype in Glioblastoma

Melis ERÇELİK[1], Berrin TUNCA[1]*, Seçil AK AKSOY[2], Çağla TEKİN[1], Gülçin TEZCAN[3]

[1]Bursa Uludağ University, Faculty of Medicine, Department of Medical Biology, Bursa, Türkiye
[2]Bursa Uludağ University, İnegol Vocation School, Bursa, Türkiye
[3]Bursa Uludağ University, Faculty of Dentistry, Department of Fundamental Sciences, Bursa, Türkiye

ABSTRACT

Objectives: The purpose of this study was to investigate the effect of *Olea europaea* L. leaf extract (OLE) on senescence and senescence-associated secretory phenotype (SASP) caused by temozolomide (TMZ) in glioblastoma (GB).

Materials and Methods: A senescence β-galactosidase assay and a colony formation assay were used to determine the effects of OLE, TMZ, and OLE + TMZ on the cellular senescence and aggressiveness of GB cell lines T98G and U87MG. mRNA expression levels of p53, a senescence factor, interleukin (IL)-6, matrix metalloproteinases (MMP)-9, and nuclear factor kappa B1 (NF-κB1) as SASP factors and Bcl-2 and Bax as senolytic markers were assessed using quantitative reverse transcription-real-time polymerase chain reaction. Cells were double-stained with acridine orange and propidium iodide to observe the cell morphology.

Results: TMZ increased the senescence rate of GB cells (p<0.001). Besides, OLE + TMZ reduced the proportion of senescent cells (p<0.001) and their capability to form colonies compared to TMZ-only-treated cells. Additionally, OLE + TMZ co-treatment elevated the mRNA expression levels of MMP-9, IL-6, NF-κB1, p53, and the Bax/Bcl-2 ratio compared to TMZ-only treatment. Especially in U87MG cells, involvement of OLE in TMZ treatments increased more than six times in the Bax/Bcl-2 ratio compared to TMZ-only, which induced the apoptosis-like morphological features (p<0.0001).

Conclusion: Collectively, our findings presented the inhibitory effect of OLE on TMZ-mediated SASP-factor production in GB and, accordingly, its potential contribution to elongate the time of recurrence.

Key words: Glioblastoma, *Olea europaea* leaf extract, temozolomide, senescence, SASP

INTRODUCTION

Cellular senescence has been recognized as an essential tumor suppressor mechanism with its ability to the cessation of cell division.[1,2] On the other hand, recent studies have evidenced a contrasting effect of cellular senescence by promoting tumor growth with stimulating growth factors, matrix proteases, and pro-inflammatory proteins, which are described as senescence-associated secretory phenotype (SASP).[2-4] Some chemotherapeutic agents, such as 5-fluorouracil, gemcitabine, doxorubicin, irinotecan, and methotrexate, induce cellular senescence.[5-8] It appeared that chemotherapeutic drug-induced aging could be beneficial with its cell proliferation inhibitory effect. However, therapy-induced senescent (TIS) cells give the tumor ability to a future relapse by producing pro-inflammatory and matrix-destroying molecules known as SASP, which alters the tumor cells' metabolism in a way that reveals an aggressive cell phenotype.[9] Therefore, the effect of chemotherapy-induced cellular senescence on tumor progression could be two-sided and might be a reason for acquired therapy resistance and tumor recurrence.

Glioblastoma (GB) is one of the deadliest cancer types and the DNA-methylating drug temozolomide (TMZ) is the most

*Correspondence: btunca@uludag.edu.tr, Phone: +90 224 295 41 61, ORCID-ID: orcid.org/0000-0002-1619-6680
Received: 09.02.2022, Accepted: 29.04.2022

©Copyright 2023 by Turkish Pharmacists' Association / Turkish Journal of Pharmaceutical Sciences published by Galenos Publishing House.
Licenced by Creative Commons Attribution-NonCommercial-NoDerivatives 4.0 (CC BY-NC-ND)

widely used chemotherapy agent for treating GB. TMZ was shown to induce senescence by the specific DNA lesion O6-methylguanine, which fails recognition of DNA damage, activation of the DNA damage response (DDR) pathway, and arrest of cells in the G2-M phase.[10,11] Considering the potential of GB cells to escape and become drug-resistant after TMZ administration due to being arrested in senescence, involvement of an additive agent with anti-senescence features in TMZ therapy is expected to reduce the risk of senescence-related symptoms and tumor relapse.[12] The therapeutic effect of various natural compounds, such as quercetin, fisetin, and curcumin, and their analogs in age-related diseases was explained with their senescence cell killing and senolytic effects.[13] Similarly, oleuropein aglycone was reported to modulate angiogenesis on senescent fibroblasts.[14] An individual study showed that oleuropein exhibits senescence inhibitory features by retaining proteasome function during replicative senescence in human embryonic fibroblasts.[15] Our previous studies indicated that *Olea europaea* L. (Oleaceae) leaf extract (OLE), which contains a high amount of oleuropein, increases the therapeutic features of TMZ in GB.[16-19] Although the effect of oleuropein on cellular senescence was described in fibroblast, its effect was not described in GB. Additionally, one of our previous studies indicated that OLE consists of several additional bioactive components, such as secoiridoids, triterpenes, and flavonoids, in trace amounts, and these minor compounds in OLE could play critical anticancer roles.[17] However, the effect of OLE on TMZ-induced SASP expression and its effect on tumor progression in GB remains unknown. Therefore, in this study, we investigated the effect of OLE on senescent cells induced by TMZ in GB cell lines with different TMZ sensitivity using *in vitro* functional analyses. Our findings identified that OLE attenuates TIS cell-promoted expression of proinflammatory SASP factors and attenuated aggressive characteristics in GB cells, independent of their TMZ sensitivity.

MATERIALS AND METHODS

Cell culture and reagents

Human GB TMZ-resistant T98G cells and TMZ-sensitive U87MG cells, and control HUVEC cells, which was used to determine the drug cytotoxicity, were obtained from Medical Biology Department, Faculty of Medicine, Bursa Uludağ University (Bursa, Türkiye). All cell lines were maintained in a Dulbecco's Modified Eagle's Medium-F12 (DMEMF12; HyClone, Utah, USA) containing L-glutamine supplemented with 10% fetal bovine serum (FBS, BIOCHROME, Berlin, Germany), 1 mM sodium pyruvate, 100 mg/mL streptomycin, and 100 U/mL penicillin. All cells were incubated in a humidified atmosphere at 37°C and 5% CO_2.

The standardized OLE (05.06.2007, 10-00014-00- 015-0) was kindly provided by Kale Naturel (Edremit, Balıkesir, Türkiye) and prepared as described in our previous study.[19] An Agilent 1200 High Performance Liquid Chromatography system (Waldbronn, Germany) identified 19.419 mg/mL of oleuropein among the phenolic compounds of the OLE fractions at 280 nm wavelength (Figure 1A).[19,20] TMZ was provided by Sigma, USA. Oleuropein was detected as 19.419 mg/mL in the standardized OLE used in this study.

Investigation of cell cytotoxicity and proliferation

The cytotoxicity of OLE and TMZ and their effect on cell proliferation was assessed using a cell proliferation kit (WST-1, Roche Applied Sciences, Mannheim, Germany) as described previously.[18] The inhibitory concentrations at which 50% of the cells die (IC_{50}) were selected to treat cells for the experiment set up. The possible additive, antagonist, and synergistic effects of OLE on TMZ treatment were calculated using a web-based tool, *i.e.* SynergyFinder (version 2.0).[21]

Apoptosis induction assay [fluorescent microscopy; acridine orange (AO)/propidium iodide (PI) double staining]

The effect of OLE on morphological features of T98G and U87MG cells was assessed by AO/PI, a double-fluorescent dye staining method.[22,23] The morphology of the cells was analyzed with an inverted fluorescent microscope (Olympus, Tokyo, Japan). Cells with intact green nuclei were considered viable; cells with dense green chromatin condensation areas in the nucleus were considered early apoptotic, cells with dense orange chromatin condensation areas were considered late apoptotic, and cells with intact orange nuclei were considered secondary necrotic.[22,23]

Evaluation of tumor aggressiveness

The CellMA™ Clonogenic assay kit (BioPioneer, USA) was used to determine the effect of OLE on colony formation in T98G and U87MG cells. The blue-colored colonies were counted under an inverted microscope under 20X magnification.

Detection of senescence-associated β-galactosidase

The rate of senescence in GB cell lines was detected using a senescence β-galactosidase staining kit (9860, Cell Signaling Technology, Danvers, MA, USA), according to the manufacturer's instructions. The blue-colored cells were visualized and counted under light microscopy using a 10X magnification.

Examination of the expression levels of senescence factors

Total RNA was isolated using a Zymo Research RNA isolation kit (Thermo Fisher Scientific, Glasgow, UK). RNA quantity and quality were assessed using a NanoDrop 2000 Spectrophotometer (Beckman Coulter, California, USA). RNA samples with a total concentration between 200 and 400 ng/µL were selected for cDNA synthesis (High-Capacity cDNA Reverse Transcription Kit; Thermo Fisher Scientific, Glasgow, UK). Quantitative reverse transcription-real-time polymerase chain reaction (RT-qPCR) analysis was performed using TaqMan gene expression assays specific to the genes related to senescence factors [p53(DM02154335-g1)], SASP factors [interleukin (IL)-6 (Hs00174131_m1), matrix metalloproteinases (MMP)-9 (Hs00957562_m1) and nuclear factor kappa B1 (NF-κB1) (Hs00428211-m1)] and senolytic effect [Bcl-2 (Hs00608023_m1) and Bax (Hs00180269 _ m1)]. Expression results were normalized to the expression of a housekeeping gene GAPDH (Hs00957562_m1). The threshold cycle for each

RNA expression was determined using a StepOne RT-PCR system (Applied Biosystems, Warrington, UK). 2-ΔCt Method calculated the fold change in RNA expression.

Statistical analysis

One-Way ANOVA was used to evaluate the findings of the WST-1 assay, and independent *t*-test analyses evaluated the difference in the number of cell colonies. The independent *t*-test analyzed the findings of the senescence-associated *β*-galactosidase assay. The independent *t*-test evaluated the findings of RT-qPCR. Data are presented as mean ± standard error of mean. Significance was established at a value of $p<0.05$. All statistical analyzes were performed using the IBM SPSS Statistics for Windows, version 23.0 (IBM Corp., Armonk, NY, USA). The findings were interpreted as graphs using the GraphPad Prism 6 (GraphPad Software Inc, San Diego, California, USA).

RESULTS

OLE inhibits the proliferation of GB cells

Previously determined effective concentrations of OLE and TMZ were confirmed using current OLE extract in laboratory conditions. OLE, TMZ, and their co-treatment reduced tumor cell proliferation in GB cell lines, T98G, and U87MG, similar to our previous findings, the effective doses of OLE + TMZ treatments were determined as 2 mg/mL OLE and 400 μM TMZ for T98G cells, while they were 1 mg/mL OLE and 300 μM TMZ for U87MG during 24 h of incubation time (Figure 1B, a-f).[24] In addition, non of the applied concentrations of OLE caused a notable cytotoxic effect on HUVEC, a non-tumor endothelial cell line (Figure 1B, g).[24] Therefore, to investigate the effect of OLE and TMZ on senescence and aggressiveness of GB cell lines, 2 mg/mL OLE and 400 μM TMZ were used for T98G, while 1 mg/mL OLE and 300 μM TMZ were used for U87MG cells for the remaining *in vitro* analysis. According to the findings, OLE + TMZ treatment showed an additive effect in T98G (SC: -8.253) and U87MG (SC: -2.078) (Figure 1C) and increased the number of cells with apoptotic morphology compared to TMZ-only treatment, suggesting that OLE provokes cell death independent from TMZ sensitivity of GB cells (Figure 2).

OLE inhibits GB tumor aggressiveness

OLE, TMZ, and their co-treatment led to a significant decrease in the number of tumor colonies of both T98G and U87MG cells compared with untreated cells (Figure 3). The number of cell colonies was 216 in untreated T98G cells, while it decreased to 38 after OLE-only, 98 after TMZ-only, and 36 after OLE + TMZ treatments ($p<0001$, Figure 3A). Additionally, the number of colonies was 235 in untreated U87MG cells, and OLE-only, TMZ-only, and OLE + TMZ treatments decreased it to 49, 64, and 46, respectively ($p<0.001$, Figure 3B), suggesting that OLE-only treatment tented to reduce the number of colonies than that of TMZ-only treatment in both T98G and U87MG cells. Additionally, the co-treatment of OLE + TMZ reduced the colony formation capacity of cells compared to TMZ-only-treated T98G cells. OLE + TMZ treatment 2.84 fold reduced the number of colonies formed by T98G cells compared to the number of colonies after TMZ-only treatment ($p<0.001$). Moreover, after alone and complementary usage of OLE, the colonies' size was smaller than those of untreated and TMZ-only-treated T98G cells. Interestingly, in U87MG, while alone usage of OLE reduced the size of colonies compared to untreated cells, it did not affect the size of TMZ-treated cells (Figure 3).

OLE reduces the senescence caused by TMZ

Untreated senescent cells were 0.8% in T98G and 3.1% in U87MG cells, respectively (Table 1). TMZ-only treatment caused a significant increase in the number of senescent cells in both T98G and U87MG cells compared with those of untreated cells (the rate of senescent cells after TMZ treatment in T98G cells: 47%, $p<0.001$; in U87MG cells: 13.4%, $p<0.001$). Although OLE-

Table 1. The effect of combination of OLE, TMZ, and OLE + TMZ on cell aging in T98G and U87MG cells

	Cell number (n: 3)			Average cell number	Number of aging cells (n: 3)			Average number of aging cells (%)
	I	II	III		I	II	III	
T98G								
Un-treated	121	111	107	113	0	3	0	1 (0.8%)
OLE	54	67	76	42	7	8	7	7 (11%)
TMZ	100	104	115	106	42	33	76	50 (47%)
OLE + TMZ	75	90	85	83	25	28	22	25 (30%)
U87MG								
Un-treated	412	418	424	418	10	13	16	13 (3.1%)
OLE	279	192	234	235	10	14	12	12 (5.1%)
TMZ	461	454	469	461	62	75	49	62 (13.4%)
OLE + TMZ	391	330	398	373	27	17	8	17.5 (4.5%)

OLE: *Olea europaea* leaf extract, TMZ: Temozolomide

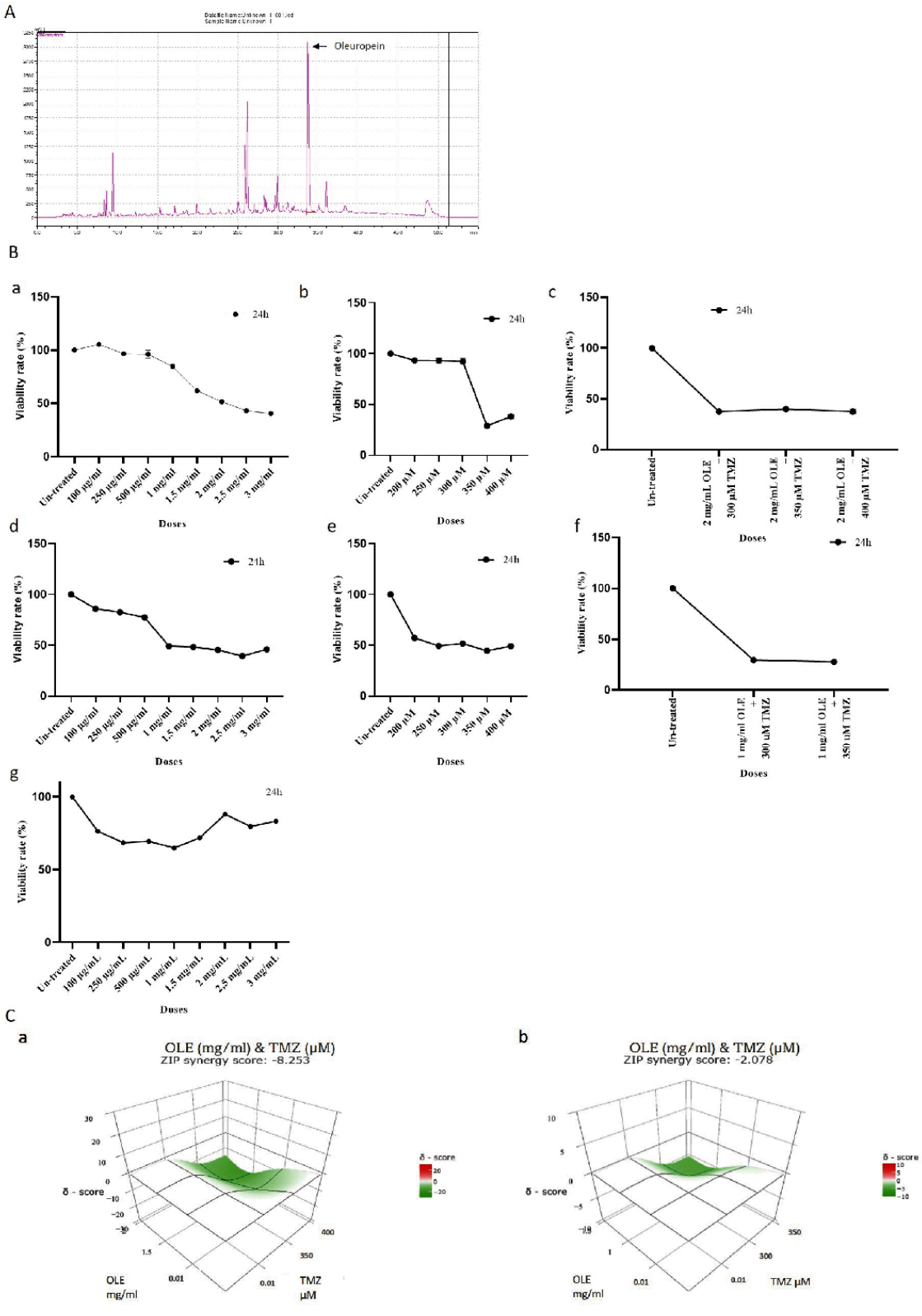

Figure 1. (A) The oleuropein content of OLE. The oleuropein concentration of OLE was detected using HPLC/DAD analyses. (B) T98G and U87MG cells viability rates of determined after treatment with OLE, TMZ, and OLE + TMZ and HUVEC cell viability rates of determined after treatment with OLE for 24 h. OLE (a), TMZ (b), OLE + TMZ (c) treatment in T98G. OLE (d), TMZ (e), OLE + TMZ (f) treatment in U87MG. OLE (g) treatment in HUVEC ($p<0.001$, one-sample *t*-test). (C) The combined effect of OLE and TMZ in T98G and U87MG cell lines. The additive effects of OLE and TMZ were detected according to the zero interaction strength synergy scoring system. The effect of OLE + TMZ in T98G cells is shown in "a", and in U87MG cells was shown in "b"

OLE: *Olea europaea* leaf extract, HPLC/DAD: High performance liquid chromatography/Diode-array detection, TMZ: Temozolomide

only treatment resulted in more senescent cells in both T98G and U87MG cells, this increase was lower than that after TMZ-only treatment (OLE-only treatment, 11% induced senescent cells in T98G cells and 5.1% in U87MG cells). Likewise, while OLE + TMZ treatment increased the number of senescent cells compared to untreated cells (in T98G cells: 30%, $p<0.001$; in U87MG: 4.5%, $p<0.001$, compared to untreated cells), the rate of this increase was lower than that of caused by TMZ-only treatment ($p<0.0001$; Figure 4). These findings showed that the involvement of OLE in the TMZ treatment reduced the senescence-provoking capacity of TMZ (Figure 4).

OLE suppresses the expression of SASP and senescence factors in GB cells

TMZ-only treatment increased the mRNA expression levels of SASP-related genes, IL-6, NF-κB1, and MMP-9, compared with untreated cells (TMZ induced IL-6: 2.03-fold; $p=0.003$, NF-κB1: 3.26-fold; $p<0.001$ and MMP-9: 6.14-fold; $p<0.001$; Figure 5). In contrast, OLE-only treatment slightly increased MMP-9 (1.54-fold, $p<0.001$) and did not affect NF-κB1 and IL-6. Additionally, a co-treatment with OLE + TMZ significantly attenuated the mRNA expression of these genes (OLE + TMZ reduced IL-6: 1.81-fold; $p=0.017$, NF-κB1: 2.35-fold; $p<0.001$ and MMP-9: 3.07-fold; $p<0.0001$ compared to TMZ-only treatment; Figure 5). Similarly, TMZ-only treatment significantly induced the mRNA expression of IL-6 (5.73-fold; $p<0.0001$), NF-κB1 (8.83-fold; $p<0.0001$), and MMP-9 (6.00-fold; $p<0.001$) in U87MG cells, compared with untreated cells. Additionally, OLE-only treatment decreased the expression of IL-6 (2.22-fold; $p<0.003$) and NF-κB1 (3.1-fold; $p=0.001$) and did not affect MMP-9 compared with untreated cells. A co-treatment with OLE + TMZ significantly reduced the expression of these genes compared with TMZ-only treatment (OLE + TMZ reduced IL-6: 14.3-fold; $p<0.0001$, NF-κB1: 13.23-fold; $p<0.0001$ and MMP-9: 2.21-fold; $p<0.001$; Figure 5). These findings showed that a mechanism of OLE to reduce GB tumor aggressive phenotype is by reducing the expression of TMZ-induced SASP factors.

Beside the reducing effect on SASP factors, OLE + TMZ significantly reduced the expression level of p53, a senescence factor, whereas it induced the ratio of Bax/Bcl-2, a senolytic effective factor compared to TMZ-only in both T98G and U87MG cells (OLE + TMZ reduced p53: 1.27-fold; $p=0.002$, and Bcl-2:

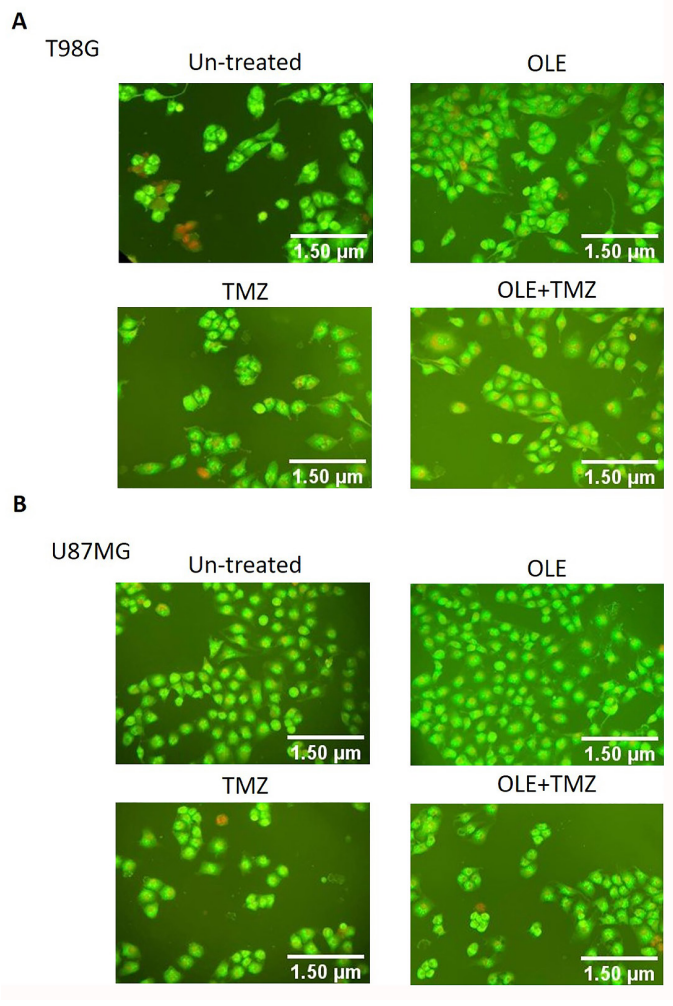

Figure 2. The effect of OLE and TMZ on GB cell morphology. Findings of AO/PI staining showed that OLE and OLE + TMZ increased the apoptosis rate in T98G (A) and U87MG cells (B). Living cells: cells with intact green nuclei; early apoptotic cells: cells with dense green chromatin condensation areas in the nucleus; late apoptotic cells: cells with dense orange chromatin condensation areas; secondary necrotic cells: cells with intact orange nuclei

OLE: *Olea europaea* leaf extract, TMZ: Temozolomide, AO: Acridine orange, PI: Propidium iodide

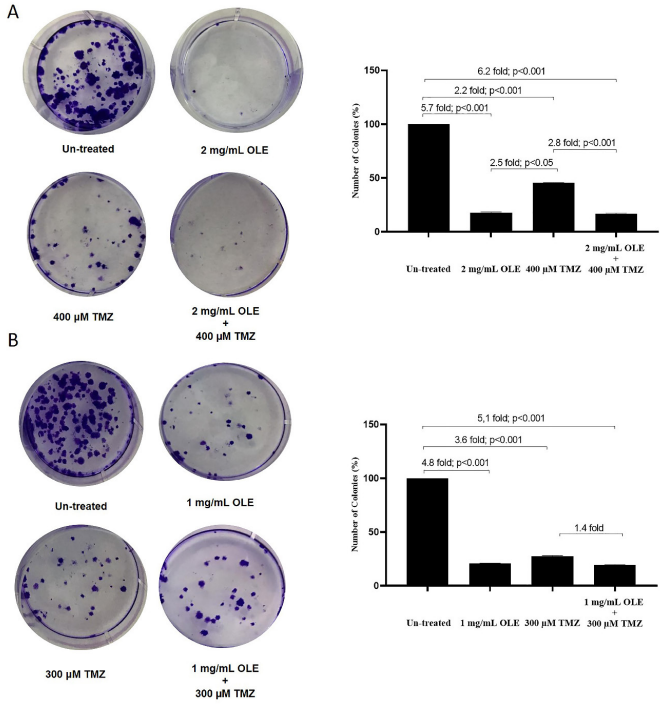

Figure 3. Effects of OLE, TMZ, and OLE + TMZ combination on colony formation of GB cells. in T98G cells OLE leaded 6.25-fold ($p<0.001$); TMZ: 2.20-fold ($p<0.001$) and OLE + TMZ 5.71-fold ($p<0.001$) (A) in U87MG cells OLE leaded 4.8-fold ($p<0.001$); TMZ: 3.60-fold ($p<0.001$) and OLE + TMZ 5.1 ($p<0.001$) (B) fold decrease compared to those of untreated cells. *P* values were calculated using an independent *t*-test (n: 3)

OLE: *Olea europaea* leaf extract, TMZ: Temozolomide, GB: Glioblastoma

1.45-fold; p=0.002, while it induced Bax: 2.02-fold; p=0.0007 and Bax/Bcl-2: 1.3-fold p>0.05 in T98G and it reduced p53: 4.66-fold; p<0.0001, and Bcl-2: 1.47-fold; p=0.0001 and induced Bax: 7.75-fold; p<0.0001 and Bax/Bcl-2: 6-fold; p<0.0001 in U87MG compared to TMZ) (Figure 6). These data provide evidence of the diverting effect of OLE on apoptosis on senescent GB cells due to TMZ treatment.

DISCUSSION

Cellular senescence arrests the cell cycle by phosphorylating p53 and the expression of p21.[2-4] One of our previous studies showed that TMZ-only treatment induces mRNA expression of p53 in GB tumors.[19] Confirming our previous findings, TMZ-only treatment induced P53 expression in T98G and U87MG cell lines in this study. Although the well-described function of p53 is activating apoptosis,[25] recent studies highlighted its regulatory role in cellular senescence *via* DDR activation.[26-28] Studies evidenced that p53 could stimulate apoptosis as a response to overwhelming stress, while it could stimulate senescence as a response to less severe damage by failing to induce pro-apoptotic factors and leading to over-expression of the pro-survival gene Bcl-2.[29-31] A very recent study of Aasland et al.[11] linked TMZ-induced p53 expression to initiation of senescence in O6-methylguanine DNA-methyltransferase (MGMT) expressing GB cell lines. Although MGMT is expressed in T98G cells, it is absent in U87MG.[32] In this study, after TMZ-only treatment, P53 and Bcl-2 expression were induced in these cell lines. Unlike apoptosis, p53-initiated cellular senescence produces diverse bioactive factors SASP.[33] Activation of SASP requires a NF-κB and C/EBPβ pathways-mediated sustained DDR. NF-κB regulates the production of IL-6, which plays a role in the maintenance and propagation of the SASP response in the tumor microenvironment.[34,35] Besides, NF-κB leads to transcriptional activation of pro-inflammatory cytokines and MMPs, such as MMP-9, a key modulator of tumor aggressiveness, in GB.[36,37] The findings of this study displayed that TMZ-only treatment induced the expression levels of NF-κB, IL-6, and MMP9. Additionally, SA-β-gal activity, which was mostly detected in senescent cells,[38] was induced after TMZ-only treatment in both cells, suggesting that TMZ-induced p53 dependent cellular senescence may be independent of MGMT in GB.

Conversely, while OLE-only did not affect p53 and slightly induced BCL2 in MGMT expressing T98G cells, it reduced p53 and had a higher capacity to induce Bcl-2 in MGMT-methylated U87MG cells. These findings indicate that the level of MGMT expression affects the expression of p53 in GB. According to our previous studies, OLE induces a methylation level of MGMT, while reducing p53 and promoting apoptosis.[39] Similarly, in this study, the complementary usage of OLE with TMZ increased the Bax/Bcl-2 ratio, which is widely used to predict the cells undergoing apoptosis.

Evidence indicated that cellular senescence promotes tumor aggressiveness and drug resistance.[40] However, in this study, OLE reduces the colony-forming ability of GB cells compared to TMZ-only-treated cells, suggesting that OLE promotes apoptosis rather than senescence. Supporting this, based on the current findings, OLE did not affect NF-κB and IL-6 in T98G cells and reduced the expression of these genes in U87MG cells. Additionally, upon senescence induced by TMZ, OLE reduced the senescence markers, including NF-κB, IL-6, and MMP-9, and β-galactosidase staining in both GB cell lines independent of MGMT expression level. Therefore, these findings provide evidence of the effect of OLE on directing TIS-GB cells to apoptosis.

CONCLUSION

This study uniquely exhibited that the enhancing effect of OLE on TMZ sensitivity in GB tumors might be associated with its attenuating capacity to TMZ-induced senescent. Advanced studies are recommended for a better understanding of the effecting mechanism of OLE on TIS and to exhibit the potential of OLE to be a complementary therapy as a senolytic agent for patients with GB.

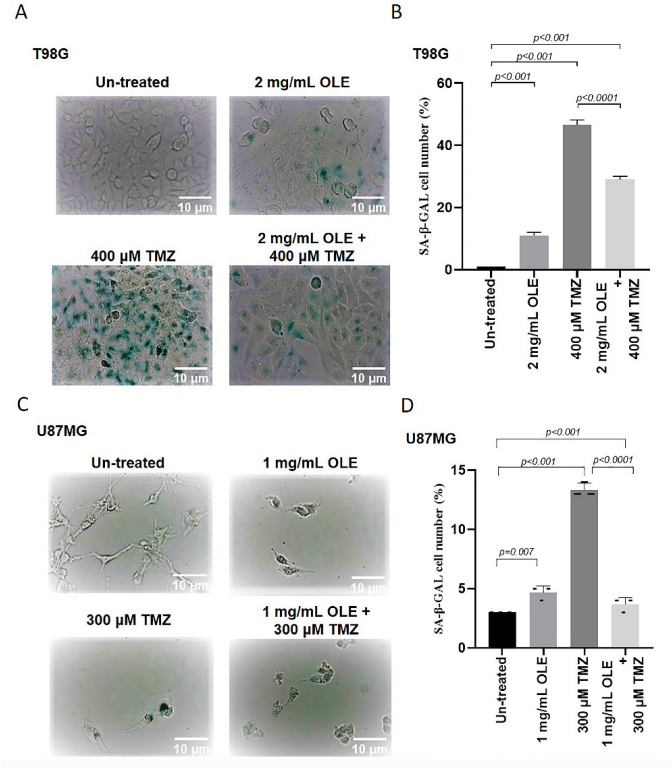

Figure 4. Effects of OLE and TMZ on cellular senescence in T98G (A) and U87MG (B) (a light microscope was analyzed using 20X objectives for T98G cells and 10X objectives for U87MG cells). A comparison of the effects of OLE and TMZ treatments on senescence in T98G (A) and U87MG cells (B)

OLE: *Olea europaea* leaf extract, TMZ: Temozolomide

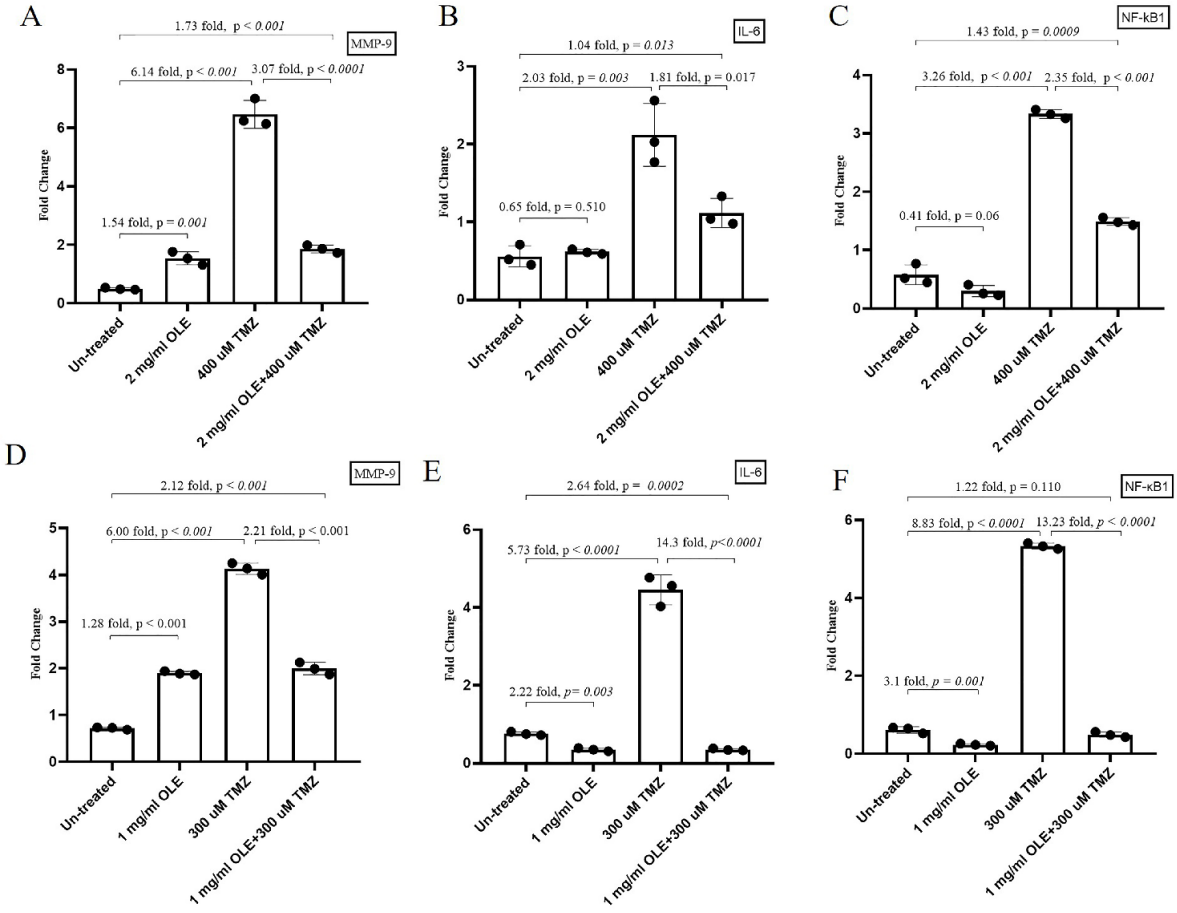

Figure 5. The effect of T98G and U87MG cells treated with OLE, TMZ, and OLE + TMZ on the expression levels of SASP factors. MMP-9 (A), IL-6 (B), and NF-κB1 (C) expression levels in T98G. MMP-9 (D), IL-6 (E), and NF-κB1 (F) expression levels in U87MG

OLE: *Olea europaea* leaf extract, TMZ: Temozolomide, SASP: Senescence-associated secretory phenotype, MMP: Matrix metalloproteinase, IL: Interleukin, NF-κB1: Nuclear factor kappa B1

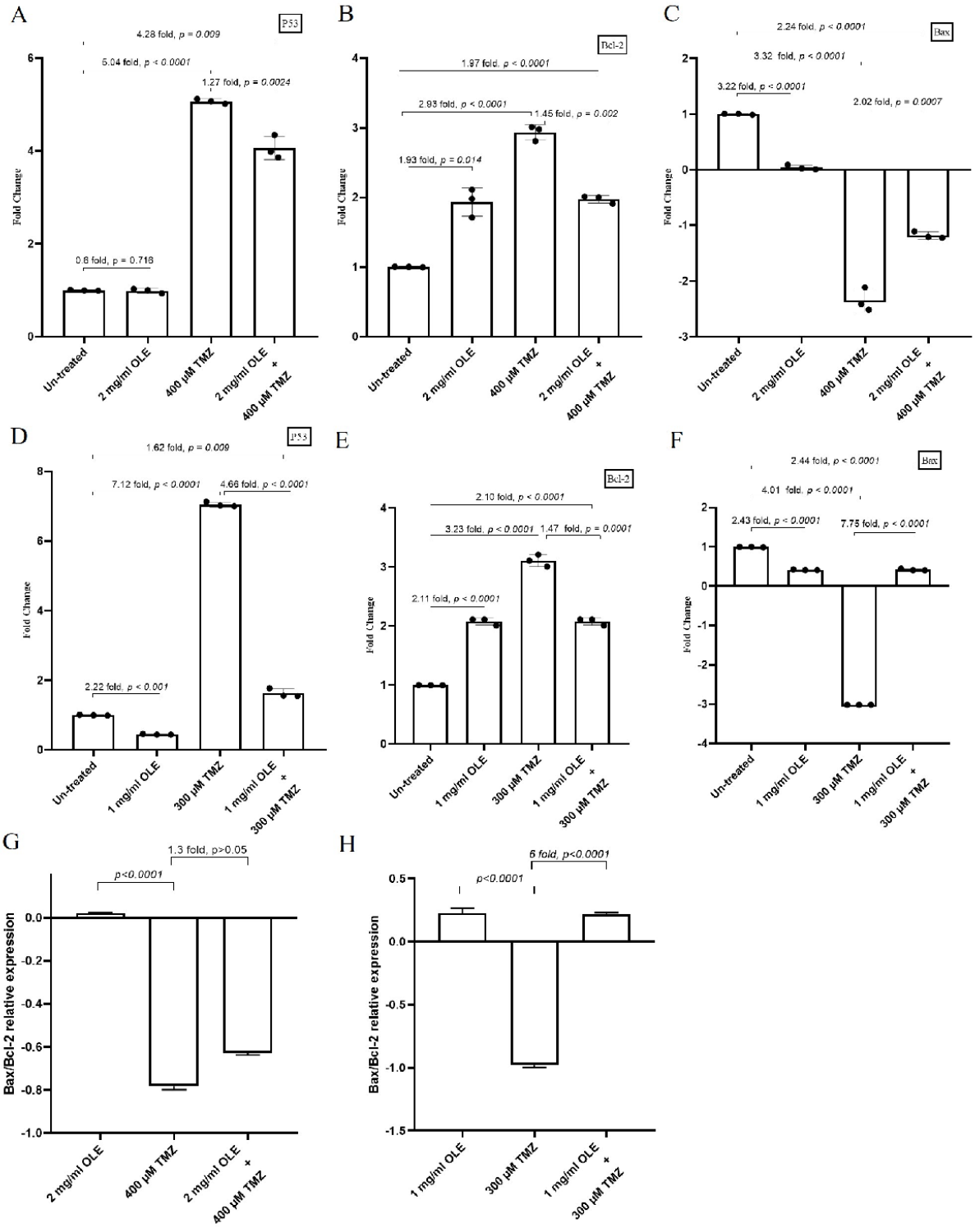

Figure 6. The effect of T98G and U87MG cells treated with OLE, TMZ, and OLE + TMZ on the expression levels of senescence factors and senolytic effect. p53 (A), Bcl-2 (B), Bax (C) expression levels in T98G. p53 (D), Bcl-2 (E), and Bax (F) expression levels in U87MG. Bax/Bcl-2 relative expression of T98G (G) and U87MG (H) cells treated with OLE, TMZ, and OLE + TMZ

OLE: *Olea europaea* leaf extract, TMZ: Temozolomide

ACNOWLEDGMENTS

We thank Prof. Ferah Budak from Bursa Uludağ University, Faculty of Medicine, Immunology Department and Assoc. Prof. Senem Kamiloğlu Beştepe from Bursa Uludağ University, Faculty of Agriculture Department of Food Sciences for their assistance in the experimental process. This work was supported by the Scientific and Technical Research Council of Türkiye (TÜBİTAK) under grant no: 118S799. One of the authors (M.E.) is a 100/2000 The Council of Higher Education Ph. D. Scholars in Molecular Biology and Genetics (Gene Therapy and Genome Studies).

Ethics

Ethics Committee Approval: Not applicable.

Informed Consent: Not applicable.

Peer-review: Externally peer-reviewed.

Authorship Contributions

Concept: M.E., B.T., Design: M.E., B.T., S.A.A., Data Collection or Processing: M.E., B.T., Ç.T., Analysis or Interpretation: M.E., Ç.T., Literature Search: M.E., B.T., S.A.A., Ç.T., G.T., Writing: M.E., B.T.

Conflict of Interest: No conflict of interest was declared by the authors.

Financial Disclosure: The authors declared that this study received no financial support.

REFERENCES

1. Schmitt R. Senotherapy: growing old and staying young? Pflugers Arch. 2017;469:1051-1059.
2. Foster SA, Wong DJ, Barrett MT, Galloway DA. Inactivation of p16 in human mammary epithelial cells by CpG island methylation. Mol Cell Biol. 1998;18:1793-1801.
3. Noda A, Ning Y, Venable SF, Pereira-Smith OM, Smith JR. Cloning of senescent cell-derived inhibitors of DNA synthesis using an expression screen. Exp Cell Res. 1994;211:90-98.
4. Coppé JP, Desprez PY, Krtolica A, Campisi J. The senescence-associated secretory phenotype: the dark side of tumor suppression. Annu Rev Pathol. 2010;5:99-118.
5. Chakrabarty A, Chakraborty S, Bhattacharya R, Chowdhury G. Senescence-induced chemoresistance in triple negative breast cancer and evolution-based treatment strategies. Front Oncol. 2021;11:674354.
6. Altieri P, Murialdo R, Barisione C, Lazzarini E, Garibaldi S, Fabbi P, Ruggeri C, Borile S, Carbone F, Armirotti A, Canepa M, Ballestrero A, Brunelli C, Montecucco F, Ameri P, Spallarossa P. 5-fluorouracil causes endothelial cell senescence: potential protective role of glucagon-like peptide 1. Br J Pharmacol. 2017;174:3713-3726.
7. Song Y, Baba T, Mukaida N. Gemcitabine induces cell senescence in human pancreatic cancer cell lines. Biochem Biophys Res Commun. 2016;477:515-519.
8. Bojko A, Czarnecka-Herok J, Charzynska A, Dabrowski M, Sikora E. Diversity of the senescence phenotype of cancer cells treated with chemotherapeutic agents. Cells. 2019;8:1501.
9. Faheem MM, Seligson ND, Ahmad SM, Rasool RU, Gandhi SG, Bhagat M, Goswami A. Convergence of therapy-induced senescence (TIS) and EMT in multistep carcinogenesis: current opinions and emerging perspectives. Cell Death Discov. 2020;6:51.
10. Villalva C, Cortes U, Wager M, Tourani JM, Rivet P, Marquant C, Martin S, Turhan AG, Karayan-Tapon L. O6-Methylguanine-methyltransferase (MGMT) promoter methylation status in glioma stem-like cells is correlated to temozolomide sensitivity under differentiation-promoting conditions. Int J Mol Sci. 2012;13:6983-6994.
11. Aasland D, Götzinger L, Hauck L, Berte N, Meyer J, Effenberger M, Schneider S, Reuber EE, Roos WP, Tomicic MT, Kaina B, Christmann M. Temozolomide induces senescence and repression of DNA repair pathways in glioblastoma cells *via* activation of ATR-CHK1, p21, and NF-κB. Cancer Res. 2019;79:99-113.
12. Demaria M, O'Leary MN, Chang J, Shao L, Liu S, Alimirah F, Koenig K, Le C, Mitin N, Deal AM, Alston S, Academia EC, Kilmarx S, Valdovinos A, Wang B, de Bruin A, Kennedy BK, Melov S, Zhou D, Sharpless NE, Muss H, Campisi J. Cellular senescence promotes adverse effects of chemotherapy and cancer relapse. Cancer Discov. 2017;7:165-176.
13. Yousefzadeh MJ, Zhu Y, McGowan SJ, Angelini L, Fuhrmann-Stroissnigg H, Xu M, Ling YY, Melos KI, Pirtskhalava T, Inman CL, McGuckian C, Wade EA, Kato JI, Grassi D, Wentworth M, Burd CE, Arriaga EA, Ladiges WL, Tchkonia T, Kirkland JL, Robbins PD, Niedernhofer LJ. Fisetin is a senotherapeutic that extends health and lifespan. EBioMedicine. 2018;36:18-28.
14. Margheri F, Menicacci B, Laurenzana A, Del Rosso M, Fibbi G, Cipolleschi MG, Ruzzolini J, Nediani C, Mocali A, Giovannelli L. Oleuropein aglycone attenuates the pro-angiogenic phenotype of senescent fibroblasts: a functional study in endothelial cells. J Funct Foods. 2019;53:219-226.
15. Katsiki M, Chondrogianni N, Chinou I, Rivett AJ, Gonos ES. The olive constituent oleuropein exhibits proteasome stimulatory properties *in vitro* and confers life span extension of human embryonic fibroblasts. Rejuvenation Res. 2007;10:157-172.
16. Tunca B, Tezcan G, Cecener G, Egeli U, Ak S, Malyer H, Tumen G, Bilir A. *Olea europaea* leaf extract alters microRNA expression in human glioblastoma cells. J Cancer Res Clin Oncol. 2012;138:1831-1844.
17. Tezcan G, Aksoy SA, Tunca B, Bekar A, Mutlu M, Cecener G, Egeli U, Kocaeli H, Demirci H, Taskapilioglu MO. Oleuropein modulates glioblastoma miRNA pattern different from *Olea europaea* leaf extract. Hum Exp Toxicol. 2019;38:1102-1110.
18. Mutlu M, Tunca B, Ak Aksoy S, Tekin C, Egeli U, Cecener G. Inhibitory effects of *Olea europaea* leaf extract on mesenchymal transition mechanism in glioblastoma cells. Nutr Cancer. 2021;73:713-720.
19. Tezcan G, Tunca B, Bekar A, Budak F, Sahin S, Cecener G, Egeli U, Taskapılıoglu MO, Kocaeli H, Tolunay S, Malyer H, Demir C, Tumen G. *Olea europaea* leaf extract improves the treatment response of GBM stem cells by modulating miRNA expression. Am J Cancer Res. 2014;4:572-590.
20. Kamiloglu S. Effect of different freezing methods on the bioaccessibility of strawberry polyphenols. Int J Food Sci Technol. 2019;54:2652–2660.
21. Ianevski A, Giri AK, Aittokallio T. SynergyFinder 2.0: visual analytics of multi-drug combination synergies. Nucleic Acids Res. 2020;48:W488-W493. Erratum in: Nucleic Acids Res. 2022;50:7198.
22. Ciapetti G, Granchi D, Savarino L, Cenni E, Magrini E, Baldini N, Giunti A. *In vitro* testing of the potential for orthopedic bone cements to cause apoptosis of osteoblast-like cells. Biomaterials. 2002;23:617-627.

23. Anasamy T, Abdul AB, Sukari MA. A phenylbutenoid dimer, *cis*-3-(3',4'-dimethoxyphenyl)-4-[(e)-3''',4'''-dimethoxystyryl] cyclohex-1-ene, exhibits apoptogenic properties in T-acute lymphoblastic leukemia cells *via* induction of p53-independent mitochondrial signalling pathway. Evid-Based Complement Alternat Med. 2013;93:9810.

24. Mutlu M, Tunca B, Aksoy SA, Tekin C, Cecener G, Egeli U. *Olea europaea* leaf extract decreases tumour size by affecting the LncRNA expression status in glioblastoma 3D cell cultures. Eur J Integr Med. 2021;45:101345.

25. Fridman JS, Lowe SW. Control of apoptosis by p53. Oncogene. 2003;22:9030-9040.

26. Giordano A, Macaluso M. Fenofibrate triggers apoptosis of glioblastoma cells *in vitro*: new insights for therapy. Cell Cycle. 2012;11:3154.

27. Surova O, Zhivotovsky B. Various modes of cell death induced by DNA damage. Oncogene. 2013;32:3789-3797.

28. Mijit M, Caracciolo V, Melillo A, Amicarelli F, Giordano A. Role of p53 in the regulation of cellular senescence. Biomolecules. 2020;10:420.

29. Vousden KH, Lane DP. p53 in health and disease. Nat Rev Mol Cell Biol. 2007;8:275-283.

30. Childs BG, Baker DJ, Kirkland JL, Campisi J, van Deursen JM. Senescence and apoptosis: dueling or complementary cell fates? EMBO Rep. 2014;15:1139-1153.

31. Tavana O, Benjamin CL, Puebla-Osorio N, Sang M, Ullrich SE, Ananthaswamy HN, Zhu C. Absence of p53-dependent apoptosis leads to UV radiation hypersensitivity, enhanced immunosuppression and cellular senescence. Cell Cycle. 2010;9:3328-3336.

32. Lee SY. Temozolomide resistance in glioblastoma multiforme. Genes Dis. 2016;3:198-210.

33. Sheekey E, Narita M. p53 in senescence - It's a marathon, not a sprint. FEBS J. 2023;290:1212-1220.

34. Nakajima K, Yamanaka Y, Nakae K, Kojima H, Ichiba M, Kiuchi N, Kitaoka T, Fukada T, Hibi M, Hirano T. A central role for Stat3 in IL-6-induced regulation of growth and differentiation in M1 leukemia cells. EMBO J. 1996;15:3651-3658.

35. Ershler WB, Keller ET. Age-associated increased interleukin-6 gene expression, late-life diseases, and frailty. Annu Rev Med. 2000;51:245-270.

36. Soubannier V, Stifani S. NF-κB signalling in glioblastoma. Biomedicines. 2017;5:29.

37. Curran S, Murray GI. Matrix metalloproteinases: molecular aspects of their roles in tumour invasion and metastasis. Eur J Cancer. 2000;36:1621-1630.

38. Kurz DJ, Decary S, Hong Y, Erusalimsky JD. Senescence-associated (beta)-galactosidase reflects an increase in lysosomal mass during replicative ageing of human endothelial cells. J Cell Sci. 2000;113:3613-3622.

39. Tezcan G, Tunca B, Demirci H, Bekar A, Taskapilioglu MO, Kocaeli H, Egeli U, Cecener G, Tolunay S, Vatan O. *Olea europaea* leaf extract improves the efficacy of temozolomide therapy by inducing MGMT methylation and reducing P53 expression in glioblastoma. Nutr Cancer. 2017;69:873-880.

40. Yang L, Fang J, Chen J. Tumor cell senescence response produces aggressive variants. Cell Death Discov. 2017;3:17049.

Turk J Pharm Sci 2023;20(2):78-83
DOI: 10.4274/tjps.galenos.2022.00334

ORIGINAL ARTICLE

Thermosensitive *In situ* Gelling System for Dermal Drug Delivery of Rutin

Sefa GÖZCÜ[1]*, Kerem Heybet POLAT[2]

[1]Erzincan Binali Yıldırım University, Faculty of Pharmacy, Department of Pharmacognosy, Erzincan, Türkiye
[2]Erzincan Binali Yıldırım University, Faculty of Pharmacy, Department of Pharmaceutical Technology, Erzincan, Türkiye

ABSTRACT

Objectives: Rutin has been broadly applied for treating several diseases due to its pharmacological activities. However, its low aqueous solubility limits its absorption and bioavailability. This research aims to increase the solubility of rutin using cyclodextrin and to develop a temperature-triggered *in situ* gelling system for dermal application.

Materials and Methods: The solubility of rutin was increased with sulfobutyl ether-β-cyclodextrin (SBE-β-CD). Rutin- SBE-β-CD inclusion complex was prepared by kneading and freeze dying method. Structural characterization was carried out using differential scanning calorimetry and fourier transform infrared spectroscopy. *In situ* gel formulations were prepared with pluronic F127 (PF127), a thermosensitive polymer, and chitosan (CH), a natural, biodegradable, and mucoadhesive hydrophilic polymer. *In situ* gel characteristics such as pH, clarity, gelation temperature, and viscosity were determined.

Results: When the solubility diagrams were examined, it was concluded that SBE-β-CD showed a linear increase, therefore, AL-type diagram was selected. The formulations were produced using different amounts of PF127 and a fixed ratio of CH. Three *in situ* gels were evaluated for their pH, gelling temperature, and the rheological behaviors, and one formulation was selected. It was observed that the formulations had a pH between 6-6.1, and their gelation temperature decreased with increasing PF127 that was between 20˚C to 34˚C. For the selected formulation (formulation E3), 0.5% rutin and rutin/SBE-β-CD were transferred to the *in situ* gelling system. Because of *in vitro* release studies, it was observed that the release of the rutin/SBE-β-CD inclusion complex containing NZ formulation showed a higher burst effect than the others and the release continued for 6 hours.

Conclusion: The results indicated that the combination of PF127 and CH can be a hopeful *in situ* gelling vehicle for dermal delivery of rutin and rutin/SBE-β-CD.

Key words: Rutin, *in situ* gel, dermal drug delivery systems, SBE-β-cyclodextrin, pluronic

INTRODUCTION

Flavonoids are secondary metabolites with phenolic structures found in many plants. According to their molecular structures, flavonoids are divided into varieties such as flavones, flavonols, isoflavones, neoflavonoids, flavans, flavanones, flavanonols, anthocyanidins, aurones, and chalcones. Flavonoids have many pharmacological activities, such as anticancer, anti-inflammatory, antioxidant, hypoglycemic, diuretic, and hepatoprotective.[1]

Rutin (quercetin-3-*O*-rutinoside) is in the form of flavonol glycoside, and is also known as vitamin P, and has a structure of 5,7,3',4'-tetrahydroxyflavone-3-rhamnoglucoside.[2-4] Rutin and other flavonoids have high antioxidant properties observed in *in vivo* and *in vitro* studies.[3,5-7] Furthermore, rutin is a non-toxic and non-oxidizing molecule, and it is not a pro-oxidant like myricetin and quercetin.[2,8] Rutin with different biological activities such as anti-inflammatory is used for treating various diseases.[3]

Recently, "*in situ* gel" as a newly developed drug delivery, extensively used in the drug delivery system area. Specific polymers that undergo sol-gel phase transition by induction of ambient conditions such as pH,[4] specific ions,[5] and temperature[6] are used in the preparation of *in situ* gels. *In situ* gel formulations are solutions or suspensions that become gels after application and thus are more acceptable to patients.[7] Studies have demonstrated that dermal contact times of some *in situ* gel

*Correspondence: sgozcu@erzincan.edu.tr, Phone: +90 446 224 53 44, ORCID-ID: orcid.org/0000-0002-0735-4229
Received: 18.01.2022, Accepted: 29.04.2022

©Copyright 2023 by Turkish Pharmacists' Association / Turkish Journal of Pharmaceutical Sciences published by Galenos Publishing House.
Licenced by Creative Commons Attribution-NonCommercial-NoDerivatives 4.0 (CC BY-NC-ND)

systems can be up to several hours and different polymer or polymeric combinations have been used successfully to adjust the desired release profile.[9]

Pluronic (poloxamer) with thermoresponsive structure widely used *in situ* gel system. These polymers exhibit amphiphilic behavior because of the hydrophilic ethylene oxide and hydrophobic propylene oxide areas. The gelation of poloxamers can be described by the observed changes in the micellar structure depending on temperature and concentration. Poloxamers with sustained drug release capability have been extensively used as drug delivery systems. On the other hand, an essential handicap of poloxamers is insufficient mucoadhesive activity, thus, some poloxamer-based drug delivery formulations have been ameliorated by the addition of polymers providing mucoadhesive properties such as, sodium hyaluronate, chitosan (CH), and carbopol.[10] CH exhibits good properties for dermal application since it is a cationic, biocompatible, and biodegradable polysaccharide. In addition, CH has mucosal adhesion properties and good antibacterial activity.[11]

Cyclodextrins (CD) are generally preferred to increase the water solubility of drugs with low water solubility and low dermal permeability. It has been determined that rutin-CD inclusion complexes are formed using different CD derivatives; nevertheless, there is no *in situ* gel formulation containing rutin/sulfobutyl ether-β-cyclodextrin (SBE-β-CD) inclusion complexes. When the literature was examined, it was determined that SBE-β-CD has higher complexation efficiency (EC) and higher solubility capacity than other β-CD derivatives.[12,13] Thus, it is preferred to develop drug delivery systems to increase permeability and drug solubility and accordingly enhance bioavailability in consequence.[14] It provides positive therapeutic effects and unimportant side effects. Therefore, it is a desirable selection for formulations of drugs with low solubilities.

The main objective of the current research is to increase the solubility of rutin with CD and placing the resulting complex in the *in situ* gel. Therefore, SBE-β-CAD was used for this purpose. *In situ* gels containing different ratios of pluronic F-127 (PF 127) (15% - 20% - 25%) with constant concentration of CH were prepared. Additionally, developed gel formulations were evaluated in terms of clarity, pH, gelation temperature, and viscosity, and an optimum formulation was selected. For the selected formulation, 0.5% rutin and 0.5% SBE-β-CD-rutin inclusion complex were added to *in situ* gelling systems and rutin release was assessed using *in situ* gel systems designed for dermal delivery.

MATERIALS AND METHODS

Materials

Rutin, PF 127, CH (low molecular weight), SBE-β-CD, phosphate buffered saline tablets, and high performance liquid chromatography (HPLC) grade acetonitrile, and methanol were purchased from Sigma, Steinheim, Germany.

Production of cyclodextrin-drug complex

Cyclodextrin-drug phase-solubility studies

Lofton and Brewster's technique[15] was used to conduct phase-solubility studies.

Increasing concentrations (0-10 mM) of SBE-β-CD solution were added into a fixed amount of rutin. The resulting mixture was stirred at room temperature for 7 days with a magnetic stirrer. A 0.22 µm membrane filter was used to filter each sample. The concentration of rutin in the supernatant was determined by an HPLC method. HPLC (Thermo Scientific, USA) analysis was carried out with a C-18 column (250 mm x 4.6 mm, 5 µm) at a 1 mL/min flow rate and a mobile phase made up from water:methanol:acetonitrile with a 50:25:25 (v/v/v) ratio. Detection wavelength for rutin was 280 nm and the injection volume of the sample was 10 µL, while the column temperature was held constant at 25°C. There were 3 sets of experiments (n: 3). The phase-solubility diagram was depicted by presenting SBE-β-CD concentration against the dissolved rutin amount.[16]

Moreover, Higuchi and Connors classification,[17] that comprises AP, AL, AN, BS, and BI diagram models, was used to determine the type of diagram obtained. The equations described below were used to estimate the complex stability constant (KS) (equation 1) and EC (equation 2).[15]

Equation 1:

$$\text{Complex stability constant} = \frac{Slope}{S0(1-slope)}$$

Intrinsic rutin solubility is shown as S, which is 0.38 mM, and the linear regression's slope of the phase-solubility diagram is presented as slope.

Equation 2:

$$\text{Complexation efficacy} = \frac{Slope}{(1-Slope)}$$

Production of cyclodextrin-drug complex

The complexes were produced by kneading and freeze-drying. Thus, the efficiency of the preparation method on complexing was evaluated.[18]

Kneading

Equimolar (EqM) amounts of rutin and SBE-β-CD were used. CD and rutin were mixed with ethanol/water (3:1 v/v) in a mortar and kneaded for 45 min. The resultant mass was stored at room temperature overnight and then dried, afterwards, the solvent was removed under reduced pressure (hot air oven, Nuve, FN 055/120, Holland) at 25 ± 1°C.

Freeze drying

Freeze-drying is another method used to prepare CD-drug complexes.[19] In short, SBE-β-CD was dissolved in water and rutin was dissolved in ethanol (EqM rate, 1:1). Then, rutin solution was transferred dropwise to the SBE-β-CD solution and mixed with a magnetic stirrer for 24 hours. Ethanol was removed

by an evaporator and the product was lyophilized. Successful preparation of the inclusion complex was determined by differential scanning calorimetry (DSC) and fourier transform infrared spectroscopy (FTIR).

Production of in situ gel

A modified cold approach was used to produce *in situ* gelling formulations.[20] PF 127 solutions (15, 20, and 25% w/v) were prepared by dissolving the polymer in water (at 4˚C) and a 6 phosphate buffer (at 4˚C). Solutions were stored in a fridge for at least 24 h to achieve thorough dissolution. Gelling system PF 127 was contained a CH solution (1% w/v) as a mucoadhesive substance. All the samples were kept at a constant 4˚C until usage. The contents of generated *in situ* gelling formulations were demonstrated in Table 1.

Characterization of in situ gel formulations

Different concentrations of PF 127 were evaluated for gelation temperature, viscosity, and pH to determine the suitability of the formulations for use as *in situ* gelling systems (Table 2).

pH

pH measurements were made with a pH Meter (Mettler Toledo) at 25˚C, and each measurement was performed in triplicate.

Gelation temperature

The cold sample solution (10 mL) was heated at 2˚C/min while mixed at 100 rpm on a magnetic stirrer (Thermomac-TM19). The temperature at which the magnetic stirring bar stopped moving was determined as the gelling temperature. Each measurement was performed thrice.

Rheological studies

The viscosity of *in situ* gels was measured using a Brookfield, DV2T-RV Viscometer (Essex, UK) with a CP 52 spindle at 10 rpm. The experiment was performed in triplicate.

Production of rutin-loaded in situ gelling systems

Rutin and rutin-SBE inclusion complex were added to the selected *in situ* gelling formulations, considering the pH, gelation temperatures, and viscosities of all formulations. These formulations were named as SV and NZ, respectively. According to the earlier research findings, rutin has an anti-inflammatory effect when used at 500 mg. Therefore, the drug concentration in our formulations was also selected to be as 0.5%. Rutin is combined with pre-optimized but freshly prepared *in situ* gelling systems. The formulations containing rutin registered in the literature and their physical structures are given in Table 3.

In vitro release studies

The dialysis bag approach was used to undertake *in vitro* release tests with the *in situ* gel formulations.[21,22] The dialysis bags were filled with 100 µL formulations stored at 4˚C, then 25 mL of pH 7.4 isotonic phosphate buffer at 37˚C was used to immerse the dialysis bags, which had been hermetically sealed. In this way, the sink condition is provided. Each time an aliquot of the medium was withdrawn (at 15, 30, 60, 90, 180, 240, and 360 min), equivalent quantities of fresh buffer media were added to replace the withdrawn samples, and the sampling was repeated. HPLC was used to assess drug concentrations in the withdrawn isotonic phosphate buffer solutions at a pH of 7.4. The rutin release profile was depicted according to the total quantity of the drug released from each formulation over time. Each measurement was repeated three times.

RESULTS AND DISCUSSION

Stability of cyclodextrin-drug complex

Phase-solubility studies are usually the preferred method for the determination of the efficacy of CD drug complexation on drug solubility.[15] CD/drug (1:1) inclusion complex is the most extensive type of association, where one drug molecule is incorporated into the cavity of a CD molecule, with a KS K1:1 for the equilibrium between free and associated species. When the solubility diagrams were examined, it was determined that SBE-β-CD concentration and solubility of the drug showed a linear increase (Figure 1). According to the phase-solubility diagram, it was decided to classify the SBE-β-CD diagram as "AL-type".

Table 1. Components of *in situ* gelling formulation

Formulation components	E1	E2	E3
PF 127 (%w/v)	25	20	15
CH (1% w/v) mL	10	10	10
Water *q.s.* to mL	100	100	100

PF 127: Pluronic F127, CH: Chitosan

Table 2. Characterization of *in situ* gel formulations

Formulation	pH (± SD)	Gelation temperature (˚C ± SD)	Viscosity (Pa.s) 25˚C
E1	6.0 ± 0.01	20 ± 1.7	168
E2	6.1 ± 0.01	25 ± 1.6	109
E3	6.1 ± 0.01	34 ± 1.1	42

(n: 3), SD: Standard deviation

Table 3. Physical properties of drug-containing formulations and their component

Formulation ingredients and physical properties	SV	NZ
Rutin (% w/v)	0.5	-
Rutin-SBE cyclodextrin (% w/v)	-	0.5
PF 127	15	15
CH (%1 w/v)	10	10
pH (± SD)	6.0 ± 0.01	6.1 ± 0.02
Gelation temperature (˚C ± SD)	34 ± 0.9	34 ± 1.3
Viscosity (Pa.s) 25˚C	42 ± 1.3	41 ± 1.7
Viscosity (Pa.s) 35˚C	159.8 ± 3.4	160.7 ± 3.8

(n: 3), PF 127: Pluronic F127, CH: Chitosan, SD: Standard deviation, SBE: Sulfobutyl ether

By examining the straight line of SBE-β-CD (r^2: 0.9196) (Figure 1), the slope was calculated as 0.5911.

EC and KS were calculated as 0.36 and 9590 M^{-1}, respectively. When the literature data is examined, the KSs reported were found between 100 and 10.000 M^{-1} as the ideal value for formation of the drug:CD complex. However, with AL type solubility curve determined by examining the diagram, the drug:CD complex ratio was decided to be 1 mM:1 mM.[23]

DSC results of rutin, SBE-β-CD, physical mixture (rutin Phy), inclusion complex produced by kneading method (rutin-Knd), and inclusion complex produced by the freeze dying method (rutin-Fdy) are shown in Figure 2. The thermogram of rutin indicates two endothermic peaks at 138°C and 215°C. However, these values were found to be compatible with the literature.[24] When rutin-Phy and rutin-Knd were examined, it was seen that the specific peak of rutin does not disappear in these samples, but the specific peak disappears in the rutin-Fdy sample.[24]

When rutin FTIR result was examined, maximum peak was seen at 3277 cm^{-1}, which was due to the hydrogen bond formed by -OH groups. The band seen at 1654 cm^{-1}, belonged to the stretching vibration of C=O. The bands at 1601 and 1505 cm^{-1} can be assigned to the aromatic ring vibrations of C=C. The stretching vibration of 3'-OH and 4'-OH appeared at 1456 cm^{-1}. However, these values were found to be compatible with the literature.[24] When rutin-Phy and rutin-Knd spectrums were examined, it was seen that the specific peaks of rutin did not disappear; however, when rutin-fyd spectrum was examined, the specific peaks of rutin was seen to disappear (Figure 3). Also, the peaks of SBE-β-CD were preserved, indicating the successful formation of the SBE-β-CD-rutin complex.

Gelation temperature

When the *in situ* gel formulations were examined, the gelation temperatures of E1 and E2 at 20°C and 25°C, respectively, were found to be low, and the gelation temperature increased with the decrease of PF 127 concentration by 15%. The gelation temperature of the E3 formulation was 34°C. In an aqueous environment, different molecules are formed in pluronics at temperatures below the critical micelle temperature (CMT), at which the critical micelle concentration occurs. Additionally, above CMT, all individual molecules are forced to form micelles, which surround the hydrophobic core by hydrophilic chains of pluronic facing the aqueous medium. CMT values are inversely proportional to the pluronic concentration.[22] This inverse ratio affects the gelling temperature as the gelling temperature is highly dependent on the concentration of pluronics. While they form monomolecular micelles at lower concentration, a multimolecular lattice structure is observed at higher concentration.[23] Due to this temperature phenomenon, it was tried bringing the gelling temperature closer to the skin temperature in the experimental formulations. Therefore, PF 127 concentrations were reduced. In the E1-E3 formulations, PF127 concentrations were decreased to increase the gelation temperature. Similar findings were observed in other studies.[25]

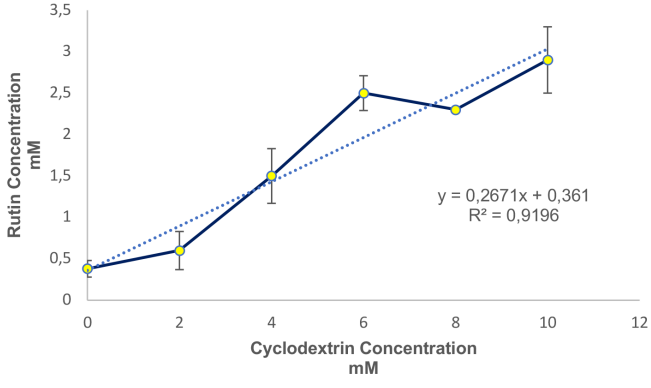

Figure 1. Phase-solubility diagram of rutin at the increasing SBE-β-CD concentration

SBE-β-CD: Sulfobutyl ether-β-cyclodextrin

pH

pH is a significant parameter in dermal formulations. Physiological pH in healthy skin and 5.5 on average. The pH of dermal carriers is a significant parameter as the change in pH of the skin will cause unwanted effects such as rash and itchiness.[21] pH of all formulations were between 6.0-6.1 as presented in Table 2.

Since CH (aq) is obtained by dispersing it in a sufficient amount of acetic acid (aq) (1% w/v), the pH of the formulations containing CH was determined as 6.0-6.1. This result supports the data we found in the literature review.[26]

Viscosity

Viscosity of the gels was increased (from 38 to 165 Pa.s at 20°C) by increasing the concentration of PF 127 (from 15% to 25%). It indicated that PF 127 concentration extremely affects the viscosity of the gels. After characterization, the optimum formulation was selected in terms of pH value, gelation temperature, and viscosity. The optimized formulation contained

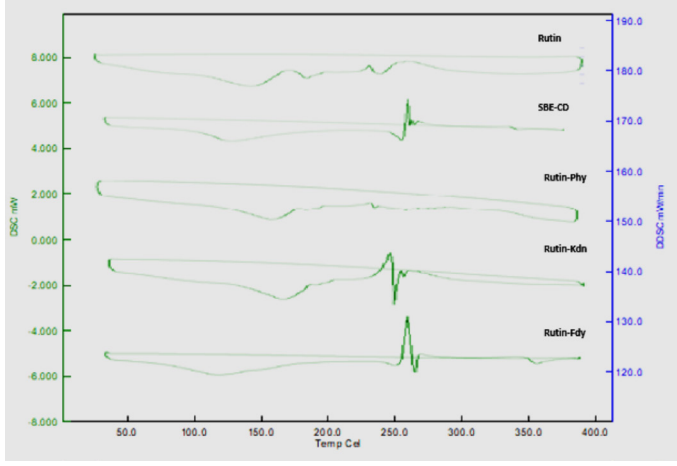

Figure 2. DSC thermogram of rutin, SBE-β-CD, rutin-Phy, rutin-Knd and rutin-Fdy

SBE-β-CD: Sulfobutyl ether-β-cyclodextrin, DSC: Differential scanning calorimetry

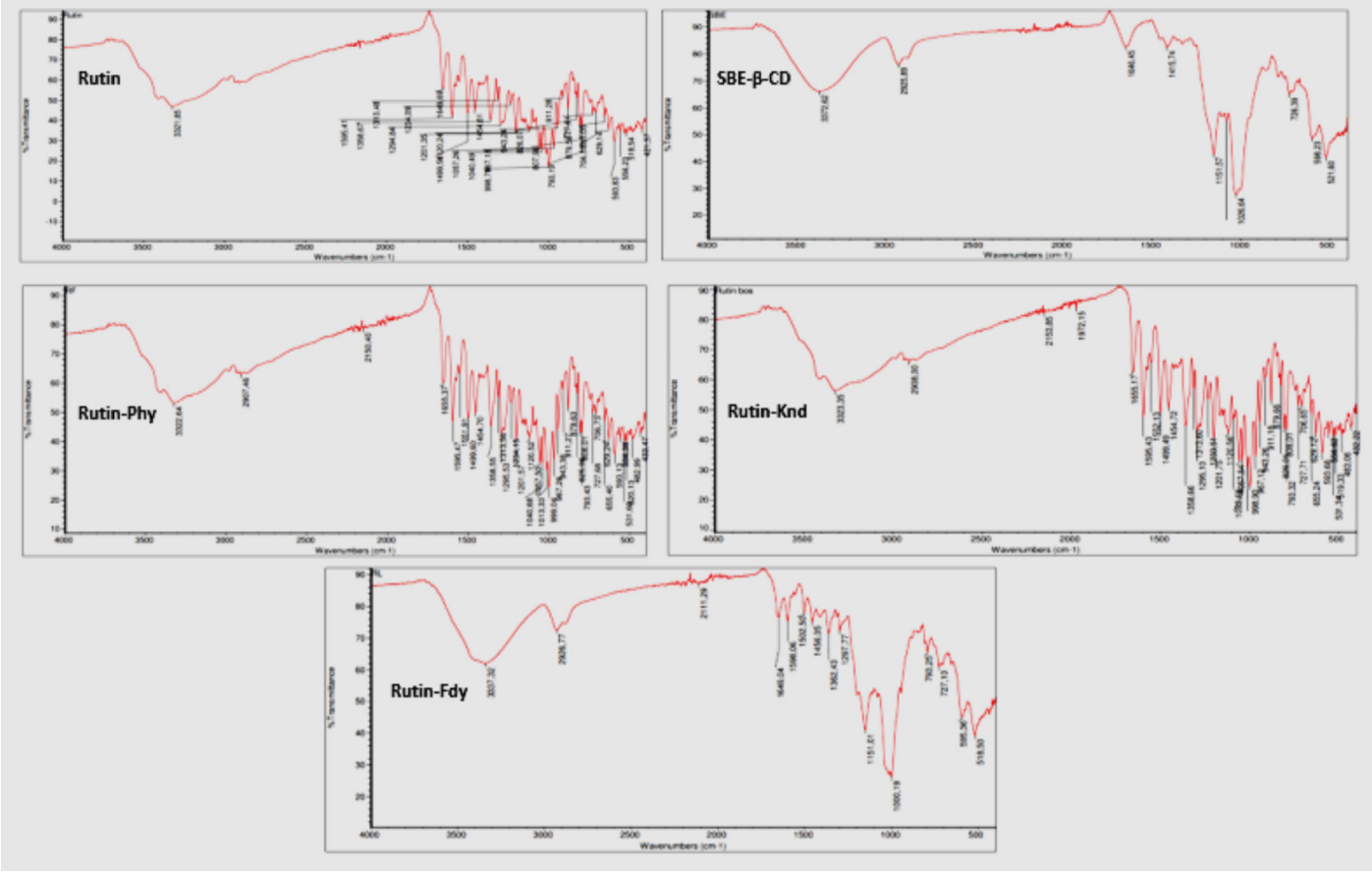

Figure 3. FTIR spectra of ruitn, SBE-β-CD, rutin-Phy, rutin-Knd and rutin-Fdy
SBE-β-CD: Sulfobutyl ether-β-cyclodextrin, FTIR: Fourier transform infrared spectroscopy

rutin (0.5% w/v), rutin-SBE-β-CD inclusion complex (0.5% w/v) in the *in situ* gelling formulations, chosen to be suitable.

These formulations are shown in Table 3 as SV and NZ. pH of the formulations was between 5.9 and 6.0 with gelling temperatures at 34˚C. Also, release of the in the NZ formulations, during the first two hours, 57% of the drug was released and the release was continued up to 77% by the end of three hours and it may be due to the concentration of PF 127 and CH. Whereas SV formulations showed <57% drug release after two hours (Figure 4). This could be due to the usage of CDs in the NZ formulation by the investigation of *in vitro* release studies results, it was found that the BRN formulation exhibits faster drug release than NI formulation. This was due to Rut-SBE-CD inclusion complex in the BRN formulation. It is believed that the CD complex caused increasing solubility of the drug. An identical result was obtained in another study, which was conducted by Polat et al.[27] They produced insert formulations containing besifloxacin HCL and besifloxacin HCl-CD inclusion complex. The results indicated that the release rate of the insert formulation containing the complex was higher than the formulation containing only the drug.[27]

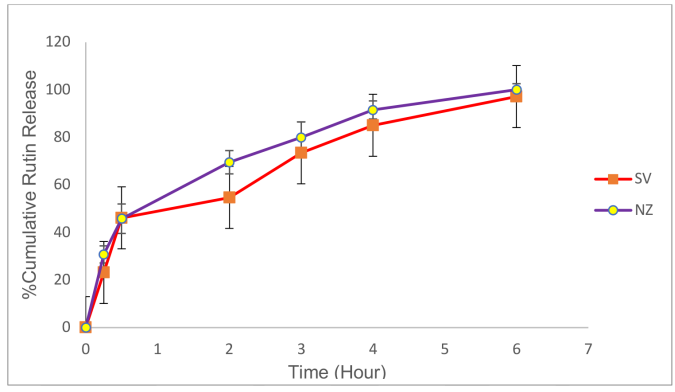

Figure 4. *In vitro* release profiles of *in situ* gel formulation

CONCLUSION

In this study, SBE-β-CD was used. SBE-β-CD was found to increase the solubility of rutin by 8 times. Inclusion complexes of drug-SBE-β-CD were produced with different methods. Due to DSC and FTIR studies, it was determined that the production was successfully carried out *via* the freeze-drying method. Furthermore, it has been determined that the prepared *in situ* gels have the optimum gelling temperature, gelling

capacity, appropriate pH point, and desired properties such as great appearance. The formulations were observed to have pseudoplastic behavior, pH: 6, and gelation temperatures between 22˚C and 34˚C. *In vitro* release studies have revealed that rutin both increases in solubility and dissolves over a longer period of 6 h. Rutin is a common anti-inflammatory natural compound effective against many diseases. The selected formulations contained 0.5% w/v. The *in situ* gel contact time with the skin is prolonged and it could provide drug release for a longer time.

Ethics

Ethics Committee Approval: Not applicable.

Informed Consent: Not applicable.

Peer-review: Externally peer-reviewed.

Authorship Contributions

Surgical and Medical Practices: S.G., K.H.P., Concept: S.G., K.H.P., Design: S.G., K.H.P., Data Collection or Processing: S.G., K.H.P., Analysis or Interpretation: S.G., K.H.P., Literature Search: S.G., K.H.P., Writing: S.G., K.H.P.

Conflict of Interest: No conflict of interest was declared by the authors.

Financial Disclosure: The authors declared that this study received no financial support.

REFERENCES

1. Nijveldt RJ, van Nood E, van Hoorn DE, Boelens PG, van Norren K, van Leeuwen PA. Flavonoids: a review of probable mechanisms of action and potential applications. Am J Clin Nutr. 2001;74:418-425.
2. Chat OA, Najar MH, Mir MA, Rather GM, Dar AA. Effects of surfactant micelles on solubilization and DPPH radical scavenging activity of rutin. J Colloid Interface Sci. 2011;355:140-149.
3. Kazłowska K, Hsu T, Hou CC, Yang WC, Tsai GJ. Anti-inflammatory properties of phenolic compounds and crude extract from *Porphyra dentata*. J Ethnopharmacol. 2010;128:123-130.
4. Srividya B, Cardoza RM, Amin PD. Sustained ophthalmic delivery of ofloxacin from a pH triggered *in situ* gelling system. J Control Release. 2001;73:205-211.
5. Liu Z, Li J, Nie S, Liu H, Ding P, Pan W. Study of an alginate/HPMC-based *in situ* gelling ophthalmic delivery system for gatifloxacin. Int J Pharm. 2006;315:12-17.
6. Polat HK. *In situ* gels triggered by temperature for ocular delivery of dexamethasone and dexamethasone/SBE-β-CD complex. J Res Pharm. 2022;26:873-883.
7. Almeida H, Amaral MH, Lobão P, Lobo JM. *In situ* gelling systems: a strategy to improve the bioavailability of ophthalmic pharmaceutical formulations. Drug Discov Today. 2014;19:400-412.
8. Almeida JS, Lima F, Ros SD, Bulhões LO, de Carvalho LM, Beck RC. Nanostructured systems containing rutin: *in vitro* antioxidant activity and photostability studies. Nanoscale Res Lett. 2010;5:1603-1610.
9. Verma A, Tiwari A, Saraf S, Panda PK, Jain A, Jain SK. Emerging potential of niosomes in ocular delivery. Expert Opin Drug Deliv. 2021;18:55-71.
10. Dumortier G, Grossiord JL, Agnely F, Chaumeil JC. A review of poloxamer 407 pharmaceutical and pharmacological characteristics. Pharm Res. 2006;23:2709-2728.
11. Muxika A, Etxabide A, Uranga J, Guerrero P, de la Caba K. Chitosan as a bioactive polymer: processing, properties and applications. Int J Biol Macromol. 2017;105:1358-1368.
12. Aiassa V, Zoppi A, Becerra MC, Albesa I, Longhi MR. Enhanced inhibition of bacterial biofilm formation and reduced leukocyte toxicity by chloramphenicol:β-cyclodextrin:*N*-acetylcysteine complex. Carbohydr Polym. 2016;152:672-678.
13. Jithan AV, Mohan CK, Vimaladevi M. Development and evaluation of a chloramphenicol hypertonic ophthalmic solution. Indian J Pharm Sci. 2008;70:66-70.
14. Zuorro A, Fidaleo M, Lavecchia R. Solubility enhancement and antibacterial activity of chloramphenicol included in modified β-cyclodextrins. Bull Korean Chem Soc. 2010; 31:3460-3462.
15. Loftsson T, Brewster ME. Pharmaceutical applications of cyclodextrins: basic science and product development. J Pharm Pharmacol. 2010;62:1607-1621.
16. Williams HD, Trevaskis NL, Charman SA, Shanker RM, Charman WN, Pouton CW, Porter CJ. Strategies to address low drug solubility in discovery and development. Pharmacol Rev. 2013;65:315-499.
17. Higuchi T. A phase solubility technique. Adv Anal Chem Instrum. 1965;4:117-211.
18. Ribeiro A, Figueiras A, Santos D, Veiga F. Preparation and solid-state characterization of inclusion complexes formed between miconazole and methyl-beta-cyclodextrin. AAPS PharmSciTech. 2008;9:1102-1109.
19. Covre JL, Cristovam PC, Loureiro RR, Hazarbassanov RM, Campos M, Sato ÉH, Gomes JÁ. The effects of riboflavin and ultraviolet light on keratocytes cultured *in vitro*. Arq Bras Oftalmol. 2016;79:180-185.
20. El-Kamel AH. *In vitro* and *in vivo* evaluation of Pluronic F127-based ocular delivery system for timolol maleate. Int J Pharm. 2002;241:47-55.
21. Polat HK, Kurt N, Aytekin E, Akdağ Çaylı Y, Bozdağ Pehlivan S, Çalış S. Design of besifloxacin HCl-loaded nanostructured lipid carriers: *in vitro* and *ex vivo* evaluation. J Ocul Pharmacol Ther. 2022;38:412-423.
22. Aytekin E, Öztürk N, Vural İ, Polat HK, Çakmak HB, Çalış S, Pehlivan SB. Design of ocular drug delivery platforms and *in vitro - in vivo* evaluation of riboflavin to the cornea by non-interventional (epi-on) technique for keratoconus treatment. J Control Release. 2020;324:238-249.
23. Escobar-Chávez JJ, López-Cervantes M, Naïk A, Kalia YN, Quintanar-Guerrero D, Ganem-Quintanar A. Applications of thermo-reversible pluronic F-127 gels in pharmaceutical formulations. J Pharm Pharm Sci. 2006;9:339-358.
24. 24. Paczkowska M, Mizera M, Piotrowska H, Szymanowska-Powałowska D, Lewandowska K, Goscianska J, Pietrzak R, Bednarski W, Majka Z, Cielecka-Piontek J. Complex of rutin with β-cyclodextrin as potential delivery system. PLoS One. 2015;10:e0120858.
25. Edsman K, Carlfors J, Petersson R. Rheological evaluation of poloxamer as an *in situ* gel for ophthalmic use. Eur J Pharm Sci. 1998;6:105-112.
26. Pawar P, Kashyap H, Malhotra S, Sindhu R. Hp-β-CD-voriconazole *in situ* gelling system for ocular drug delivery: *in vitro*, stability, and antifungal activities assessment. Biomed Res Int. 2013;2013:341218.
27. Polat HK, Bozdağ Pehlivan S, Özkul C, Çalamak S, Öztürk N, Aytekin E, Fırat A, Ulubayram K, Kocabeyoğlu S, İrkeç M, Çalış S. Development of besifloxacin HCl loaded nanofibrous ocular inserts for the treatment of bacterial keratitis: *In vitro*, *ex vivo* and *in vivo* evaluation. Int J Pharm. 2020;585:119552.

Turk J Pharm Sci 2023;20(2):84-90
DOI: 10.4274/tjps.galenos.2022.07277

ORIGINAL ARTICLE

Development and Evaluation of a Turkish Scale to Assess Medication Literacy for Adults

Ozgenur TORUN[1], İlkay MEMİÇ[1], Pınar AY[2], Mesut SANCAR[1], Aysu SELCUK[3], Ecehan BALTA[4], Vildan OZCAN[4], Betul OKUYAN[1]*

[1]Marmara University, Faculty of Pharmacy, Department of Clinical Pharmacy, İstanbul, Türkiye
[2]Marmara University, Faculty of Medicine, Department of Public Health, İstanbul, Türkiye
[3]Ankara University, Faculty of Pharmacy, Department of Clinical Pharmacy, Ankara, Türkiye
[4]Turkish Pharmacists' Association, Ankara, Türkiye

ABSTRACT

Objectives: This study aimed to develop a Turkish scale to assess medication literacy and to evaluate its psychometric properties among adults having at least 12 years of education in Türkiye.

Materials and Methods: After the composition of a preliminary set of items, the content validity of the scale was assessed by an e-Delphi process and a pilot study. The psychometric properties of the scale were evaluated in 358 participants, who had above 12 years of education: university students, academics and, administrative staff from two faculties (pharmacy and law) in two universities located in two major cities (İstanbul and Ankara) in Türkiye between March and May, 2021. The test-retest validity was assessed by Spearman's rho and Wilcoxon test. Internal consistency was evaluated by Kuder Richardson 20. Principal component analysis was conducted.

Results: The last version of the medication literacy scale consisted of 8 items. There was a positive correlation (Spearman's rho: 0.570; $p<0.01$) and no significant difference ($p=0.308$) between the scores of the scale at baseline and after a two-week interval. Kuder Richardson 20 coefficient was 0.659. Students and graduates of health sciences and participants with high reading ability of health-related information had significantly higher scores on the medication literacy scale ($p<0.001$).

Conclusion: Turkish version of the Medication Literacy Scale for Adults is a valid tool for evaluate medication literacy among adults, who have above 12 years of education in Türkiye. The generalizability of our findings should be evaluated with caution since this study was conducted in a sample with a significant representation from healthcare professionals. It would be useful to conduct further studies evaluating the psychometric properties of this scale in participants with diverse characteristics.

Key words: Medication literacy, scale, clinical pharmacy, validation, measure, health literacy

INTRODUCTION

Medication literacy is defined as "the degree to which individuals can obtain, comprehend, communicate, calculate, and process patient-specific information about their medications to make informed medication and health decisions in order to safely and effectively use their medications, regardless of the mode by which the content is delivered (*e.g.*, written, oral, and visual)".[1]

Medication literacy is essential for enabling individuals to safely use unprescribed medications, herbal products, and dietary supplements in addition to the prescribed medications.[2] Individuals with poor medication literacy could improperly manage their medications, leading to medication-related problems, including medication adherence.[3] Promoting individuals' capability toward rationale medication use is crucial to avoiding potential medication-related problems.

A medication literacy scale, which is designed to evaluate the counseling and educational needs of healthy individuals in primary care (such as community pharmacies) and clinical settings, should be valid and reliable as well as not time-consuming and easily applicable. Worldwide, there are only a few specific tools or scales for measuring medication literacy.[4,5] The Recognition and Addressing of Limited Pharmaceutical

*Correspondence: betulokuyan@yahoo.com, Phone: +90 533 330 03 53, ORCID-ID: orcid.org/0000-0002-4023-2565
Received: 24.03.2022, Accepted: 05.05.2022

©Copyright 2023 by Turkish Pharmacists' Association / Turkish Journal of Pharmaceutical Sciences published by Galenos Publishing House.
Licenced by Creative Commons Attribution-NonCommercial-NoDerivatives 4.0 (CC BY-NC-ND)

Literacy (RALPH), developed by Vervloet et al.[6], is an interview guide for pharmacists in identifying the individuals with limited medication literacy implicitly. RALPH interview guide determines medication literacy by asking questions about the medications used by the patient. However, this scale is not applicable to healthy individuals, who do not use medication regularly.[7] There are also scales that are constructed based on vignette scenarios and medication leaflets and instructions.[2,8-10] Vignette-based questions with instructions assess individuals' understanding and interpretation of medication information. However, vignette-based scales are mostly composed of questions specific to the health system of the country, where the scale had been developed,[2,8] so, they are not suitable for cultural adaption.

In Türkiye, more than half of the adults have inadequate or limited health literacy levels. This problem is clear also among participants who are university graduates and/or who have a higher educational level (https://sggm.saglik.gov.tr/Eklenti/39699/0/soya-rapor-1pdf.pdf) Accessed date: 1 April 2022. Still, there is currently no Turkish scale to evaluate individuals' medication literacy levels.

This study aimed to develop a scale of medication literacy in Turkish [Medication Literacy Scale for Adults (MELSA-TR)] and evaluate its psychometric properties among adults having at least 12 years of education (including Turkish university students, academics, and administrative staff) in Türkiye.

MATERIALS AND METHODS

Ethical approval

Ethical approval for this study was received from Marmara University, Institute of Health Science Ethical Board Committee, İstanbul, Türkiye (date: 14/09/2020; file number: 77). Participants were provided electronic informed consent to participate in the study.

The study was reported on the basis of the recommendations of the consensus-based standards for selecting health status measurement instruments (COSMIN) statement.[11] The study design is presented in Figure 1.

Composition of a preliminary set of items

The scale items were developed considering the literature.[2,9,12,13] The research team also reviewed drug leaflets and patient education brochures to generate the items. As the first version of MELSA-TR, twenty-seven draft items were created using virtual medicine boxes and instructions. Both performance-based (such as calculation) and perception-based (interpretation of instructions given) items related to the prescribed medications/non-prescribed medications/dietary supplements/herbal medicines were included. These items were created based on numeracy, prose, and document literacy.[2] Each item of the scale had a dichotomous score (1: for the correct response and 0: for the wrong response and the option of no idea/don't know).

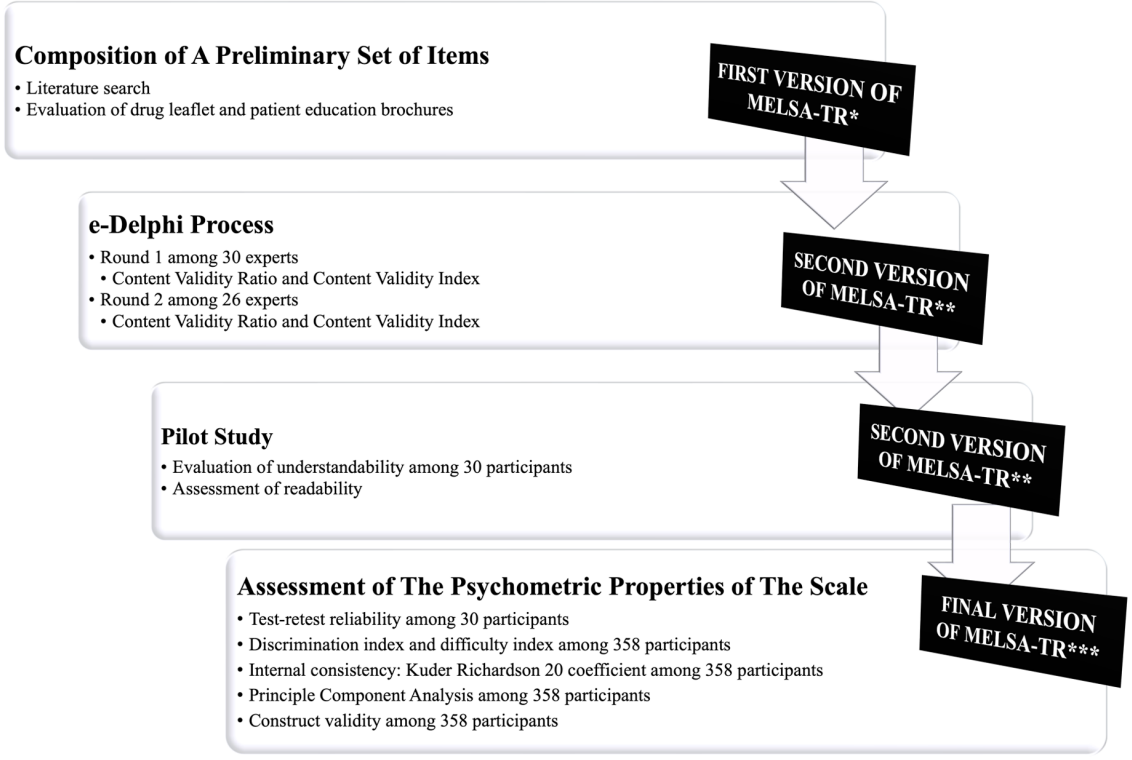

Figure 1. Flowchart representing the development and evaluation of MELSA-TR process. *It consisted of 27 items, **It consisted of 23 items, ***It consisted of 8 items

e-Delphi process

The content validity of the scale was assessed by an e-Delphi process between December 2020 and February 2021. A national multidisciplinary group of experts working on health literacy (including community pharmacists, hospital pharmacists, a health sociologist, a clinical psychologist, a public health expert, nurses, a pharmacologist, clinical pharmacists, physicians, a pedagogist, and an education specialist) participated in the e-Delphi process. A link to the online survey was generated on the Marmara University Questionnaire System, which is powered by the Lime Survey©, and invitation letters were sent to the experts by email. After receiving their informed consent electronically, the questionnaire link was sent individually with a password. The participants were asked to complete the questionnaire within three weeks.

The experts were asked whether the items would be relevant to medication literacy. The experts rated each item with a 4-point Likert scale [from very irrelevant (1) to very relevant (4)] and provided suggestions and comments to evaluate the clarity and comprehensibility of the questions (about the type, visual, and grammar of the items) by filling in the comment box for each item. At the end of each round, the content validity ratio (CVR) and the content validity index (CVI) were calculated for each item.[14] If the item-CVI was less than 0.70, the item was excluded from the scale. If the item CVI was in the range of 0.70-0.79, it was revised. If CVR value of the item was negative, it was excluded from the scale.[15]

Two separate rounds were conducted within four weeks intervals for the e-Delphi study. Thirty-six experts from various disciplines were invited to the e-Delphi study. Thirty experts participated in round 1. At the end of round 1, four items in the scale were excluded based on the CVR and CVI findings. The items were re-written according to the feedback and suggestions of the experts. Twenty-six experts participated in round 2. No items were excluded and no other items were added to the scale in round 2, while the second version of MELSA-TR consisted of 23 items.

Pilot study

A pilot study was conducted on 30 adults (a separate sample of individuals who were recruited neither in the test-retest nor the psychometric study) for the second version of MELSA-TR. The participants assessed the comprehensibility of the items. It took an average of 10-15 minutes to complete the scale. The readability of the total scale was evaluated by the Turkish evaluation formula, which was developed by Ateşman[16] and it was found to be average, with a score of 65.3.

Assessment of the psychometric properties of the scale

An online survey was conducted between March and May, 2021. The sample size for validation studies is recommended to be ten times the number of items in the scale, so it was calculated that at least 300 participants would be required for an adequate sample size.[17] The study population consisted of university students, academics, and administrative staff from two faculties (pharmacy and law) in two universities located in two cities (İstanbul and Ankara) in Türkiye. Because of the restrictions (including a curfew and social distance) during the coronavirus disease-2019 (COVID-19) pandemic, an online survey was conducted in both Delphi processes and the psychometric analysis. Due to the difficulties in reaching individuals with low education levels, this study was conducted only on individuals with an education level of above 12 years using convenience sampling. In Türkiye, the compulsory education year has been 12 since 2012 (https://www.resmigazete.gov.tr/eskiler/2012/04/20120411-8.htm Accessed date: 1 February 2022). The population of this study had a medium to high level of education according to the International Standard Classification of Education (https://ec.europa.eu/eurostat/statistics-explained/index.php?title=International_Standard_Classification_of_Education_(ISCED)#Implementation_of_ISCED_2011_.28levels_of_education.29 Accessed date: 1 February 2022).

Socio-demographic variables [age, sex, faculty, and degree (year), having a bachelor's degree or associate degree in health sciences for academic and administrative staff, perceived socioeconomic status, use of prescribed medication/unprescribed medication/vitamin, and perceived general health assessment] were collected.

Turkish version of the Single Item Literacy Screener developed by Morris et al.[18] was used to evaluate the need for individuals for reading and comprehension of health-related materials. The item was as follows: "How often do you need someone to help you, when you read instructions, pamphlets, or other written material from your doctor or pharmacy?". A 5-Likert scale (ranging from never to always) was used in this self-report instrument, and the cut-off was greater than 2 to identify subjects with limited reading ability for health-related information.

Two-week test-retest reliability for the second and final versions of MELSA-TR was evaluated on 30 participants (a separate sample of individuals who were recruited neither in the test-retest nor the psychometric study). The discrimination index (which was considered as excellent if it was greater than 0.4) and the difficulty index (which is considered as difficult if it was less than 30%) were calculated.[19]

Kuder Richardson 20 coefficient was calculated to determine the internal consistency of the scale. A shorter and more reliable version of the scale with 8 items was created taking into consideration the discrimination index, the difficulty index, and Kuder Richardson 20 coefficient. Principal component analysis was conducted.

The following hypothesis was tested to evaluate the construct validity of the scale: *Students (fourth and fifth-grade students of faculty of pharmacy) and graduates (academic and administrative staff with bachelor's degree or associate degree in health science) of health science have higher scores on the medication literacy scale compared with participants who did not have any education in health sciences.* The study was conducted among all university students, regardless of their grades. However, the hypothesis was restricted to only the fourth and fifth-grade students of the faculty of pharmacy because the pharmacy students have been receiving professional pharmacy courses in these grades

according to the national pharmacy core education program in Türkiye (https://www.yok.gov.tr/Documents/Kurumsal/egitim_ogretim_dairesi/Ulusal-cekirdek-egitimi-programlari/eczacilik_cep.pdf Accessed date: 1 February 2022).

Statistical analysis

Descriptive data were presented as medians (25^{th}-75^{th} percentiles) and numbers (percentages), where appropriate. Kolmogorov-Smirnov test was used to assess the normality of the data. Since the data did not follow a normal distribution, continuous variables for two and more than two groups were compared with Mann-Whitney *U* and Kruskal-Wallis tests, respectively. Kuder Richardson 20 coefficient was calculated to determine internal consistency. Principal component analysis was conducted. Spearman's correlation and Wilcoxon test were used to evaluate test-retest reliability. $P<0.05$ was set as the level of statistical significance. Data analysis was performed by IBM® SPSS® 11 software.

RESULTS

The online survey link was accessed by 752 participants. Fourteen participants declined to participate. Three hundred eighty participants did not complete the survey. Therefore, 358 of 752 (47.6%) were included in the analysis. The median (25^{th}-75^{th} percentiles] age was 22 (21-24) years (minimum-maximum: 19-62). The characteristics of the participants (n: 358) are presented in Table 1.

For the final version of MELSA-TR, the test-retest reliability (n: 30) showed a positive correlation between the scores of the scale at baseline and after a two-week interval (Spearman's rho: 0.570; $p<0.01$). There was no significant difference between the test and retest scores ($p=0.308$) (data not shown).

Kuder Richardson 20 coefficient was 0.762 for the second version of MELSA-TR. The final version was limited to 8 items taking into consideration the content of the items, discrimination index, the difficulty index, and Kuder Richardson 20 coefficient. Kuder Richardson 20 coefficient was 0.659 for the final version consisting of 8 items. The median (25^{th}-75^{th} percentiles) score of the scale was 8.0 (7.0-8.0). Kaiser-Meyer-Olkin Measure of Sampling Adequacy was 0.776 with Bartlett's Test of Sphericity was significant ($p<0.001$). Only one factor was extracted by principal component analysis. The content of the items, the proportion of correct responses, corrected item-total correlation, and Kuder Richardson 20 coefficient if item deleted for each item are presented in Table 2.

Students (fourth and fifth-grade students of faculty of pharmacy) and graduates (academic and administrative staff with bachelor's degrees or associate degrees in health science) of health science had significantly higher scores on the medication literacy scale compared with the participants who did not have any education on health sciences [the median (25^{th}-75^{th} percentiles): 8.0 (8.0-8.0) *vs.* 7.0 (6.0-8.0), respectively; $p<0.001$]. Female participants had significantly higher scores on medication literacy scale compared with the males [the median (25^{th}-75^{th} percentiles): 8.0 (7.0-8.0) *vs.* 7.0 (6.0-8.0), respectively; $p=0.001$]. Participants with the high reading ability of health-related information had significantly higher scores on the medication literacy scale compared with those having the limited reading ability [the median (25^{th}-75^{th} percentiles): 8.0 (7.0-8.0) *vs.* 7.0 (6.0-8.0), respectively; $p=0.002$]. Medication literacy scale scores by participants' characteristics are presented in Table 3.

DISCUSSION

Content validity, the test-retest validity, internal consistency, and construct validity of MELSA-TR were confirmed in this study. Like the previously developed medication literacy scales,[2,8,10] Kuder Richardson 20 coefficient of MELSA-TR was determined as 0.659 and acceptable. Therefore, we suggest that MELSA-TR is a valid tool for adults having at least 12 years of education. However, we used a sample with a significant representation from healthcare professionals so the generalizability of our

Table 1. Characteristics of the participants (n: 358)

	n (%)
Sex	
Female	272 (76.0)
Male	86 (24.0)
Students* or graduates of health sciences**	
Yes	134 (37.4)
No	224 (62.6)
Perceived socioeconomic status	
Low	3 (0.8)
Low-moderate	82 (22.9)
Moderate	186 (52.0)
High-moderate	75 (20.9)
High	12 (3.4)
Use of prescribed medications/unprescribed medication/vitamins	
Yes	105 (29.3)
No	253 (70.7)
Perceived general health	
Perfect	16 (4.5)
Pretty good	135 (37.7)
Good	161 (45.0)
Not bad	43 (12.0)
Bad	3 (0.8)
SILS	
High reading ability for health-related information	289 (80.7)
Limited reading ability for health-related information	69 (19.3)

SILS: Single Item Literacy Screener, *Fourth and fifth-grade students of the faculty of pharmacy **Academic and administrative staff with bachelor's degree or associate degree in health science

findings for adults with a medium to high level of education should be evaluated with caution. It would be useful to conduct further studies evaluating the psychometric properties of this scale in participants with diverse characteristics.

Like similar medication literacy scales,[2,8-10] our scale consisted of numeracy questions (including calculation of dose and refill prescription date) items related to prose and document literacy. Neiva Pantuzza et al.[5] defined four constructs of medication literacy: functional literacy, communicative literacy, critical literacy, and numeracy. The items in MELSA-TR had items to assess all these constructs. During the COVID-19 pandemic, an infodemic had arisen,[20] so, we included two items related to critical and communicative literacy about the news on social media/television and purchasing herbal medicine on the internet, the advice taken from relatives/friends, and communication with physicians/pharmacists.

Study limitations

We used an online survey to determine the psychometric properties of the scale due to COVID-19 pandemic, which might have resulted with a selection bias. The participants who used the internet more frequently and/or were more interested in medication information might have participated more, resulting with an overestimation of total scores. Also, in an online survey, the participants might have gotten some guidance in filling out the questionnaire. The participants were adults with medium to high level of education who had worked and/or studied at universities, and some of them were health science students and/or professionals, which also limit the generalizability of the findings.

CONCLUSION

MELSA-TR could be used to evaluate the medication literacy levels of adults having at least 12 years of education in Türkiye. There is still a need to test the psychometric properties of the scale on diverse populations, particularly on socioeconomic disadvantaged groups, before using it extensively. This scale has many advantages, such as being a self-reported, valid, easily applicable, and not time-consuming tool. It also does not consist

Table 2. Content of the items and proportion of correct responses, corrected item-total correlation and Kuder Richardson 20 Coefficient if item deleted for each item of MELSA-TR (n: 358)

Items	Classification	Content of the item	Proportion of correct responses n (%)	Corrected item-total correlation	Kuder Richardson 20 coefficient if item deleted
Item-1	e-Medication literacy	After the news on social media/television about its harmful effects, deciding to continue taking a regularly used medicine, if the physicians'/pharmacists tell it is safe	319 (89.1)	0.306	0.639
Item-2	Dose	Selecting appropriate pediatric dose of paracetamol suspension according to child's age and weight (a dose table presented to the participants)	292 (81.6)	0.343	0.633
Item-3	Indication	Selecting the right medicine for heartburn according to indication information on the medicine box (the virtual medicine boxes presented to the participants)	266 (74.3)	0.376	0.628
Item-4	Calculating total daily dose	Calculating the total daily paracetamol dose in two products containing paracetamol (daily dose regimen and the virtual medicine boxes presented to the participants)	315 (88.0)	0.470	0.596
Item-5	Calculating time for dose	Calculating administration timing of an antibiotic dose	328 (91.6)	0.368	0.625
Item-6	Dose administration	Deciding whether a re-shake is needed or not before each dose of antibiotic suspension if it has been diluted, prepared, and shake in the initial use. The antibiotic suspension had a warning as "shake before each dose"	354 (98.9)	0.336	0.651
Item-7	Potential drug-drug interaction	Selecting appropriate administration timing of two medications (levothyroxine and iron product) that should be taken at different times because of a potential drug-drug interaction (the virtual instruction presented to the participants)	327 (91.3)	0.451	0.606
Item-8	Storage	Deciding about the storage conditions of an oral suspension bottle (the virtual instruction presented to the participants)	313 (87.4)	0.300	0.641

MELSA-TR: Medication Literacy Scale for Adults-Türkiye

Table 3. MELSA-TR scores by participants' characteristics (n: 358)

	MELSA-TR score Median (25^{th}-75^{th} percentiles)	*p* value
Sex		
Female	8.0 (7.0-8.0)	0.001
Male	7.0 (6.0-8.0)	
Students* or graduates of health sciences**		
Yes	8.0 (8.0-8.0)	<0.001
No	7.0 (6.0-8.0)	
Perceived socioeconomic status		
Low and low-moderate	8.0 (6.5-8.0)	0.844
Moderate	8.0 (6.75-8.0)	
High and high-moderate	7.0 (7.0-8.0)	
Use of prescribed medication/unprescribed medication/vitamin		
Yes	8.0 (7.0-8.0)	0.127
No	7.0 (6.0-8.0)	
Perceived general health		
Perfect and pretty good	8.0 (7.0-8.0)	0.188
Good	8.0 (7.0-8.0)	
Bad and not bad	7.0 (6.0-8.0)	
SILS		
High reading ability for health-related information	8.0 (7.0-8.0)	0.002
Limited reading ability for health-related information	7.0 (6.0-8.0)	

SILS: Single Item Literacy Screener; *Fourth and fifth-grade students of the faculty of pharmacy **Academic and administrative staff with bachelor's degree or associate degree in health science, MELSA-TR: Medication Literacy Scale for Adults-Türkiye

of items related to the country-based healthcare system. Still, we note that further studies among participants with diverse characteristics (particularly on socioeconomic disadvantaged groups) would be useful for evaluating psychometric properties in more detail.

Ethics

Ethics Committee Approval: Ethical approval for this study was received from Marmara University, Institute of Health Science Ethical Board Committee, İstanbul, Türkiye (date: 14/09/2020; file number: 77).

Informed Consent: Participants provided electronic informed consent to participate in the study.

Peer-review: Externally peer-reviewed.

Authorship Contributions

Concept: O.T., İ.M., P.A., M.S., B.O., Design: O.T., İ.M., P.A., M.S., B.O., Data Collection or Processing: O.T., İ.M., A.S., E.B., V.O., B.O., Analysis or Interpretation: O.T., İ.M., P.A., M.S., A.S., E.B., V.O., B.O., Literature Search: O.T., İ.M., P.A., M.S., B.O., Writing: O.T., İ.M., P.A., M.S., A.S., E.B., V.O., B.O.

Conflict of Interest: No conflict of interest was declared by the authors.

Financial Disclosure: The project entitled "A Scale Development Study to Determine Individuals' Medication Literacy, and Attitudes Regarding Rational Medication Use" was supported by the TÜBİTAK 2209-A program (no: 1919B012001763).

REFERENCES

1. Pouliot A, Vaillancourt R, Stacey D, Suter P. Defining and identifying concepts of medication literacy: an international perspective. Res Social Adm Pharm. 2018;14:797-804.
2. Sauceda JA, Loya AM, Sias JJ, Taylor T, Wiebe JS, Rivera JO. Medication literacy in Spanish and English: psychometric evaluation of a new assessment tool. J Am Pharm Assoc (2003). 2012;52:e231-e240.
3. Koster ES, Philbert D, van Dijk L, Rademakers J, de Smet PAGM, Bouvy ML, Vervloet M. Recognizing pharmaceutical illiteracy in community pharmacy: agreement between a practice-based interview guide and questionnaire based assessment. Res Social Adm Pharm. 2018;14:812-816.
4. Gentizon J, Hirt J, Jaques C, Lang PO, Mabire C. Instruments assessing medication literacy in adult recipients of care: a systematic review of measurement properties. Int J Nurs Stud. 2021;113:103785.
5. Neiva Pantuzza LL, Nascimento ED, Crepalde-Ribeiro K, Botelho SF, Parreiras Martins MA, Camila de Souza Groia Veloso R, Gonzaga do Nascimento MM, Vieira LB, Moreira Reis AM. Medication literacy: a conceptual model. Res Social Adm Pharm. 2022;18:2675-2682.
6. Vervloet M, van Dijk L, Rademakers JJDJM, Bouvy ML, De Smet PAGM, Philbert D, Koster ES. Recognizing and addressing limited pharmaceutical literacy: development of the RALPH interview guide. Res Social Adm Pharm. 2018;14:805-811.
7. Zheng F, Ding S, Lai L, Liu X, Duan Y, Shi S, Zhong Z. Relationship between medication literacy and medication adherence in inpatients with coronary heart disease in Changsha, China. Front Pharmacol. 2020;10:1537.
8. Yeh YC, Lin HW, Chang EH, Huang YM, Chen YC, Wang CY, Liu JW, Ko Y. Development and validation of a Chinese medication literacy measure. Health Expect. 2017;20:1296-1301.
9. Stilley CS, Terhorst L, Flynn WB, Fiore RM, Stimer ED. Medication health literacy measure: development and psychometric properties. J Nurs Meas. 2014;22:213-222.
10. Horvat N, Kos M. Development, validation and performance of a newly designed tool to evaluate functional medication literacy in Slovenia. Int J Clin Pharm. 2020;42:1490-1498.
11. Gagnier JJ, Lai J, Mokkink LB, Terwee CB. COSMIN reporting guideline for studies on measurement properties of patient-reported outcome measures. Qual Life Res. 2021;30:2197-2218.
12. Ubavić S, Krajnović D, Bogavac-Stanojević N. Pharmacotherapy literacy questionnaire for parents of pre-school children in Serbia: construction and psychometric characteristics. Vojnosanitetski Pregled. 2019;76:1054-1061.

13. Kripalani S, Henderson LE, Jacobson TA, Vaccarino V. Medication use among inner-city patients after hospital discharge: patient-reported barriers and solutions. Mayo Clin Proc. 2008;83:529-535.

14. Lawshe CH. A quantitative approach to content validity 1. Personnel Psychology. 1975;28:563-75.

15. Rodrigues IB, Adachi JD, Beattie KA, MacDermid JC. Development and validation of a new tool to measure the facilitators, barriers and preferences to exercise in people with osteoporosis. BMC Musculoskelet Disord. 2017;18:540.

16. Ateşman E. Measuring readability in Turkish. AU Tömer Language Journal. 1997;58:171-174.

17. Streiner DL, Kottner J. Recommendations for reporting the results of studies of instrument and scale development and testing. J Adv Nurs. 2014;70:1970-1979.

18. Morris NS, MacLean CD, Chew LD, Littenberg B. The Single Item Literacy Screener: evaluation of a brief instrument to identify limited reading ability. BMC Fam Pract. 2006;7:21.

19. Mitra N, Nagaraja H, Ponnudurai G, Judson J. The levels of difficulty and discrimination indices in type A multiple choice questions of pre-clinical semester 1 multidisciplinary summative tests. IeJSME. 2009;3:2-7.

20. The Lancet Infectious Diseases. The COVID-19 infodemic. Lancet Infect Dis. 2020;20:875.

Turk J Pharm Sci 2023;20(2):91-99
DOI: 10.4274/tjps.galenos.2022.01346

ORIGINAL ARTICLE

Radiolabeling, Quality Control, and Cell Binding Studies of New ^{99m}Tc-Labeled Bisphosphonates: ^{99m}Tc-Ibandronate Sodium

Meliha EKİNCİ, Derya İLEM ÖZDEMİR*, Emre ÖZGENÇ, Evren GÜNDOĞDU, Makbule AŞIKOĞLU

Ege University, Faculty of Pharmacy, Department of Radiopharmacy, İzmir, Türkiye

ABSTRACT

Objectives: Early detection of bone cancer is critical for treating symptoms, minimizing pain, and increasing overall quality of life. It is critical to develop novel radiopharmaceuticals with high labeling efficiency and stability for the diagnosis of bone cancer. This research aims to design a novel radiopharmaceutical that may be used to diagnose bone cancer.

Materials and Methods: In this study, ibandronate sodium (IBD), a bisphosphonate analog, was radiolabeled with technetium-99m [^{99m}Tc] and quality control tests on the newly developed radiopharmaceutical ([^{99m}Tc]Tc-IBD) were performed using radioactive thin layer chromatography. After that, the incorporation of [^{99m}Tc]Tc-IBD into hydroxyapatite (HA) crystals and a human bone osteosarcoma cell line (U2OS) was tested.

Results: According to the results obtained, optimal radiolabeling procedure was obtained for [^{99m}Tc]Tc-IBD with 200 µg.mL^{-1} IBD, 20 µg stannous chloride, and ^{99m}Tc with 37 MBq radioactivity. The reaction mixture was adjusted to pH 5.5 and incubated at room temperature for 15 min. The radiochemical purity of [^{99m}Tc]Tc-IBD was found to be greater than 95% at room temperature for up to 6 h. Additionally, chromatography analysis showed >95% [^{99m}Tc]Tc-IBD complex formation with promising stability for up to 24 h in saline and up to 2 h in cell medium. The percentage binding of IBD to HA was 83.70 ± 3.67 and the logP of [^{99m}Tc]Tc-IBD was -1.1014. The radiolabeled complex exhibited a higher rate of cell incorporation to U2OS cells compared to Reduced/Hydrolyzed $^{99m}TcO_4^-$.

Conclusion: The newly produced radiopharmaceutical is very promising according to the results of *in vitro* cell culture, HA binding, and quality studies, and will be a step forward for further studies in nuclear medicine for bone cancer diagnostics.

Key words: Ibandronate sodium, technetium-99m, radiopharmaceuticals, radiolabeling, bone cancer cells

INTRODUCTION

Bisphosphonates (BPs) are a group of medications used to help prevent and treat bone loss.[1] They are structural counterparts of pyrophosphate molecules that occur, when the oxygen atom in the phosphorus-oxygen-phosphorus (P-O-P) bond in pyrophosphates is replaced with a carbon atom, resulting in the formation of a phosphorus-carbon-phosphorus (P-C-P) bond.[2] Since BPs bind to hydroxyapatite crystals (HA), they have a high affinity for bone minerals, like their natural analog pyrophosphates. Non-nitrogen-containing BPs (non-N-BPs) and nitrogen-containing BPs (non-N-BPs) are the two types of BPs (N-BPs). Ibandronate (IBD) is a very powerful oral N-BP that comprises a core P-C-P structure that is required for binding to the mineral surface of the bone and prevents osteoclast-mediated bone resorption.[2,3] IBD's main pharmacological impact on bone tissue is due to its affinity for HA, which is a component of bone's mineral matrix.[4] The bone affinity of IBD is significantly high because of phosphonate groups and the chemical structure of IBD is ({1-hydroxy-3-[methyl(pentyl) amino] propane-1,1-diyl}bis (phosphonic acid).[5] The possible schematic design of the direct radiolabeling method for [^{99m}Tc] Tc-IBD is shown in Figure 1.

Early and accurate identification of bone cancer, followed by proper therapy, is crucial for managing symptoms and extending life expectancy. Because radiolabeled BPs are used as bone-seeking radiopharmaceuticals, bone scintigraphy has

*Correspondence: deryailem@gmail.com, Phone: +90 232 311 19 63, ORCID-ID: orcid.org/0000-0002-1062-498X
Received: 24.03.2022, Accepted: 09.05.2022

©Copyright 2023 by Turkish Pharmacists' Association / Turkish Journal of Pharmaceutical Sciences published by Galenos Publishing House.
Licenced by Creative Commons Attribution-NonCommercial-NoDerivatives 4.0 (CC BY-NC-ND)

become one of the most extensively used diagnostic nuclear medicine procedures, providing earlier diagnosis or detecting more lesions than conventional radiographic approaches.[6-9]

In the past decades, several BPs compounds such as alendronate (ALD), risedronate, and zoledronate were radiolabeled with technetium-99m [^{99m}Tc] for use as a bone imaging agent to diagnose various clinical diseases that typically result in widespread skeletal metastases.[10-14]

In radiopharmaceuticals, there are radioactive and pharmaceutical parts together. A suitable radionuclide for radiolabeling experiments can be determined by considering aspects including radiation dose, cost, and availability. ^{99m}Tc has recently become the most widely used radionuclide for labeling research.[15] By many procedural advantages related to the physical properties of this isotope, the use of ^{99m}Tc may enhance the quality of images and radiation protection for patients and staff.[16] ^{99m}Tc is a radionuclide with monoenergetic gamma rays of 140 KeV, with a half-life of 6 h, and diverse chemistry for forming complexes.[17]

Although animal experimental studies are important for cancer detection, *in vitro* cell culture research was used to assess various cancer binding affinities. Many researchers prefer to do binding studies using cell lines before performing animal experiments, when developing a new radiopharmaceutical for imaging.[18-24] In this procedure, radiolabeled pharmaceuticals or formulations are treated to various types of cells, and then, the radioactivity in the cells and cell medium is measured at various time intervals.

This study aimed to develop a novel radiopharmaceutical for use in the detection of bone cancer. IBD was radiolabeled with ^{99m}Tc for this purpose. Labeling efficiency and stability of the compound were studied. Cell incorporation tests were used to assess the newly produced radiopharmaceutical's binding affinity to cancer cells. In human bone osteosarcoma cell line, incorporation of [^{99m}Tc]Tc-IBD to cancer line was examined as part of cell culture research (U2OS).

MATERIALS AND METHODS

Materials

Roche (Germany) provided IBD, while Merck (Germany) provided stannous chloride and ascorbic acid as well as all the solvents. Molybdenum-99 (^{99}Mo)/^{99m}Tc generator produced $^{99m}TcO_4^-$ (Ege University, Türkiye). Pall Life Science provided 0.22 µm pore size syringe filter. Gibco Invitrogen (Grand Island, NY) provided cell culture products and supplies. American Type Culture Collection (ATCC) provided the U2OS cell line. All other solvents were of analytical quality and were not purified further. A dose calibrator (AtomLab 100), a TLC scanner (BioScan AR 2000), and a gamma counter (Sesa Uniscaller) were used to count radioactive samples.

Radiolabeling studies

Varying amounts of reducing agent were used to test the radiolabeling of [^{99m}Tc]Tc-IBD. With ascending radioactive thin layer chromatography (RTLC) studies, radiochemical purity (RP) was assessed. To obtain the best outcome, the role of antioxidant agent amount, incubation time, radiation dose, pH, and filtration parameters were examined.

Effect of reducing agent amount on labeling

$^{99m}TcO_4^-$ was eluted from ^{99}Mo/^{99m}Tc generator in +7 oxidation level. For ^{99m}Tc, this level is unable to label with any component or formulation when added directly. Before the radiolabeling, ^{99m}Tc must be reduced to lower oxidation levels to form complexes with the ligand and synthesize the radiopharmaceutical. For this purpose, various reduction agents, such as stannous chloride, stannous tartrate, sodium borohydride, sodium dithionite, hydrohalic acids, formamidine, sulfonic acid, and others, have been employed by the researchers. Because of its non-toxic and stable properties, stannous chloride is widely used as a reductant within them.[25]

The role of reducing agent quantity on labeling was tested using stannous chloride in this study. IBD (100 µg) was dissolved in 0.5 mL of 0.9% sodium chloride solution (SF). Under the influence of a bubbling nitrogen environment, stannous chloride was added to the stock solution. $^{99m}TcO_4^-$ was reduced using different amounts of stannous chloride (5, 10, 20, 50, and 100 µg) at neutral pH (pH: 7.0) (1 mg reducing agent diluted in 1 mL pure water). In 0.1 mL SF, 37 MBq $^{99m}TcO_4^-$ was used for radiolabeling and before the radiochemical testing, the [^{99m}Tc]Tc-IBD was left at room temperature for 15 min.

Effect of antioxidant agent amount on labeling

Auto radiolysis occurs in ^{99m}Tc radiopharmaceuticals at all stages of production, including preparation, release, and storage. As a result, it is critical to use a stabilizer to prevent radiopharmaceuticals' auto radiolysis. Antioxidant agents like ascorbic acid, gentisic acid, and *p*-aminobenzoic acid, which quickly react with hydroxyl and superoxide radicals, have been used as stabilizers to reduce ^{99m}Tc radiopharmaceutical radiolytic disintegration.[26]

Ascorbic acid as an antioxidant agent was used to investigate the effect of the quantity of antioxidant agent on labeling in this study. Radiolabeling experiments were carried out in the presence of ascorbic acid and in the absence of ascorbic acid. In 0.5 mL SF, IBD (100 µg) was dissolved. Each of the three vials was added 20 µg of stannous chloride. Then, before labeling, 1 and 2 µg of ascorbic acid were added to two vials, respectively, while no ascorbic acid is added to the 3rd vial. 37 MBq/0.1 mL of $^{99m}TcO_4^-$ was used for radiolabeling. The labeling efficiency was determined using RTLC after a 15 min incubation period.

Effect of incubation time on labeling

To generate a complex with high labeling efficiency and stability, radiopharmaceuticals should be left to stand for a while after labeling. RP of the [^{99m}Tc]Tc-IBD was studied by RTLC tests at 5, 15, 30, 45, and 60 min post-labeling to examine the incubation time.

Effect of radioactivity doses on labeling

Because of the personnel's and the area's radiation safety, *in vitro* radiolabeling investigations were performed with 37 MBq of $^{99m}TcO_4^-$. Also, the RP of [^{99m}Tc]Tc-IBD was investigated with 185 and 370 MBq radiation doses in addition to the 37 MBq radiation

dose because human research including radiopharmaceuticals require higher radiation doses.

Effect of pH on labeling

For stability and integrity, all radiopharmaceuticals should have a suitable pH value. The ideal pH of a radiopharmaceutical is 7.4 (pH of the blood), yet, it can vary between 2.0 and 9.0 due to the blood's high buffering capacity.[20] Although [^{99m}Tc]Tc-IBD should be compatible with body pH, small-volume preparations are adjusted to pH stable.

In this work, using 0.1 N NaOH and HCl, the role of pH on RP of [^{99m}Tc]Tc-IBD was investigated for pH 4.0-7.4.

Effect of filtration on labeling

Because radiopharmaceuticals are administered *via* the parenteral route, they must be sterilized using the appropriate procedure. Filtering with a membrane filter with a particle size of 0.22 µm enables sterile filtration for radiopharmaceuticals, while also removing reduced/hydrolized (R/H) $^{99m}TcO_4^-$ from the medium to improve image quality.

Two batches of radiopharmaceuticals were prepared with only 20 µg of stannous chloride to see whether filtration had any effect on labeling. While one group was filtered after a 15 min incubation period, the other was not. A RTLC scanner was used to assess the labeling stability of the two groups.

In vitro stability

After ^{99m}Tc labeling, IBD was the left in SF for 24 h at 25°C and in cell medium for 2 h at 37°C. RTLC experiments at predetermined time intervals were used to evaluate the complex's labeling stability.

Stability of [^{99m}Tc]Tc-IBD in SF

To 0.9 mL SF, 0.1 mL of [^{99m}Tc]Tc-IBD reaction media was added. For 24 h, the mixture was incubated at 25°C. To test the stability of [^{99m}Tc]Tc-IBD in SF, one drop of radiolabeled solution was spotted on chromatography papers at various times (0, 1, 2, 3, 4, 5, 6, and 24 h) and RTLC experiments were carried.

Stability of [^{99m}Tc]Tc-IBD in cell medium

[^{99m}Tc]Tc-IBD reaction medium (0.1 mL) was mixed with 0.9 mL Dulbecco's modified essential medium (DMEM) containing 10% fetal bovine serum (FBS). The radiolabeled solution was incubated for 2 h at 37°C. To determine the stability of [^{99m}Tc] Tc-IBD in cell medium, 2-3 µL of sample was spotted on chromatographic paper at pre-determined times (0, 30, 60, and 120 min) and RTLC studies were performed.

RTLC procedure

In RTLC studies, ITLC-SG chromatographic sheets were used as stationary phase. In [^{99m}Tc]Tc-IBD solution, free $^{99m}TcO_4^-$ and R/H $^{99m}TcO_4^-$ were determined by 100% acetone and acetonitrile/water/trifluoroacetic acid (ACN/W/TFA; 50/25/1.5) solvent system as the mobile phase. The radioactivity of the sheets was assessed *via* a TLC scanner and the RP (%) of [^{99m}Tc]Tc-IBD was determined using equation (1) by subtracting the sum of the detected impurity percentages from 100:

RP (%) = 100 - [free $^{99m}TcO_4^-$ (%) + R/H $^{99m}TcO_4^-$ (%)] (1)

Cell culture studies

U2OS cell line was grown in DMEM solution supplemented 10% FBS. 3 x 10^5 cells were seeded in six wells with a transwell insert filter to form cell monolayers. The cells were kept at 37°C, 90% humidity, and 5% CO_2. The adherent cells were split daily with trypsin/ethylene diamine tetraacetic acid in a 1:20 ratio.

In vitro incorporation studies

In vitro incorporation tests with the U2OS cells were used to compare the incorporation of [^{99m}Tc]Tc-IBD and R/H $^{99m}TcO_4^-$ to human bone osteosarcoma cells. For this experiment, cells were incubated with 3.7 MBq [^{99m}Tc]Tc-IBD for 30, 60, and 120 min at 37°C. The samples were collected from the cell medium and placed in tubes after the incubation time. Adherent cells were also trypsinized, washed in phosphate buffered saline (PBS) once, and transferred to tubes. A gamma counter was used to count the amount of radioactivity in the cell media and U2OS cells. The cellular uptake was calculated by dividing the total activity counted by the proportion of activity counted in the cells. The following equation, (equation 2), was used to determine the radioactivity (%) of cells.

Radioactivity of cells (%) = (radioactivity of cells/total radioactivity) x 100 (2)

Hydroxyapatite-binding studies

HA binding test was performed with only minor changes to the procedure previously described.[9] In a short, HA (5 mg, synthetic, powder) was added to PBS (1 mL) at the pH of 7.4. After that, 10 µL (0.5 MBq) of [^{99m}Tc]Tc-IBD were added to each HA solution, and the suspensions were shaken for 1 h at 37°C. A 50 µL sample of each sample's supernatant was tested for radioactivity in a gamma counter after 10 min of 5000 rpm centrifugation. The same process was used to obtain and count a control sample that did not contain HA. The following equation 3 was used to calculate the percentage of HA binding:

% HA binding = [1- (radioactivity of sample/radioactivity of control)] x 100 (3)

Biological tests of [^{99m}Tc]Tc-IBD

Because radiopharmaceuticals are applied to people, they must be sterile, isotonic, and free of pyrogens. The sterility, isotonicity, and pyrogenicity of [^{99m}Tc]Tc-IBD were tested for this purpose.

Sterility test

Sterility of the IBD solution was determined using the British Pharmacopoeia's direct inoculation method.[27] The IBD solution was inoculated aseptically into the sterilized terrific broth medium and tryptic soy broth tubes and incubated for 7 days at 35 ± 2°C. The growth of microorganisms in the tubes was assessed at the end of the incubation period.

Isotonicity test

The IBD solution's isotonicity was determined using an osmometer. The calibrated instrument was used to analyze the samples in eppendorf tubes.

Pyrogenicity test

In a bacterial endotoxins test, pyrogenicity of the IBD solution was determined using the gel-clot technique. In terms of pyrogenicity, pyrogenicity of the prepared IBD solution and the standard endotoxin solution was compared. According to the European protocol, Limulus amebocyte lysate test was performed to validate radiopharmaceutical preparation.[27,28]

Lipophilicity studies

For lipophilicity tests of [^{99m}Tc]Tc-IBD, *n*-octanol and PBS (pH: 7.4) were used. In a centrifuge tube, 500 µL *n*-octanol, 500 µL PBS (pH: 7) and 150 µL [^{99m}Tc]Tc-IBD were mixed and centrifuged at 2500 rpm for 30 min. The mixture was separated into two phases after centrifugation. A gamma counter was used to count 100 µL of each phase activities. This process was carried out for four times.[20]

Statistical analysis

Microsoft Excel was used to calculate the means and standard deviations (SD). The *t*-test was used to evaluate statistical significance. Differences were considered significant at 95 percent confidence level (p>0.05). Unless otherwise noted, all experiments were carried out in triplicate. The results are presented as a mean with SD.

RESULTS

Radiolabeling studies

Our research group developed the radiolabeling of [^{99m}Tc]Tc-IBD. The best results were obtained by experimenting with radiolabeling parameters.

Effect of reducing agent amount on labeling

Labeling tests were carried out to determine how the amount of reducing agent affected the labeling yield. The labeling yield was low, and the chromatograms were irregular at lower concentrations of stannous chloride than the optimal value. The labeling yield was significantly decreased by increasing the reducing agent concentration above the optimal limits. In this study, RP (%) of formulations containing various concentrations of stannous chlorides is shown in Figure 2.

The amount of reducing agent that was shown to be the most effective was 20 µg, according to the findings. Labeling efficiency was above 95% under these situations and did not alter much after 6 h at room temperature.

Effect of antioxidant agent amount on labeling

Stability of the complex increased slightly in the presence of ascorbic acid, but not significantly. A decrease in the R/H $^{99m}TcO_4^-$ percentage increases labeling efficiency. Figure 3 was illustrated the results. Since the amount of auxiliary material should always be decreased, ascorbic acid-free samples were chosen for continued study.

Effect of incubation time on labeling

Stannous chlorides (20 µg) including formulations were labeled with 37 MBq $^{99m}TcO_4^-$. RP of the complexes was studied by RTLC tests done at 5, 15, 30, 45, and 60 min after radiolabeling. According to the trials, the best radiolabeling yield (~98%) was obtained after a 15 min incubation time (Figure 4).

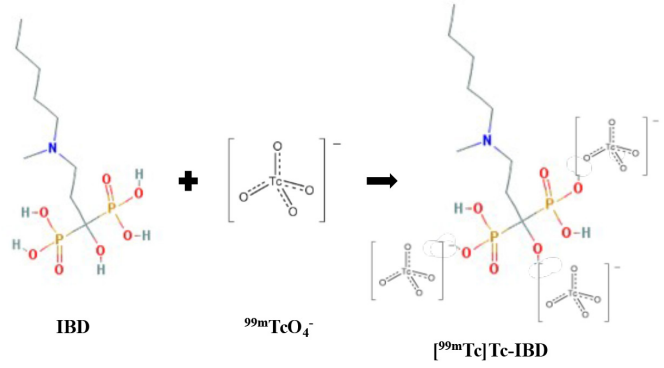

Figure 1. The possible direct radiolabeling approach for [^{99m}Tc]Tc-IBD

^{99m}Tc: Technetium-99m, IBD: Ibandronate sodium

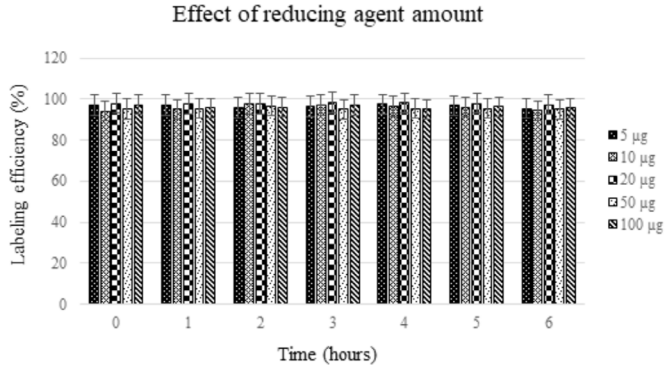

Figure 2. The labeling efficiency of [^{99m}Tc]Tc-IBD in which different amounts of stannous chlorides

^{99m}Tc: Technetium-99m, IBD: Ibandronate sodium

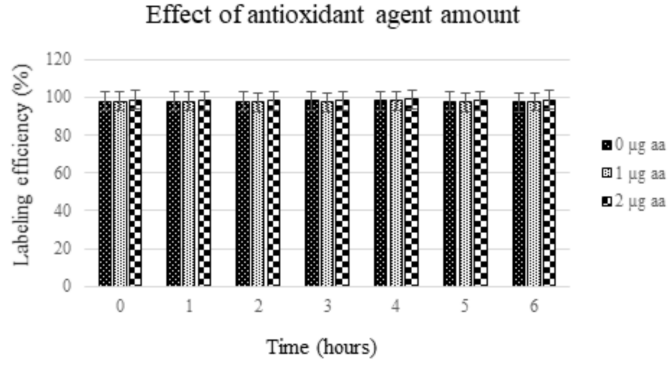

Figure 3. The labeling efficiency of [^{99m}Tc]Tc-IBD in the absence and presence of ascorbic acid

^{99m}Tc: Technetium-99m, IBD: Ibandronate sodium

Effect of radioactivity doses on labeling

IBD was radiolabeled with radiation dosages of 37, 185, and 370 MBq $^{99m}TcO_4^-$. With increasing radioactivity, RP of the [^{99m}Tc]Tc-IBD complex decreased slightly (Figure 5).

Effect of pH on labeling

For pH 4.0 and 7.4, influence of pH on the labeling efficiency of [^{99m}Tc]Tc-IBD was investigated. According to the results of the experiments, pH of the reaction medium plays a significant role in the labeling process (Figure 6). RP was altered, while the other reaction parameters remained constant, and the pH of the reaction was modified from 4.0 to 7.4. The best labeling efficiency was found at pH 5.5, which is the same as IBD's pH.

The effect of filtration on labeling

The labeling efficiency was reduced when [^{99m}Tc]Tc-IBD was filtered. The outcomes are represented in Figure 7.

In vitro stability

Stability of [^{99m}Tc]Tc IBD in saline

The produced radiopharmaceutical's stability was tested at room temperature for up to 24 h. [^{99m}Tc]Tc-IBD was confirmed to be stable in saline over the test period as indicated by RTLC (Figure 8).

Stability of [^{99m}Tc]Tc-IBD in cell medium

The compound was stable in cell media during the test period as assessed by RTLC. The percentage of [^{99m}Tc]Tc-IBD did not significantly decrease within 2 h as demonstrated in Figure 9.

RTLC procedure

Our research group has developed an innovative, basic, fast, and effective direct technique for ^{99m}Tc labeling of IBD. RTLC tests were used to examine the labeling efficiency of the [^{99m}Tc]Tc-IBD. The quantities of radioactive impurities (free $^{99m}TcO_4^-$ and R/H $^{99m}TcO_4^-$) were determined using two solvent systems.

RTLC tests were used to evaluate the RP and stability of [^{99m}Tc]Tc-IBD. Free $^{99m}TcO_4^-$ migrated with the solvent front in RTLC tests using acetone as the solvent, while [^{99m}Tc]Tc-IBD and R/H $^{99m}TcO_4^-$ remained at the spotting point. R/H $^{99m}TcO_4^-$ was identified using the mobile phase ACN/W/TFA (50/25/1.5), where R/H $^{99m}TcO_4^-$ remained at the site of spotting, whereas free $^{99m}TcO_4^-$ and [^{99m}Tc]Tc-IBD migrated with the solvent front. Figure 10 shows RTLC chromatogram of [^{99m}Tc]Tc-IBD. RP of [^{99m}Tc]Tc-IBD obtained using RTLC was >95%.

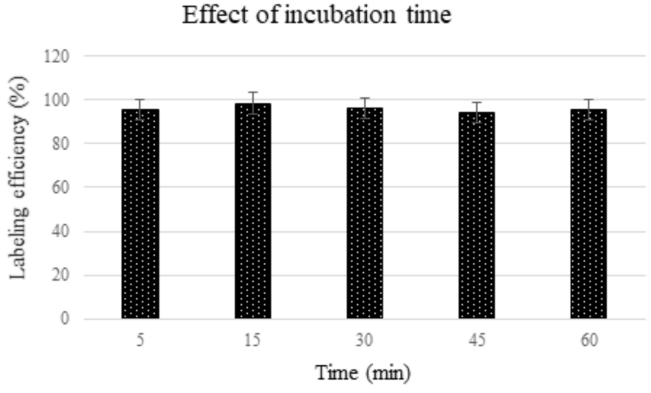

Figure 4. The labeling efficiency of [^{99m}Tc]Tc-IBD at different times post-labeling

^{99m}Tc: Technetium-99m, IBD: Ibandronate sodium

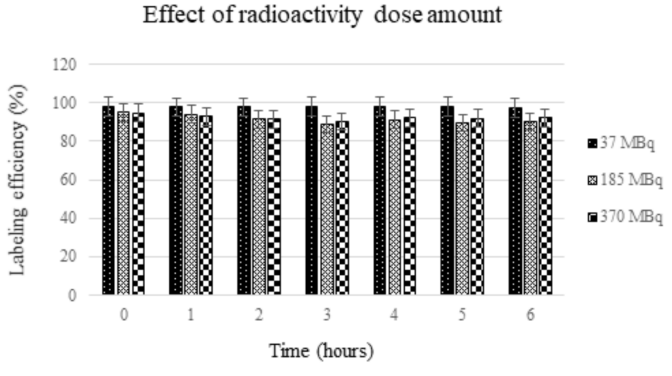

Figure 5. The labeling efficiency of [^{99m}Tc]Tc-IBD in different radioactivity doses

^{99m}Tc: Technetium-99m, IBD: Ibandronate sodium

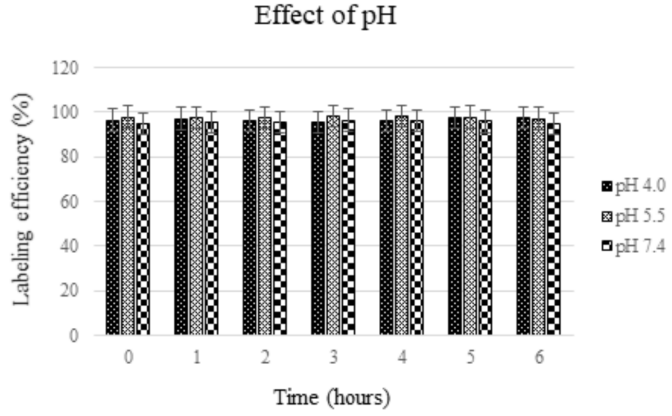

Figure 6. The labeling efficiency of [^{99m}Tc]Tc-IBD on different pH value

^{99m}Tc: Technetium-99m, IBD: Ibandronate sodium

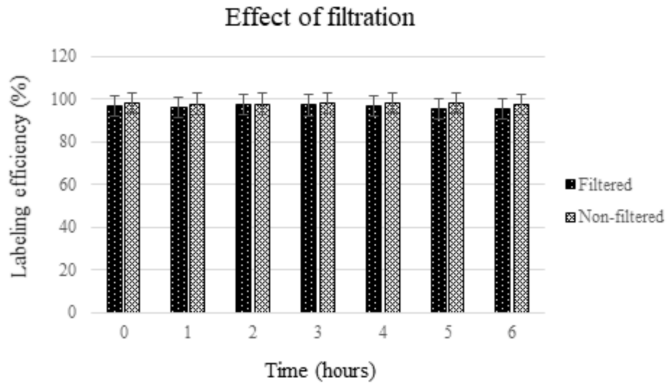

Figure 7. The labeling efficiency of [^{99m}Tc]Tc-IBD in terms of filtration

^{99m}Tc: Technetium-99m, IBD: Ibandronate sodium

In vitro incorporation studies

The percentage of [^{99m}Tc]Tc-IBD and R/H $^{99m}TcO_4^-$ incorporated into U2OS cell line was investigated in this research. Figure 11 shows the percentage of [^{99m}Tc]Tc-IBD and R/H $^{99m}TcO_4^-$ incorporated into U2OS cell lines after 30, 60, and 120 min of incubation. During the test period, the maximum incorporation percentage (~80%) was observed with [^{99m}Tc]Tc-IBD up to 2 h. The incorporation percentage of R/H $^{99m}TcO_4^-$ was decreased during the test period.

Hydroxyapatite-binding studies

The higher binding affinity to bone minerals is responsible for very selective localization and stability of therapeutically used radiolabeled BPs on bone. To determine the bone-seeking properties of [^{99m}Tc]Tc-IBD, *in vitro* HA absorption tests were conducted. In a 5 mg.mL^{-1} suspension, the percentage of IBD binding to HA was found to be 83.70 ± 3.67. HA experiment revealed that IBD has a significant capacity for binding to HA than [^{99m}Tc]Tc-MDP (methylene diphosphonate, bone imaging agent in clinical routine), whose binding efficiency was 63.10 ± 3.0%.

Biological tests of [^{99m}Tc]Tc-IBD

Sterility test

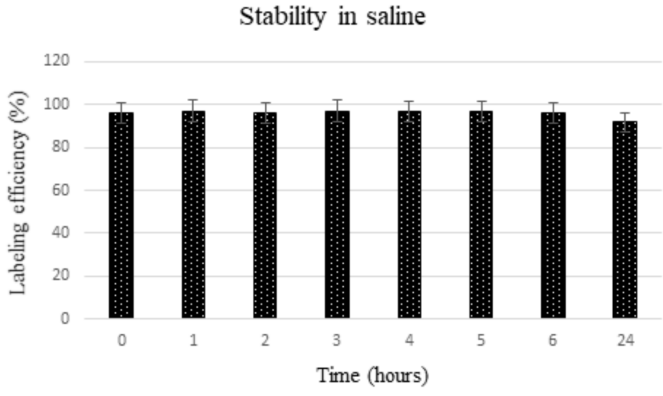

Figure 8. The stability of [^{99m}Tc]Tc-IBD in saline up to 24 h

^{99m}Tc: Technetium-99m, IBD: Ibandronate sodium

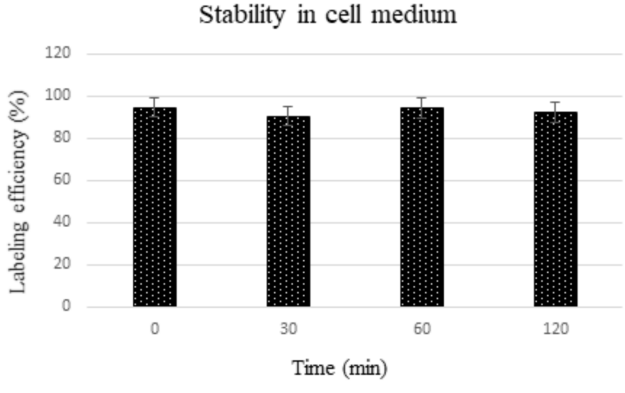

Figure 9. The stability of [^{99m}Tc]Tc-IBD in cell medium up to 2 h

^{99m}Tc: Technetium-99m, IBD: Ibandronate sodium

Sterility of the IBD solution was demonstrated by the absence of clearly visible microbial growth in the vials at the end of the sterility test.

Isotonicity test

According to British Pharmacopeia, isotonizing of the IBD solution was found to be 302 mOsm.mL^{-1}, which was suitable for injectable formulation.

Pyrogenicity test

The pyrogenicity test revealed that the IBD solution was non-pyrogenic.

Lipophilicity studies

logP value is a precious measure that, when combined with other factors, may be used to understand a drug's behavior, and predict its distribution throughout the body. logP of the [^{99m}Tc]Tc-IBD was found to be -1.0104. Due of the anionic nature of the produced complexes and the BP groups, the radiolabeled molecule has very polar properties (logP <1).[29]

DISCUSSION

BPs, such as MDP, ALD, and IBD, have long been used to control cancer-induced bone resorption in cancer patients.[30] IBD's bone-seeking feature has been used for cancer imaging and therapy in various ways, including direct conjugation or conjugation to a cargo. The clinical pharmacokinetics of IBD indicate that this BP has powerful bone mineral affinity.[31]

Because of its good physical features and low availability from a generator, ^{99m}Tc has become the most essential nuclide for organ imaging in nuclear medicine. BPs can be labeled with ^{99m}Tc and used for bone imaging because of their good localization in the skeleton and fast clearance from soft tissues. Since Qiu et al.[32] discovered that BPs have a high affinity for bone minerals in 1968, several ^{99m}Tc-labeled phosphate compounds have been developed for skeletal imaging.

$^{99m}TcO_4^-$ was eluted from ^{99}Mo/^{99m}Tc generator in +7 oxidation level. Since the chemical reactivity of the $^{99m}TcO_4^-$ anion is so minimal, presence of a suitable reducing agent in the proper ratio is essential for successful direct labeling with ^{99m}Tc. Because to its quick action, perfect redox characteristics, and efficacy at room temperature, stannous chloride is the most often used reducing agent.[25] Here, stannous chloride was used as a reducing agent.

In the preparation of [^{99m}Tc]Tc-IBD, three types of ^{99m}Tc could be present: (1) $^{99m}TcO_4^-$ that has not been reduced by stannous chloride, (2) R/H $^{99m}TcO_4^-$ that did not react with IBD and was bonded to hydrolyzed stannous chloride, and (3) [^{99m}Tc]Tc-IBD (the desired molecule).

Generally, using an excess of stannous chloride for ^{99m}Tc reduction can result in the desired radiolabeled complexes, but it can also create unwanted radiocolloids that are uptaken by macrophages and so concentrate in RES organs, irradiating them unnecessarily. For this reason, the amount of reducing agent is one of the most important parameters in the radiolabeling procedure of any molecule with ^{99m}Tc. The amount

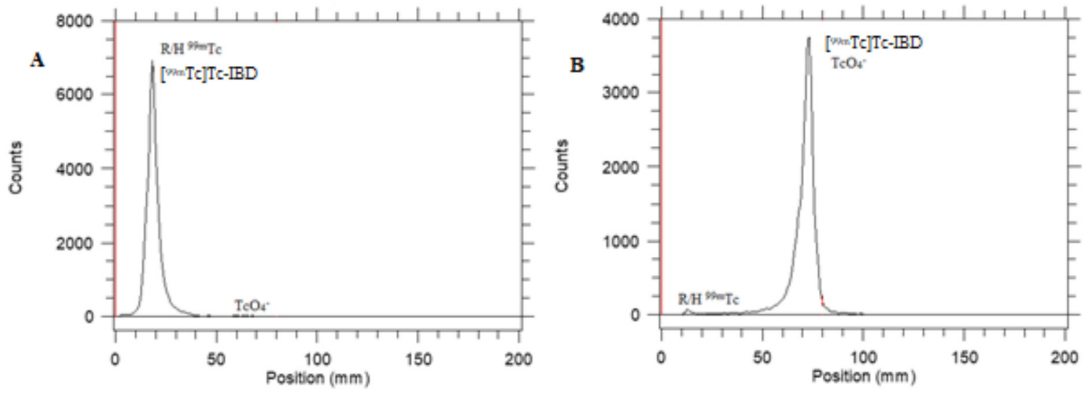

Figure 10. RTLC chromatogram of [^{99m}Tc]Tc-IBD in different mobile phases: A: acetone, B: ACN/W/TFA (50/25/1.5)

^{99m}Tc: Technetium-99m, IBD: Ibandronate sodium, RTLC: Radioactive thin layer chromatography, ACN/W/TFA: Acetonitrile/water/trifluoroacetic acid

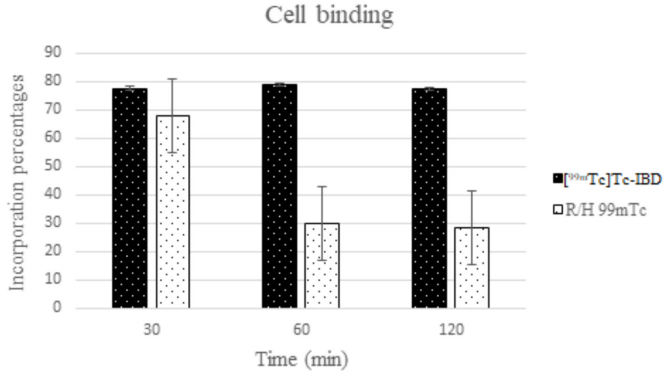

Figure 11. Incorporation percentage of [^{99m}Tc]Tc-IBD and R/H ^{99m}Tc to the U2OS cell lines for 30, 60, and 120 min

^{99m}Tc: Technetium-99m, IBD: Ibandronate sodium

of stannous chloride needed for efficient ^{99m}Tc labeling of IBD was found to be 20 µg (Figure 2).

For RTLC studies, ITLC-SG with two mobile phases [acetone and ACN/W/TFA (50/25/1.5)] (Figure 10) was used to study the effects of reaction pH and incubation time, and the amount of the reducing agent on the radiolabeling yield and stability of [^{99m}Tc]Tc-IBD. IBD was radiolabeled with ^{99m}Tc with high yields (95%) at pH 5.5 (Figure 6). After 15 min at room temperature, radiolabeling was confirmed to be complete (Figure 4). No further purification was required because the radiolabeling yield of [^{99m}Tc]Tc-IBD complexes was greater than 95%. Additionally, [^{99m}Tc]Tc-IBD was quite stable and labeling efficiency was found >90% for 24 h in SF (Figure 8) and >90% for 2 h in cell medium (Figure 9).

In vitro cell binding tests revealed that [^{99m}Tc]Tc-IBD had the highest cell binding capability for U2OS cells, and that binding ratio of [^{99m}Tc]Tc-IBD to bone cancer cells was higher than that of R/H $^{99m}TcO_4^-$. According to the data, the cell binding ratio did not alter at any of the time periods (30, 60 or 120 min) (Figure 11). In addition to this result, the percentage of IBD binding to HA was found to be 83.70 ± 3.67 that has high incorporated to bone minerals.

IBD was previously labeled with ^{99m}Tc and bone uptake was evaluated.[33] According to this study, IBD (300 µg) was radiolabeled with high radiolabeling efficiency (98.6%) using 25 µg of stannous chloride at room temperature at pH 7 for 15 min incubation time. Then, the radiolabeled complex was purified by high performance liquid chromatography (HPLC). Although the *in vitro* stability study was determined for 8 h, [^{99m}Tc]Tc-IBD was found to be stable for 6 h. According to the performed biodistribution study, [^{99m}Tc]Tc-IBD indicated high uptake and long retention in bone (44.32 % ID/organ) at (1 h) post-injection. Thus, it was concluded that [^{99m}Tc]Tc-IBD could be used as a selective potential imaging agent for diagnosis of bone diseases.[33]

CONCLUSION

In this study, we demonstrated that IBD can be labeled with ^{99m}Tc with high RP (>95%) using a simple RTLC approach. The resultant complex was extremely stable with labeling efficiency maintaining up to 6 h. At pH 5.5, formulations containing 20 µg stannous chloride and 37 MBq $^{99m}TcO_4^-$ yielded the highest RP.

According to the cell culture data, [^{99m}Tc]Tc-IBD was demonstrated to be a valuable tool for determining the cancer cell binding affinity *in vitro*. Incorporation of [^{99m}Tc]Tc-IBD to U2OS cells was greater than that of R/H $^{99m}TcO_4^-$. Because of these encouraging radiolabeling and cell culture results, [^{99m}Tc]Tc-IBD will be studied further in nuclear medicine patients for bone cancer diagnosis.

ACNOWLEDGMENTS

TLC scanner used herein was funded by Prime Ministry State Planning Organization Foundation of Republic of Türkiye (grant project number: 09DPT001), which the authors gratefully acknowledge. The authors further acknowledge the Nuclear Medicine Department at Ege University for supplying the radioisotope ($^{99m}TcO_4^-$) and Dr. Petek Ballar-Kırmızıbayrak for contributing the cell line (U2OS) used in this study.

Ethics

Ethics Committee Approval: Not applicable.

Informed Consent: Not applicable.

Peer-review: Externally peer-reviewed.

Authorship Contributions

Surgical and Medical Practices: M.E., D.İ.Ö., Concept: M.E., D.İ.Ö., M.A., Design: M.E., D.İ.Ö., Data Collection or Processing: M.E., D.İ.Ö., E.Ö., Analysis or Interpretation: M.E., D.İ.Ö., E.G., Literature Search: M.E., D.İ.Ö., Writing: M.E.

Conflict of Interest: No conflict of interest was declared by the authors.

Financial Disclosure: The authors declared that this study received no financial support.

REFERENCES

1. Bartl R, Frisch B, Tresckow E, Christoph B. Bisphosphonates. In: Bartl R, Frisch B, Tresckow E, Christoph B, eds. Biphosphonates in Medical Practice. (1st ed). Springer, Berlin, Heidelberg; 2007:33-70.
2. Bauss F, Schimmer RC. Ibandronate: the first once-monthly oral bisphosphonate for treatment of postmenopausal osteoporosis. Ther Clin Risk Manag. 2006;2:3-18.
3. Abtahi J, Klintström B, Klintström E. Ibandronate reduces the surface bone resorption of mandibular bone grafts: a randomized trial with ınternal controls. JBMR Plus. 2021;5:e10468.
4. Epstein S, Zaidi M. Biological properties and mechanism of action of ibandronate: application to the treatment of osteoporosis. Bone. 2005;37(4):433-440.
5. Bittner B, McIntyre C, Jordan P, Schmidt J. Drug-drug interaction study between a novel oral ibandronate formulation and metformin. Arzneimittelforschung. 2011;61:707-713.
6. Palma E, Oliveira BL, Correia JD, Gano L, Maria L, Santos IC, Santos I. A new bisphosphonate-containing (99m)Tc(I) tricarbonyl complex potentially useful as bone-seeking agent: synthesis and biological evaluation. J Biol Inorg Chem. 2007;12:667-679.
7. Ogawa K, Kawashima H, Shiba K, Washiyama K, Yoshimoto M, Kiyono Y, Ueda M, Mori H, Saji H. Development of [90Y]DOTA-conjugated bisphosphonate for treatment of painful bone metastases. Nucl Med Biol. 2009;36:129-135.
8. Suzuki K, Satake M, Suwada J, Oshikiri S, Ashino H, Dozono H, Hino A, Kasahara H, Minamizawa T. Synthesis and evaluation of a novel 68Ga-chelate-conjugated bisphosphonate as a bone-seeking agent for PET imaging. Nucl Med Biol. 2011;38:1011-1018.
9. Makris G, Tseligka ED, Pirmettis I, Papadopoulos MS, Vizirianakis IS, Papagiannopoulou D. Development and pharmacological evaluation of new bone-targeted (99m)Tc-radiolabeled bisphosphonates. Mol Pharm. 2016;13:2301-2317.
10. Gundogdu E, Ilem-Ozdemir D, Asikoglu M. *In vitro* incorporation studies of 99mTc-alendronate sodium at different bone cell lines. J Radioanal Nucl Chem. 2014;299:1255-1260.
11. Ilem Ozdemir D, Gundogdu E, Ekinci M, Ozgenc E, Asikoglu M. Comparative permeability studies with radioactive and nonradioactive risedronate sodium from self-microemulsifying drug delivery system and solution. Drug Dev Ind Pharm. 2015;41:1493-1498.
12. Elitez Y, Ekinci M, Ilem-Ozdemir D, Gundogdu E, Asikoglu M. Tc-99m radiolabeled alendronate sodium microemulsion: characterization and permeability studies across Caco-2 Cells. Curr Drug Deliv. 2018;15:342-350.
13. Motaleb HA, Ibrahim IT, El-Tawoosy M, Mohamed MI. Synthesis, preclinical, and pharmacokinetic evaluation of a new zoledronate derivative as a promising antiosteoporotic candidate using radiolabeling technique. J Labelled Comp Radiopharm. 2017;60:542-549.
14. Gundogdu E, Ekinci M, Ozgenc E, Ozdemir DI, Asikoglu M. Development and evaluation of liquid and solid lipid based drug delivery systems containing technetium-99m-radiolabeled alendronate sodium. Curr Radiopharm. 2018;11:100-108.
15. Ilem-Ozdemir D, Atlihan Gundogdu E, Ekinci M, Ozgenc E, Asikoglu M. In: Grumezescu AM, ed. Nuclear medicine and radiopharmaceuticals for molecular diagnosis. I Biomedical Applications of Nanoparticles. (1st ed). Elsevier Inc. 2019:457-490.
16. Ekinci M, İlem-Özdemir D. Radyofarmasötikler ve teranostikler. J Lit Pharm Sci. 2021;10:119-132.
17. Ting G, Chang CH, Wang HE. Cancer nanotargeted radiopharmaceuticals for tumor imaging and therapy. Anticancer Res. 2009;29:4107-4118.
18. Ekinci M, Ilem-Ozdemir D, Gundogdu E, Asikoglu M. Methotrexate-loaded chitosan nanoparticles: preparation, radiolabeling and *in vitro* evaluation for breast cancer diagnosis. J Drug Deliv Sci Technol. 2015;30:107-113.
19. Ozgenc E, Ekinci M, Ilem-Ozdemir D, Gundogdu E, Asikoglu M. Radiolabeling and *in vitro* evaluation of ^{99m}Tc-methotrexate on breast cancer cell line. J Radioanal Nucl Chem. 2016;307:627-633.
20. Ekinci M, Öztürk AA, Santos-Oliveira R, İlem-Özdemir D. The use of Lamivudine-loaded PLGA nanoparticles in the diagnosis of lung cancer: preparation, characterization, radiolabeling with 99mTc and cell binding. J Drug Deliv Sci Technol. 2022;69:103139.
21. Gundogdu E, Ilem-Ozdemir D, Ekinci M, Ozgenc E, Asikoglu M. Radiolabeling efficiency and cell incorporation of chitosan nanoparticles. J Drug Deliv Sci Technol. 2015;29:84-89.
22. İlem-Özdemir D, Karavana SY, Şenyiğit ZA, Çalışkan Ç, Ekinci M, Asikoglu M, Baloğlu E. Radiolabeling and cell incorporation studies of gemcitabine HCl microspheres on bladder cancer and papilloma cell line. J Radioanal Nucl Chem. 2016;310:515–522.
23. Ilem-Ozdemir D, Atlihan-Gundogdu E, Ekinci M, Halay E, Ay K, Karayildirim T, Asikoglu M. Radiolabeling and *in vitro* evaluation of a new 5-fluorouracil derivative with cell culture studies. J Label Compd Radiopharm. 2019;62:874-884.
24. İlem-Özdemir D, Ekinci M, Gündoğdu E, Aşıkoğlu M. Estimating binding capability of radiopharmaceuticals by cell culture studies. Int J Med Nano Res. 2016;3:014.
25. Spies H, Pietzsch HJ. Stannous chloride in the preparation of 99mTc pharmaceuticals. In: Zolle I, ed. Technetium-99m pharmaceuticals: preparation and quality control in nuclear medicine. Springer, Berlin, Heidelberg. 2007:59-66.
26. Liu S. 6-hydrazinonicotinamide derivatives as bifunctional coupling agents for 99mTc-labeling of small biomolecules. Top Curr Chem. 2005;252:117-153.
27. British Pharmacopoeia 2019. London; 2018.
28. EANM Radiopharmacy Committee. Guidelines on current good radiopharmacy, practice (CGRPP) in the preparation of radiopharmaceuticals. 2007. https://www.eanm.org/publications/guidelines/gl_radioph_cgrpp.pdf

29. Chadha N, Sinha D, Tiwari AK, Chuttani K, Mishra AK. Synthesis, biological evaluation and molecular docking studies of high-affinity bone targeting *N,N*(')-bis(alendronate) diethylenetriamene-*N,N'*-triacetic acid: a bifunctional bone scintigraphy agent. Chem Biol Drug Des. 2013;82:468-476.

30. Chavdarova L, Piperkova E, Tsonevska A, Timcheva K, Dimitrova M. Bone scintigraphy in the monitoring of treatment effect of bisphosphonates in bone metastatic breast cancer. J BUON. 2006;11:499-504.

31. Ringe JD, Body JJ. A review of bone pain relief with ibandronate and other bisphosphonates in disorders of increased bone turnover. Clin Exp Rheumatol. 2007;25:766-774.

32. Qiu L, Cheng W, Lin J, Luo S, Xue L, Pan J. Synthesis and biological evaluation of novel $^{(99m)}$Tc-labelled bisphosphonates as superior bone imaging agents. Molecules. 2011;16:6165-6178.

33. Soliman M. ^{99m}Tc-ibandronate as imaging radiopharmaceutical for early detection of bone diseases. Bull Fac Sci Zagazig Univ. 2020. https://bfszu.journals.ekb.eg/article_119256.html

Turk J Pharm Sci 2023;20(2):100-107
DOI: 10.4274/tjps.galenos.2022.50887

ORIGINAL ARTICLE

Effect of Oligopeptides-Homologues of the Fragment of $ACTH_{15-18}$ on Morphogenetic Markers of Stress in the Adrenal Glands on the Model of Acute Cold Injury in Rats

Olesia KUDINA*, Sergii SHTRYGOL', Yulia LARJANOVSKA

National University of Pharmacy, Department of Pharmacology and Pharmacotherapy, Kharkiv, Ukraine

ABSTRACT

Objectives: Aim of the current study was to evaluate the stress-protective effect of oligopeptides-homologues of the adrenocorticotropic hormone (ACTH) fragment 15-18 on morphogenetic signs of stress reaction of the adrenal glands under acute cold exposure (CE) in rats.

Materials and Methods: The acute cold stress was reproduced by placing random-bred male rats in a freezer at a temperature of -18°C for 2 hours. The peptides-homologous of $ACTH_{15-18}$ acetyl-(D-Lys)-Lys-Arg-Arg-amide (KK-1) and acetyl-(D-Lys)-Lys-(D-Arg)-Arg-amide (KK-5) and the reference medicine (Sema) were administered intranasally in a dose of 20 mg/kg 30 minutes before and after CE. Rectal temperature was measured before and 10 min after CE. *Zona glomeruloza*, *zona fasciculata*, *zona reticularis*, and the area of cells and nuclei of adrenocorticocytes of the *zona fasciculata* were measured.

Results: KK-1 significantly prevented structural changes in the adrenal cortex and medulla and stabilized the secretory activity of glucocorticoid-producing cells. However, the congestion of the capillaries of the *zona fasciculata* and *zona reticularis* remained in some locations. *Zona fasciculata* cells had a marked tendency to decrease, and the area of nuclei significantly decreased ($p<0.05$) recovering the width to control animals' markers. KK-5 had a more marked recovery of the adrenal glands (a greater saturation of cytoplasm of adrenocorticocytes of *zona glomerulosa* and *zona fasciculata*). The number of chromaffin cells at rest was increased in the *adrenal medulla*. KK-5 statistically significantly normalized both the area of cells ($p<0.05$) and the area of nuclei ($p<0.05$) of the *zona fasciculata*, unlike KK-1, which reliably restored only the marker of the nuclei area. Some morphometric parameters of acute stress hypertrophy remained in the adrenal glands of rats receiving Sema.

Conclusion: KK-1 and KK-5 prevented the manifestation of acute stress reactions in the adrenal cortex of rats. KK-5 had a more marked stress-protective effect compared with the peptide KK-1. Both study substances exceeded the reference medicine Sema. KK-5 is a promising stres-sprotector and frigoprotector.

Key words: Stres sprotectors, acute cold stress, cold trauma, adrenal gland morphology, neuropeptides, oligopeptides-homologues of the fragment of $ACTH_{15-18}$

INTRODUCTION

Stress underlies the pathogenesis of many diseases of the cardiovascular, immune, central nervous, and other systems.[1] Prolonged stress exposure reduces the adaptive capabilities of the body and leads to the development of adaptation disease.[2] One of the leading links in the harmful effects of stress is the disruption of the peptidergic system,[3,4] which makes it relevant to search for stress detectors among these substances. The range of peptidergic drugs having stress-protective activity is narrow. It is known that stress activates the release of adrenocorticotropic hormone (ACTH), which led to glucocorticoid hormone release by adrenal glands. Taking into account the leading role of the hypothalamus-pituitary-adrenal axis in regulating the body's response to stress,[5,6] it seems promising to search for stress detectors among oligopeptides-

*Correspondence: olesiakudina@gmail.com, Phone: +38 057 706 30 69, ORCID-ID: orcid.org/0000-0002-8080-2286
Received: 21.03.2022, Accepted: 14.06.2022

©Copyright 2023 by Turkish Pharmacists' Association / Turkish Journal of Pharmaceutical Sciences published by Galenos Publishing House.
Licenced by Creative Commons Attribution-NonCommercial-NoDerivatives 4.0 (CC BY-NC-ND)

homologues of the fragment of ACTH. Peptides-homologues of the fragment of $ACTH_{15-18}$ (Lys-Lys-Arg-Arg) were obtained at the Institute of Highly Pure Biopreparations (St. Petersburg, Russia). In previous studies, we have established the stress-protective effect of peptides on models of acute immobilization[7,8] and acute cold stress on the effect on behavioral reactions, anxiety, and physical endurance of animals,[9] markers of carbohydrate metabolism,[10] blood systems.[11] The issue of the morphogenesis changes in the adrenal response to acute cold stress and the influence of frigoprotectors on these processes has been insufficiently studied, but such data are important for optimizing the frigoprotective effect. Taking into account that adrenal glands have one of the main roles in the body-response to stress, purpose of the current study is to evaluate the stress-protective effect of oligopeptides-homologues of the ACTH fragment 15-18 on morphogenetic signs of stress reaction of adrenal glands under acute cold exposure (CE) in rats.

MATERIALS AND METHODS

Experimental animals and ethical clearance

30 adult (3 months old) random-bred male rats (249 ± 5 g) were taken from the vivarium of the National University of Pharmacy (Kharkiv, Ukraine). The animals were housed in standard polypropylene cages at 22-24°C and 50% humidity in the well-ventilated room with a 12 hour light/dark cycle and free access to food and water. The work was carried out in the Educational and Scientific Institute of Applied pharmacy of the National University of Pharmacy in compliance with Directive 2010/63/EU of the European Parliament and the Council "On the protection of animals used for scientific purposes" (Brussels, 2010). All experimental protocols were approved by the Bioethics Commission of the National University of Pharmacy (no: 6, 8 June, 2021).

Drugs and chemicals

Peptide homologs of the fragment of $ACTH_{15-18}$ (Lys-Lys-Arg-Arg) under the laboratory codes KK-1 [acetyl-(D-Lys)-Lys-Arg-Arg-amide] and KK-5 [Acetyl-(D-Lys)-Lys-(D-Arg)-Arg-amide] were synthesized at the Institute of Highly Pure Biopreparations by A. A. Kolobov. The peptides were obtained by solid-phase synthesis methods using Boc-technology and purified by preparative reverse-phase chromatograph; their purity was at least 98%. In these compounds, one (KK-1) or two (KK-5) natural amino acids are replaced by the corresponding D-stereomer. Peptides do not relieve any hormonal activity and due to the presence of D-amino acids have increased resistance to human serum proteases, are practically non-toxic substances.[12]

Study design

The model of acute cold stress was reproduced by placing animals in a freezer "NordInter-300" at a temperature of -18° C for 2 hours in individual plastic pencil cases with a volume of 5 dm^3 without limiting airflow and motor activity.[13,14] This experimental model was chosen according to the aim study and the results of a previous investigation that showed a positive influence of peptide homologs of the fragment of $ACTH_{15-18}$ on behavioral reactions, anxiety, and physical endurance of animals,[9] markers of carbohydrate metabolism,[10] and blood systems.[11] The peptides-homologous of the fragment of $ACTH_{15-18}$ were administered intranasally (*i/n*) in the form of a solution in an effective stress-protective dose of 20 mcg/kg 30 min before and after CE. This dosage was chosen to take into account the cerebroptotective and stressprotective properties relieved in previous investigations.[7-11] The reference medicine, Sema (peptogen, RF), was administered *i/n* at a dose of 20 mcg/kg in a similar treatment. Heptapeptide semax (Met-Glu-His-Phe-Pro-Gly-Pro) is a synthetic analog of ACTH fragment 4-7 without hormonal activity. It is used to increase the adaptive capacity of the body under stress.[15]

The animals were divided into 5 groups (6 rats in each group). Group 1: control; group 2: CE (rats were exposed to acute cold stress); groups 3-5 - animals with CE who received experimental therapy: group 3: CE + KK-1, group 4: CE + KK-5, group 5: CE + Sema. Rectal temperature was measured with a WSD-10 thermometer before and 10 min after CE.

Adrenal gland histopathology

Animals were removed from the experiment 2 h after cold stress exposure by decapitation under thiopental anesthesia (40 mg/kg). Adrenal glands of the animals were fixed in a 10% formalin solution, dehydrated in alcohols of increasing concentration, and poured into paraffin. The sections were stained with hematoxylin and eosin.[16]

The photographs were processed on a Pentium 2.4 GHz computer using the Toup View program. In the photographs, using the Toupcam Granum program, the width of zones of the adrenal gland cortex (microns, μm) was measured: the *zona glomeruloza* (WZG), the *zona fasciculata* (WZF), the *zona reticularis* (WZR); the area of cells and nuclei (microns, μm^2) of adrenocorticocytes of *zona fasciculata* (AcZF, AnZF).

Statistical analysis

Statistical processing was carried out by methods of variational statistics using a standard package of statistical programs "Statistica, V. 6.0".[17-19] The results are expressed as mean ± standard error of mean (the level of statistical significance was considered $p<0.05$) or Me (LQ;UQ). Statistical differences between groups were analyzed using the parametric Student's *t*-test in cases of normal distribution and non-parametric Mann-Whitney *U* test and Kruskal-Wallis test in cases of its absence.

RESULTS

After the 24 h acute CE in rats of the group with CE, the rectal temperature significantly decreased by an average of 3°C ($p<0.05$), or 8% relative to the initial level (Table 1). All three peptides decreased the severity of hypothermia compared to the CE group: body temperature decreased by 1.0°C, or 2.7% (KK-1); by 0.3°C, or 0.8% (KK-5), and 0.4°C, or 1.1% (Semax). This decrease was statistically significant for all groups, respectively ($p<0.05$). The temperature of rats treated with the oligopeptides being studied did not differ from that of intact animals.

The histostructure of the adrenal cortex and medulla of the rats of the intact control group fully corresponds to the status of a physiologically functioning organ (Figure 1).

According to morphometry, functional state of adrenal glands of control rats is characterized by the following indicators: WZG was 44.64 microns, WZF-174.1 microns, WZR-78.4 microns; AcZF-168.8 microns 2, and AnZF-34.1 microns (Table 2).

In the majority of rats in the CE group, focal disorientation of connective tissue fibers in the capsule, their plasma impregnation, and tearing were observed (Figure 2A, B).

In *zona fasciculata*, linearity of corticocyte strands is broken in places, there is a decrease in their vacuolization, appearance of areas of complete cell defatting, which sometimes extends to the outer zone up to *zona glomerulosa*. Some nuclei had not a rounded, but a more elongated, "lobed" shape. The boundary between *zona glomerulosa* and *zona fasciculata* is not always clear, while the capillary net is expanded and congested (Figure 2C-E). The cells of *zona reticularis* have not been visually changed. The expansion and congestion of the venous-capillary net of *zona reticularis* were observed (Figure 3F). In the *adrenal medulla*, number of the cells with basophilic cytoplasm increased markedly with a decrease in the number or absence of vacuoles (Figure 2G).

According to morphometric measurements, WZF in the rats of CE group had significantly increased. There was a clear tendency toward an increase in AcZF and a significant increase

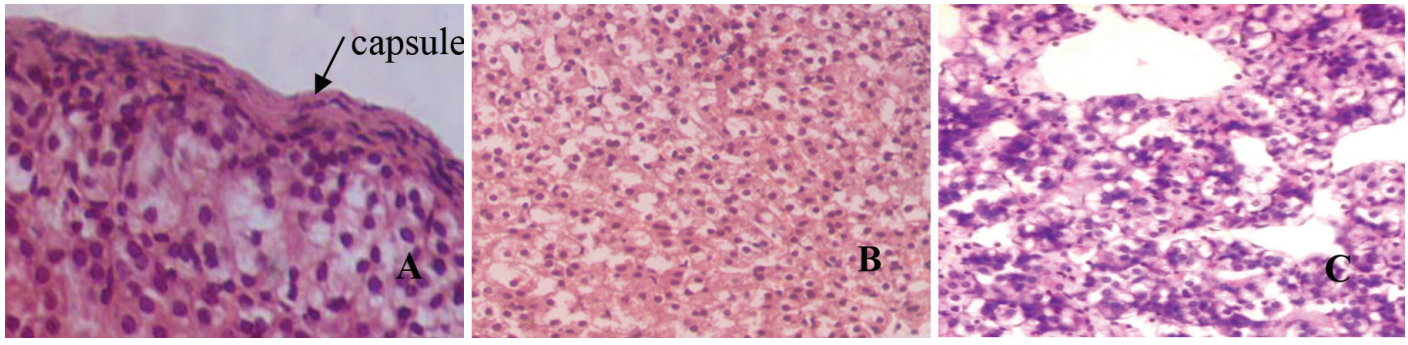

Figure 1. The adrenal gland of a control rat. (A) Capsule and cells of *zona glomeruloza* (arrow), hematoxylin-eosin, x400; (B) *zona fasciculata*, hematoxylin-eosin, x400; (C) chromaffin cells of the *adrenal medulla*, hematoxylin-eosin, x250

Table 1. The effect of the peptides KK-1, KK-5, and Sema on the body temperature of rats before and after a 24 h cold exposure at -18°C

Observation period	Group of animals, body temperature (°C)				
	Control	CE	CE + KK-1	CE + KK-5	CE + Sema
Before CE	36.8 ± 0.21	37.4 ± 0.38	37.5 ± 0.5	36.6 ± 0.35	37.1 ± 0.45
10 minutes after CE	-	34.4 ± 0.21*	36.5 ± 0.4#	36.3 ± 0.4#	36.7 ± 0.57#

*p<0.05 compared with intact, #p<0.05 compared with the CE group (Student's criterion). CE: Cold exposure

Table 2. The effect of acute cold stress on the morphometric markers of the adrenal glands of rats (Me (LQ; UQ)

Group of animals	Markers				
	WZG, μm	WZF, μm	WZR, μm	AcZF, μm^2	AnZF, μm^2
Control	44.64 (38.03; 45.15)	174.1 (163.6; 181.3)	78.4 (72.4; 86.9)	168.8 (159.7; 187.6)	34.1 (32.9; 35.1)
Cold exposure	43.90 (43.09; 45.10)	187.5 (179.1; 191.6)*	86.2 (74.3; 88.4)	186.4 (175.3; 199.1)	39.0 (38.8; 39.4)*
Cold exposure + KK-1	41.56 (33.34; 50.63)	179.8 (169.3; 190.1)	75.7 (61.3; 88.4)	177.6 (156.3; 191.6)	33.3 (30.3; 38.8)^
Cold exposure + KK-5	41.08 (39.85; 42.28)	173.2 (166.7; 182.8)^	77.4 (75.4; 80.3)	157.0 (149.1; 161.1)^	32.9 (32.4; 36.3)^
Cold exposure + Sema	40.47 (39.07; 47.84)	181.7 (180.3; 186.8)	81.6 (68.1; 85.5)	205.2 (188.2; 219.0)*#	36.1 (34.9; 39.1)*#
p	0.9235	0.2468	0.8303	0.0075	0.0011

p: The level of statistical significance when comparing samples (Kruskal-Wallis criterion), *p<0.05 compared with the control group (Mann-Whitney U criterion); ^p<0.05 compared with the cold exposure group (Mann-Whitney U criterion); #p<0.05 compared with the group of animals treated with KK-5 peptide (Mann-Whitney U criterion)

in AnZF, whereas WZG and WZR did not change in comparison with the markers of control (Table 2).

Changes in the connective tissue fibers of the adrenal capsule of rats that received KK-1 peptide under acute general hypothermia was expressed insignificantly. There is only a weakly pronounced focal tearing of the capsule. The cells of *zona glomerulosa* retain their location and their cytoplasm contains a different number of vacuoles. Cytoplasm vacuolization was increased in corticocytes of *zona fasciculata* and there were no marks of defatting (Figure 3A). The congestion of the capillaries of *zona fasciculata* and *zona reticularis* is preserved in some locations. The number of cells with basophilic cytoplasm and the presence of vacuoles in the medulla is increased (Figure 3B).

Results of the morphometric analysis confirmed positive effect of KK-1 peptide on prevention of adrenal gland hypertrophy under acute cold stress. Thus, AcZF had a marked tendency to decrease and AnZF significantly decreased compared with rats of the CE group. All this contributed to the recovery of WZF to the markers of control animals (Table 2).

Peptide KK-5 had a more marked positive effect on the histostructure of the adrenal glands. This was expressed in greater and evenly saturation of the cytoplasm of adrenocorticocytes both of *zona glomerulosa* and *zona fasciculata* (Figure 4A). More chromaffin cells of the medulla were in a state of functional rest (Figure 4B).

Morphometric markers of the adrenal cortex confirmed the marked positive effect of KK-5 peptide on the adrenal glands under acute stress hypertrophy. WZF, AcZF, and AnZF were significantly reduced in comparison with the markers of the CE group and practically reached the level of control (Table 2). Normalization of AcZF and AnZF significantly exceeded such markers of the reference drug.

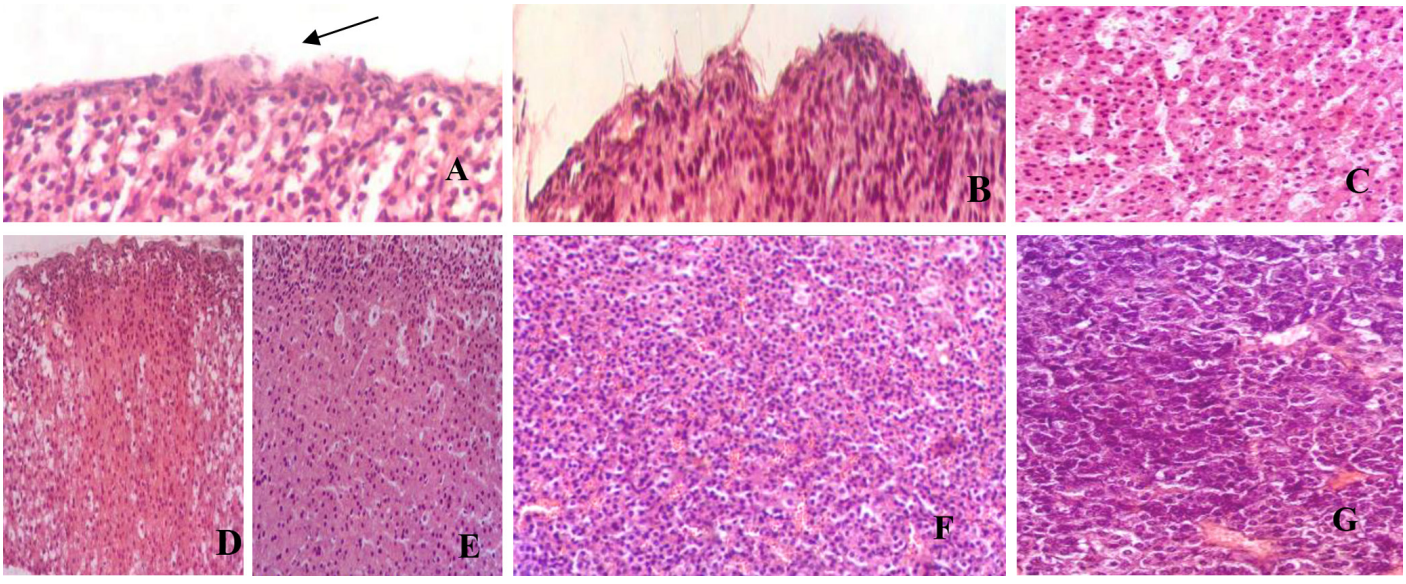

Figure 2. The adrenal gland of the animals of the cold exposure group (acute cold stress): (A) the disorientation of fibers, plasmatic impregnation in capsule (arrow); (B) disruption of arcade-like arrangement of corticocytes, the absence of vacuolization of the cytoplasm of cells; hematoxylin-eosin, x250; (C) reduction of vacuolization of the cytoplasm of corticocytes of *zona fasciculata*, expansion and congestion of the capillaries; hematoxylin-eosin, x250; (D, E) different size plots of complete defatting of corticocytes; hematoxylin-eosin, x250; (F) expansion and congestion of the venous-capillary net of *zona reticularis*; hematoxylin-eosin, x200; (G) an increase in endocrine cells with basophilic cytoplasm of the medulla, decrease or absence of vacuolization of the cytoplasm; hematoxylin-eosin, ×250

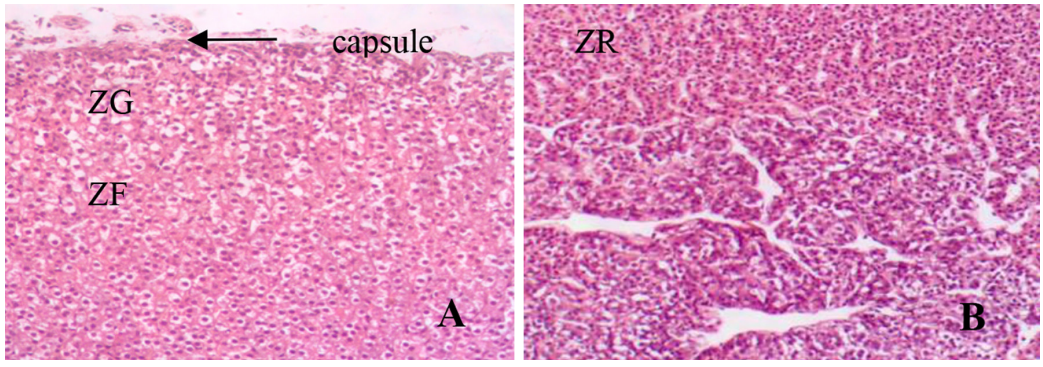

Figure 3. The adrenal gland of a rat received KK-1 peptide under acute cold stress. (A) Recovering of the functional state of *zona glomerulosa* (ZG) and *zona fasciculata* (ZF); hematoxylin-eosin, x200; (B) the normal state of cells and capillary net of *zona reticularis* (ZR), an increase in chromaffin cells of the *adrenal medulla*, which is relevant to the state of rest; hematoxylin-eosin, x200

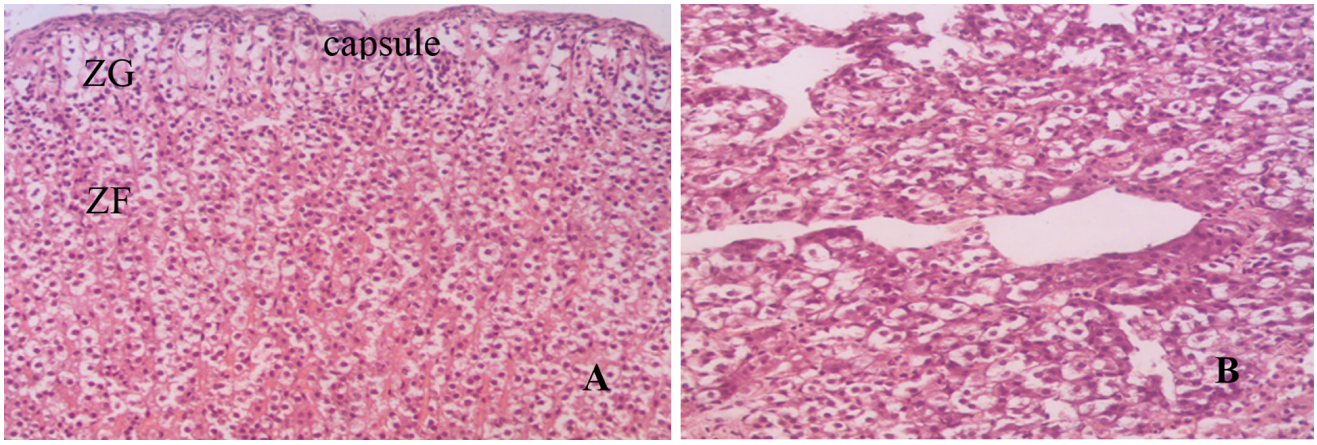

Figure 4. The adrenal gland of the rat received the peptide KK-5 under acute general hypothermia. (A) Complete recovering of the structural and functional state of *zona glomerulosa* (ZG) and *zona fasciculata* (ZF); hematoxylin-eosin, x200; (B) a significant number of chromaffin cells of the *adrenal medulla* in a state of functional rest; hematoxylin-eosin, x250

Small focal segments with disorientation, plasma impregnation, and fibrillation of connective tissue fibers are observed in the adrenal capsule of some rats having received Sema. The structure of *zona glomerulosa* is mostly restored, although there were small areas with indistinctness of arcade-like cell formation. There was not always clear linearity of the location of corticocytes in *zona fasciculata*; there were still enough cells with a decrease/absence of cytoplasm vacuolization. Foci of cell defatting with different severity were also observed in the middle and outer sections of *zona fasciculata* (Figure 5A, B).

In some locations, extension and congestion of capillaries are observed both in *zona fasciculata* and *zona reticularis*. The state of chromaffin cells of the medulla varied in different animals from the condition of rest to functional tension (Figure 5C, D). Morphometric parameters of the adrenal glands of rats after administration of Sema, the reference medicine, indicated that some markers of acute stress hypertrophy remained (Table 2). Thus, AcZF and AnZF had no statistically significant differences compared with animals in the CE group.

DISCUSSION

Stress is essential in the body's adaptation to adverse environmental factors, which, with prolonged exposure, turns into a pathogenic process.[2,20] One of the most common stressful factors is cold stress, which negatively affects health and productivity.[21] Due to the complexity of the pathogenesis of cold injury associated with cardiovascular, endocrine, central nervous, respiratory, immune, and other systems, the treatment is a challenging problem.[1] Considering that stress leads to disruption of the functioning of the peptidergic system,[4] it is advisable to study the stress-protective properties of neuropeptides. Since hypothalamus-pituitary-adrenal system participates in the mechanism of stress,[22] neuropeptides-homologues of ACTH deserve special attention in this aspect. Among such medicines, synthetic $ACTH_{1-24}$ Tetracosactide (Synacthen Depot®) is known, which is used for treating disseminated sclerosis, and a number of allergic diseases;[23] Sema is a synthetic analog of ACTH 4-10 with a nootropic and

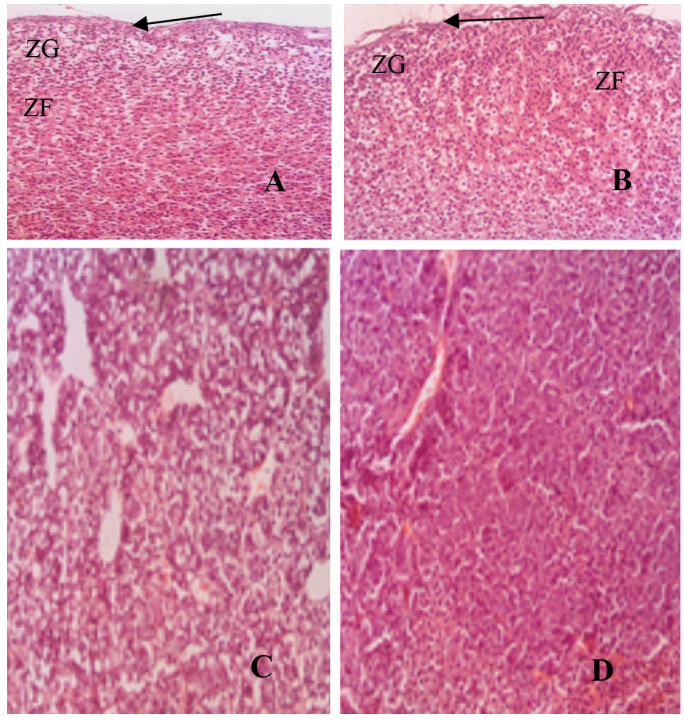

Figure 5. The adrenal gland of a rat that received Sema under acute cold stress. (A) A small area of disorientation of fibers in the capsule, incomplete recovering of the structure of *zona glomerulosa* (ZG), lack of linearity of the location of corticocytes of *zona fasciculata*, a moderate increase in vacuolization of the cytoplasm of cells of *zona fasciculata* (ZF); hematoxylin-eosin, x200. (B) Tearing of the capsule fibers, a site of a violation of the structure of *zona glomerulosa* (ZG), a site of complete defatting of the middle and outer sections of *zona fasciculata* (ZF); hematoxylin-eosin, x200. (C, D) Different functional states of chromaffin cells of the *adrenal medulla*: from a condition of rest (C) to tension (D). Hematoxylin-eosin x200

neuroprotective activity.[24,25] Stress-protective properties of these peptides are being studied currently.[26-29]

In our previous studies on the model of acute immobilization stress in rats, stress-protective properties of oligopeptides homologous to the primary amino acid sequence of $ACTH_{15-18}$ were revealed.[7,8] Under acute cold stress, a positive effect

of peptides on behavioral reactions, physical endurance, and carbohydrate metabolism was shown.[9,10] In the current study, using a model of acute cold injury, we confirmed the frigoprotective properties of these peptides to reduce hypothermia and found their marked protective effect on the histostructure of adrenal glands of rats under cold stress.

Exposure to acute cold stress caused marked morphological changes in all areas of the adrenal glands of rats that did not receive experimental therapy. Thus, there was a disorientation of connective tissue fibers in the capsule, a violation of the arcade-like arrangement of cells in the *zona glomerulosa* was observed, in *zona fasciculata* part of the nuclei had not a rounded, but an elongated shape. All these morphological changes indicate the functional tension of the adrenal glands. It is believed that this is a compensatory mechanism that intensifies metabolic processes by increasing the surface of the junction of the nuclear and cytoplasmic parts.[30]

Hypertrophy of the adrenal cortex was characterized by an increase in the area of adrenocorticocytes of *zona fasciculata* of adrenal cortex and their nuclei, which led to the expansion of this zone. An increase in the zone of adrenocorticocytes is also typically for models of chronic immobilization stress[31,32] and chronic variable/unpredictable stress in rats.[33] However, the level of corticosterone did not change in these stress models. Under acute cold stress in our study, an increase in cell size is accompanied by defatting the adrenal cortex, which indicates functional stress associated with stimulation of glucocorticoid hormone production. An increase in corticosterone production under stress is typically for both acute and chronic heat stress in rats.[34,35] Activation of the adrenal cortex under acute cold stress is accompanied by changes in its vascular system; expansion and congestion of capillaries, which coincides with the data of other scientists.[36]

KK-1 peptide significantly prevented structural changes in the adrenal cortex and medulla under acute cold stress, stabilized the secretory activity of glucocorticoid-producing cells, and contributed to the maintaining of lipid saturation. However, the congestion of capillaries of *zona fasciculata* and *zona reticularis* remained in some locations.

Much more complete recovery of the adrenal glands of rats receiving KK-5 peptide was observed, which was reflected in greater and uniform saturation of the cytoplasm of adrenocorticocytes of *zona glomerulosa* and *zona fasciculata*. The number of chromaffin cells in the state of rest was increased in *adrenal medulla*. The peptide KK-5 statistically significantly normalized both AcZF and AnZF, unlike KK-1 peptide, which reliably restored only the marker of AnZF.

The results of our study demonstrate a marked frigo- and stress-protective effects of peptides, which might be connected with a reduction in the effect of ACTH on the synthesis of glucocorticoids in *zona fasciculata* and release of epinephrine in *adrenal medulla*. It is known that ACTH belongs to the melanocortin family.[37,38] The ACTH receptor, known as MC2R, is located in *zona fasciculata* and *zona reticularis* of the adrenal cortex[22,39] and selectively binds only to ACTH.[40] Stimulation of MC2R promotes the production of glucocorticoids and mineralocorticoids by adrenal cortex under stress.[41] The sequence of amino acids of ACTH at positions 15-19 is responsible for its binding to MC2R.[42] In addition, it is supposed that ACTH participates in the regulation of its own secretion through negative feedback *via* MC2R mRNA detected in the pituitary gland.[43] We assume that stress-protective effect of the peptides-homologues being studied of the fragment of $ACTH_{15-18}$ is realized due to affinity to MC2R receptors, which leads to the prevention of the effect of ACTH on the development of histostructure changes in both the cortex and the *adrenal medulla* under stress.

The reduction range of morphogenetic marks of a stress reaction in the adrenal glands does not directly depend on the severity of the antihypothermic effect of the peptides under study. Thus, despite almost the same indicators of body temperature in the groups of animals receiving the peptide KK-5 and Sema under CE, morphological changes in the adrenal glands are almost absent in animals treated with the peptide KK-5, but moderately expressed in rats treated with Sema.

Thus, both peptides under study, especially KK-5, reduce morphogenetic signs of a stress reaction in the adrenal glands of rats under acute cold injury, surpassing Sema, the reference medicine. KK-5 peptide can be considered as the most promising frigoprotector.

Study limitations

The absence of discussion of hormonal status is the limitation of our study.

CONCLUSION

1. On the model of acute cold injury in rats, peptides-homologues of the fragment of $ACTH_{15-18}$ [acetyl-(D-Lys)-Lys-Arg-Arg-amide and acetyl-(D-Lys)-Lys-(D-Arg)-Arg-amide] and Sema, the reference medicine (Met-Glu-His-Phe-Pro-Gly-Pro), prevent hypothermia.

2. Acute cold exposure causes acute stress hypertrophy of the adrenal cortex in rats, which is characterized by an increase in the area of adrenocorticocytes of *zona fasciculata* and *zona reticularis* of the cortex. These changes are accompanied by defatting the adrenal cortex. This indicates functional tension associated with stimulation of glucocorticoid hormone production.

3. Peptides-homologues of the ACTH fragment 15-18 [acetyl-(D-Lys)-Lys-Arg-Arg-amide and acetyl-(D-Lys)-Lys-(D-Arg)-Arg-amide] prevent the manifestation of acute stress reactions in adrenal cortex of rats, which is proven by the absence of structural changes in the cortex. Also, the peptides stabilized the secretory activity of the glucocorticoid-producing cells and contributed to the maintaining of their lipid saturation. Thus, preserving the reserve capabilities of secretory cells, acetyl-(D-Lys)-Lys-Arg-Arg-amide and acetyl-(D-Lys)-Lys-(D-Arg)-Arg-amide peptides increase the resistance of adrenal cortex to the action of a cold factor having a stress-protective effect.

4. According to severity of the stress-protective effect, acetyl-(D-Lys)-Lys-(D-Arg)-Arg-amide has a more marked stress-protective effect compared to acetyl-(D-Lys)-Lys-Arg-Arg-amide, and both study substances exceed Sema, the reference medicine.

Ethics

Ethics Committee Approval: The work was carried out in the Educational and Scientific Institute of Applied Pharmacy of the National University of Pharmacy in compliance with Directive 2010/63/EU of the European Parliament and the Council "On the protection of animals used for scientific purposes" (Brussels, 2010). All experimental protocols were approved by the Bioethics Commission of the National University of Pharmacy (no: 6, 8 June, 2021).

Informed Consent: Not applicable.

Peer-review: Externally peer-reviewed.

Authorship Contributions

Surgical and Medical Practices: O.K., Y.L., Concept: O.K., Y.L., Design: S.S., Data Collection or Processing: O.K., Y.L., Analysis or Interpretation: S.S., O.K., Y.L., Literature Search: O.K., Y.L., Writing: O.K., S.S., Y.L.

Conflict of Interest: No conflict of interest was declared by the authors.

Financial Disclosure: The research was carried out within the framework of the topic "Experimental substantiation for improving the effectiveness of prevention and treatment of cold injuries" of the list of scientific studies of the Ministry of Health of Ukraine, carried out at the expense of the state budget of Ukraine no. 0120u102460 (Order of the Ministry of Health of Ukraine no. 2651 of 17.11.2020).

REFERENCES

1. Selye H. Stress and disease. Science. 1955;122:625-631.
2. Selye H. The general adaptation syndrome and the diseases of adaptation (two parts). J Allergy Clin Immunol. 1946;17: 231-247.
3. Shabanov PD, Lebedev AA. Kortikoliberinovye mekhanizmy rasshirennoy mindaliny i gipotalamusa: uchastie v formirovanii stressa, podkrepleniya i deystviya narkogenov [Corticoliberin mechanisms of the enlarged amygdala and hypothalamus: participation in the formation of stress, reinforcement and the action of narcotics]. Zhurnal Psikhofarmakol Biol Narkol. 2007;Spet.issue, part 2: 2011.
4. Heck AL, Crestani CC, Fernández-Guasti A, Larco DO, Mayerhofer A, Roselli CE. Neuropeptide and steroid hormone mediators of neuroendocrine regulation. J Neuroendocrinol. 2018;30:e12599.
5. Kopin IJ. Catecholamines, adrenal hormones, and stress. Hosp Pract. 1976;11:49-55.
6. Goldstein DS. Adrenal responses to stress. Cell Mol Neurobiol. 2010;30:1433-1440.
7. Kudina OV, Shtrygol' SYu, Tsyvunin VV, Kolobov AA. Stressprotektornoe deystvie novykh oligopeptidov – analogov fragmenta $AKTG_{15-18}$ – na modeli ostrogo immobilizatsionnogo stressa [Stress-protective activity of new oligopeptides – $ACTH_{15-18}$ analogues on the model of acute immobilization stress]. Éksp Klin Farmakol. 2018;81:12-16 [in Russian].
8. Kudina OV, Shtrygol' SY, Kolobov A.A, Lar'yanovska YuB. Vliyanie oligopeptidov - gomologov fragmenta $AKTG_{15-18}$ na sostoyanie pecheni i nadpochechnikov krys na modeli ostrogo immobilizatsionnogo stressa [The influence of oligopeptides - the homologues of $ACTH_{15-18}$ on the liver and adrenal glands in the rats on the model of acute immobilization stress]. Rev Clin Pharmacol Drug Therapy. 2017;4:30-37 [in Russian].
9. Kudina OV, Shtrygol' SYu, Kolobov AA. Doklinichne doslidzhennja stresprotektornyh vlastyvostej oligopeptydiv - gomologiv fragmenta $AKTG_{15-18}$ na modeli gostrogo holodovogo stresu [Preclinical investigation of stress-protective properties of oligopeptides - homologs of the $ACTH_{15-18}$ fragment on the model of acute cold stress]. Pharmacol Drug Toxicol. 2018;58:41-48 [in Ukrainian].
10. Kudina OV, Shtrygol' SYu, Kolobov AA. Vliyanie oligopeptidov - gomologov fragmenta $AKTG_{15-18}$ na pokazateli uglevodnogo obmena v usloviyakh ostrogo kholodovogo stressa [Effect of oligopeptides - homologues of the $ACTH_{15-18}$ fragment on parameters of carbohydrate metabolism on in terms of acute cold stress]. Vestnik Farmatsii. 2019;1:64-70 [in Russian].
11. Kudina OV, Shtrygol' SYu, Kolobov AA. Vplyv oligopetydiv-gomologiv $AKTG_{15-18}$ na adaptacijni reakcii' krovi shhuriv na modeli gostrogo holodovogo stresu [The effect of oligopeptides-homologs of the $ACTH_{15-18}$ fragment on the adaptive response of rat blood on the acute cold stress model]. Ukrainian Biopharm J. 2020;65(4):40-45 [in Ukrainian].
12. Kovalitskaya YuA, Sadovnikov VB, Zolotarev YuA, Navolotskaya EV. Stressprotektornaya aktivnost' sinteticheskogo peptida CH3CO-Lys-Lys-Arg-Arg-NH 2 (protektina) [Stress-protective activity of the synthetic peptide CH_3CO-Lys-Lys-Arg-Arg-NH 2 (protectine)]. Bioorganicheskaya Khimiya. 2009;35:493-500.
13. Bondariev YV, Shtrygol' SY, Drogovoz SM, Shchokina KG. Holodova travma: doklinichne vyvchennja likars'kyh preparativ z fygoprotektornymy vlastyvostjamy: metod. rec. [Cold injury: preclinical study of drugs with frigoprotective properties. Guidelines]. Kharkiv; 2018.
14. Kapelka I, Shtrygol' S, Koiro O, Merzlikin S, Kudina O, Yudkevich T. Effect of arachidonic acid cascade inhibitors on body temperature and cognitive functions in rats in the Morris water maze after acute cold injury. Pharmazie. 2021;76:313-316.
15. Ashmarin IP, Levitskaya NG, Kamenskiy AA, Myasoedov NF. Semaks - novoe lekarstvennoe sredstvo dlya korrektsii krovoobrashcheniya mozga, gipoksicheskikh sostoyaniy i povysheniya umstvennoy rabotosposobnosti [Semax is a new medicine for the treatment of cerebral circulation, hypoxic conditions and increasing mental activity]. Farmateka. 1997;4:32-33 [in Russian].
16. Merkulov GA. Kurs patologogistologicheskoy tekhniki [Course of pathological and histological techniques]. Moscow; Meditsina; 1969 [in Russian].
17. Khalafyan AA. STATISTICA 6. Statisticheskiy analiz dannykh (3-e izd) [STATISTICA 6. Statistical data analysis (3rd ed)]. Moscow; OOO «Binom-Press»; 2007 [in Russian].
18. Lapach SN, Chubenko AV, Babich PN. Statisticheskie metody v mediko-biologicheskikh issledovaniyakh s ispol'zovaniem Excel [Statistical methods in biomedical research using Excel]. Kyiv; Morion; 2001 [in Russian].
19. Oyu R. Statisticheskiy analiz meditsinskikh dannykh. Primenenie paketa prikladnykh programm STATISTICA [Statistical analysis of medical data. Usage of the application package STATISTICA]. Moscow; MediaSfera; 2006 [in Russian].
20. Lecic-Tosevski D, Vukovic O, Stepanovic J. Stress and personality. Psychiatriki. 2011;22:290-297.

21. Castellani JW, Tipton MJ. Cold stress effects on exposure tolerance and exercise performance. Compr Physiol. 2015;6:443-469.

22. Berger I, Werdermann M, Bornstein SR, Steenblock C. The adrenal gland in stress - adaptation on a cellular level. J Steroid Biochem Mol Biol. 2019;190:198-206.

23. Panikratova YR, Lebedeva IS, Sokolov OY, Rumshiskaya AD, Kupriyanov DA, Kost NV, Myasoedov NF. Functional connectomic approach to studying selank and semax effects. Dokl Biol Sci. 2020;490:9-11.

24. Glazova NY, Manchenko DM, Volodina MA, Merchieva SA, Andreeva LA, Kudrin VS, Myasoedov NF, Levitskaya NG. Semax, synthetic ACTH(4-10) analogue, attenuates behavioural and neurochemical alterations following early-life fluvoxamine exposure in white rats. Neuropeptides. 2021;86:102114.

25. Medvedeva EV, Dmitrieva VG, Limborska SA, Myasoedov NF, Dergunova LV. Semax, an analog of $ACTH_{(4-7)}$, regulates expression of immune response genes during ischemic brain injury in rats. Mol Genet Genomics. 2017;292:635-653.

26. Fomenko EV, Bobyntsev II, Ivanov AV, Belykh AE, Andreeva LA, Myasoedov NF. Effect of selank on morphological parameters of rat liver in chronic foot-shock stress. Bull Exp Biol Med. 2019;167:293-296.

27. Mukhina AY, Mishina ES, Bobyntsev II, Medvedeva OA, Svishcheva MV, Kalutskii PV, Andreeva LA, Myasoedov NF. Morphological changes in the large intestine of rats subjected to chronic restraint stress and treated with selank. Bull Exp Biol Med. 2020;169:281-285.

28. Svishcheva MV, Mukhina AY, Medvedeva OA, Shevchenko AV, Bobyntsev II, Kalutskii PV, Andreeva LA, Myasoedov NF. Composition of colon microbiota in rats treated with ACTH(4-7)-PGP peptide (semax) under conditions of restraint stress. Bull Exp Biol Med. 2020;169:357-360.

29. Samotrueva MA, Yasenyavskaya AL, Murtalieva VK, Bashkina OA, Myasoedov NF, Andreeva LA, Karaulov AV. Experimental substantiation of application of semax as a modulator of immune reaction on the model of "social" stress. Bull Exp Biol Med. 2019;166:754-758.

30. Stepanyan YuS. Strukturnye izmeneniya nadpochechnikov pri kholodovoy travme [Structural changes in the adrenal glands under cold injury]. Problemy Ekspertizy v Meditsine. 2009;36-4:21-23 [in Russian].

31. Aguilera G, Kiss A, Lu A, Camacho C. Regulation of adrenal steroidogenesis during chronic stress. Endocr Res. 1996;22:433-443.

32. Aguilera G, Kiss A, Sunar-Akbasak B. Hyperreninemic hypoaldosteronism after chronic stress in the rat. J Clin Invest. 1995;96:1512-1519.

33. Ulrich-Lai YM, Figueiredo HF, Ostrander MM, Choi DC, Engeland WC, Herman JP. Chronic stress induces adrenal hyperplasia and hypertrophy in a subregion-specific manner. Am J Physiol Endocrinol Metab. 2006;291:E965-973.

34. Wang LI, Liu F, Luo Y, Zhu L, Li G. Effect of acute heat stress on adrenocorticotropic hormone, cortisol, interleukin-2, interleukin-12 and apoptosis gene expression in rats. Biomed Rep. 2015;3:425-429.

35. Koko V, Djordjeviae J, Cvijiae G, Davidoviae V. Effect of acute heat stress on rat adrenal glands: a morphological and stereological study. J Exp Biol. 2004;207:4225-4230.

36. Ryzhavskiy BYa. Postnatal'nyy ontogenez korkovogo veshchestva nadpochechnikov [Postnatal ontogenesis of the adrenal cortex]. Novosibirsk; Nauka; 1989 [in Russian].

37. Fridmanis D, Roga A, Klovins J. ACTH receptor (MC2R) specificity: what do we know about underlying molecular mechanisms? Front Endocrinol (Lausanne). 2017;8:13.

38. Metz JR, Peters JJ, Flik G. Molecular biology and physiology of the melanocortin system in fish: a review. Gen Comp Endocrinol. 2006;148:150-162.

39. Mountjoy KG, Bird IM, Rainey WE, Cone RD. ACTH induces up-regulation of ACTH receptor mRNA in mouse and human adrenocortical cell lines. Mol Cell Endocrinol. 1994;99:R17-20.

40. Gantz I, Fong TM. The melanocortin system. Am J Physiol Endocrinol Metab. 2003;284:468-474.

41. Labrie F, Giguere V, Proulx L, Lefevre G. Interactions between CRF, epinephrine, vasopressin and glucocorticoids in the control of ACTH secretion. J Steroid Biochem. 1984;20:153-160.

42. Costa JL, Bui S, Reed P, Dores RM, Brennan MB, Hochgeschwender U. Mutational analysis of evolutionarily conserved ACTH residues. Gen Comp Endocrinol. 2004;136:12-16.

43. Morris DG, Kola B, Borboli N, Kaltsas GA, Gueorguiev M, McNicol AM, Ferrier R, Jones TH, Baldeweg S, Powell M, Czirják S, Hanzély Z, Johansson JO, Korbonits M, Grossman AB. Identification of adrenocorticotropin receptor messenger ribonucleic acid in the human pituitary and its loss of expression in pituitary adenomas. J Clin Endocrinol Metab. 2003;88:6080-6087.

Turk J Pharm Sci 2023;20(2):108-114
DOI: 10.4274/tjps.galenos.2022.60669

ORIGINAL ARTICLE

The Effect of Herbal Penetration Enhancers on the Skin Permeability of Mefenamic Acid Through Rat Skin

Anayatollah SALIMI[1,2]*, Sahba SHEYKHOLESLAMI[2]

[1]Nanotechnology Research Center, Ahvaz Jundishapur University of Medical Sciences, Ahvaz, Iran
[2]Department of Pharmaceutics, Faculty of Pharmacy, Ahvaz Jundishapur University of Medical Sciences, Ahvaz, Iran

ABSTRACT

Objectives: Mefenamic acid (MA) is a strong non-steroidal anti-inflammatory drug, but because of its limited oral bioavailability and the side effects that come with taking it systemically, it is better to apply it topically. The major goal of this study was to see how certain permeation enhancers affected MA is *in vitro* skin permeability. In manufactured Franz diffusion cells, MA permeability tests using rat skin pretreatment with several permeation enhancers such as corn oil, olive oil, clove oil, eucalyptus oil, and menthol were conducted and compared to hydrate rat skin as a control.

Materials and Methods: The steady-state flux (Jss), permeability coefficient (Kp), and diffusion coefficient are among the permeability metrics studied. The permeability enhancement mechanisms of the penetration enhancer were investigated using fourier transform infrared spectroscopy (FTIR) to compare changes in peak position and intensities of asymmetric and symmetric C-H stretching, C=O stretching, C=O stretching (amide I), and C-N stretching of keratin (amide II) absorbance, as well as differential scanning calorimetry (DSC) to compare mean transition temperature and their enthalpies.

Results: Clove oil, olive oil, and eucalyptus oil were the most effective enhancers, increasing flux by 7.91, 3.32, and 2.6 times, as well as diffusion coefficient by 3.25, 1.34, and 1.25, respectively, when compared to moist skin. FTIR and DSC data show that permeation enhancers caused lipid fluidization, extraction, disruption of lipid structures in the SC layer of skin, and long-term dehydration of proteins in this area of the skin.

Conclusion: According to the findings, the permeation enhancers used improved drug permeability through excised rat skin. The most plausible mechanisms for greater ERflux, ERD, and ERP ratios were lipid fluidization, disruption of the lipid structure, and intracellular keratin irreversible denaturation in the SC by eucalyptus oil, menthol, corn oil, olive oil, and clove oil.

Key words: Mefenemic acid, percutaneous absorption, natural enhancers, differential scanning calorimetry, fourier transform infrared spectroscopy

INTRODUCTION

Transdermal drug delivery, based on medication permeation *via* the skin, has a number of benefits, including controlled and continuous drug delivery, which is important for drugs with short biological half-lives and low therapeutic indice, first-pass intestinal and hepatic bypass; avoidance of gastrointestinal irritation, which is common with oral medication, and easier drug localization at the target site.[1]

Partitioning and diffusion across *stratum corneum* (SC) and viable epidermis, transit into the dermis, and eventually systemic absorption or penetration into deeper tissues are the two key phases in skin permeation. SC, the skin's outermost layer, is the most effective barrier against drug penetration. Many techniques have been employed to increase medication access into the lower skin layer and deeper tissues. Permeation enhancers, both chemical and physical, have been developed to help carry high medication concentrations over the skin and into the systemic circulation or deeper tissues. Types of enhancers employed and their mechanisms of action differ.[2] Penetration enhancers work by increasing drug diffusion in the skin, lipid fluidization in SC, and increasing drug thermodynamic activity in the skin and vehicles as well as influencing drug partition coefficient.

*Correspondence: anayatsalimi2003@yahoo.com, Phone: 09163130905, ORCID-ID: orcid.org/0000-0003-1505-7969
Received: 01.04.2022, Accepted: 04.06.2022

©Copyright 2023 by Turkish Pharmacists' Association / Turkish Journal of Pharmaceutical Sciences published by Galenos Publishing House.
Licenced by Creative Commons Attribution-NonCommercial-NoDerivatives 4.0 (CC BY-NC-ND)

Mefenamic acid (MA), an enolic acid-class non-steroidal anti-inflammatory medication, is often used to treat mild-to-moderate pain, such as headaches, tooth discomfort, dysmenorrhea, rheumatoid arthritis, osteoarthritis, and other joint problems. MA is classified as a class II biopharmaceutical, meaning it is highly permeable across biological membranes, but has poor water solubility.[3] Although oral administration of MA is widely used, it necessitates frequent dosing every 6 h to maintain steady-state plasma concentrations.[4] This route is associated with gastrointestinal side effects such as ulceration, bleeding or perforation of the stomach, small intestine or large intestine, which can be fatal; as a result, it is contraindicated in patients with active ulceration or chronic inflammation of the upper or lower gastrointestinal tract.[5] As a result, the only way to get MA through the skin is through a transdermal administration.

Investigation of the microstructure of intercellular or lipids in the SC layer of the skin is necessary to create transdermal medication delivery methods. Differential scanning calorimetry (DSC) and fourier transform infrared spectroscopy (FTIR) have been used in recent research to investigate the organization of lipids and skin microstructure. FTIR analysis of skin may be a useful method for researching the interaction of chemical enhancers with SC that produce bands with varied wave numbers.[6]

Molecular analyses of the entire rat skin were conducted using DSC and FTIR to determine the mechanism by which the characteristics of enhancers/retardants vary in a specific medium.[7] Several infrared spectral bands of the skin are attributed to vibration of protein and lipid molecules in SC.[8] Lipid vibration is a good way to look at the microstructure of lamellar lipids in the intercellular region of SC layer. Many of the skin's infrared spectral bands are caused by the vibration of protein and lipid molecules in SC. Lipid vibration is a good predictor of the architecture of lamellar lipids in the intercellular area of SC layer. SC stretching vibrations of C-H symmetric vibration (about 2850 cm^{-1}) and C-H asymmetric vibration (around 2920 cm^{-1}) have been recorded. The wave number and width of C-H stretching peaks increase, when the lipids in SC fluidize. If the shift is to a higher wavenumber (blue shift), it means that SC membrane (lipid bilayer) is fluidizing, which contributes to the breakdown of the barrier properties, allowing more material to pass through SC. Lipid groups, on the other hand, reorient, producing a change in wave number (*e.g.*, red shift) and strengthening of subcutaneous-barrier characteristics, which slows permeant transit through the skin. The phase transition of the lipids is illustrated by an increase or drop in the band position (wavenumber) of the signals at 2920, 2850, and about 1738 cm^{-1}, when the penetration modifier acts on the lipid pathway.[9-12] Thermal analysis methods such as DSC have been used to investigate thermal transitions in mammalian SC. Thermodynamic analysis techniques such as DSC have been used to study temperature (Tm) transitions in SC. The skin's barrier function is controlled by SC, which is the epidermis' outermost layer.[13]

DSC method is commonly used to study lipid melting, lipid bilayer phase transitions, and protein denaturation in SC layer. A DSC investigation was planned to learn more about the lipid components and protein conformational stability of the entire skin rat treated with enhancers.[14]

The thermotropic behavior of the treated skin was examined by comparing the mean transition Tm and enthalpies (H). Any decrease in Tm might be the result of lipid breakdown in the bilayer and irreversible protein denaturation in the SC. Enthalpy loss is often linked to lipid fluidization in lipid bilayers and protein-lipid interactions.[15]

MATERIALS AND METHODS

Ramopharmin pharmaceutical firm donated MA (Tehran, Iran). Barij Essence Iranian Company in Kashan (Iran) provided eucalyptus oil, olive oil, corn oil, clove oil, and menthol.

Animal experiments

For *in vitro* permeation investigation, male Wistar rats weighing 200-250 g were employed. The abdomen skin hair was meticulously cut using an electric clipper and razor after the animal was sacrificed under ether anesthesia. The skin was dissected, and any excess subcutaneous fat from the dermal surface was removed. The animals were cared for accordance with the guidelines for the care and use of laboratory animals, and the experiments were approved by the Ahvaz Jundishapur University of Medical Sciences' Ethical Committee (IR.AJUMS.REC.1396.295). The National Academy of Sciences issued recommendations, which were published by the National Institutes of Health (U.S. Department of Health and Human Services, Office of Laboratory Animal Welfare).[16,17]

Skin permeation experiments

Permeation tests were conducted using specifically built diffusion cells with an effective area of about 4.906 cm^2. In the donor phase, 2 mL of each natural permeation enhancer was applied to the surface of the skin for 2 or 4 h. After that, the donor and receptor compartments were rinsed and filled with 5.5 mL of MA suspension (1%, w/v) and 30 mL of phosphate buffer solution (PBS, pH 7.4), respectively. As a control, fully hydrated samples were used. On a magnetic stirrer with a heater, the diffusion cell was inserted and clamped in a water bath at 37 ± 0.05°C. A tiny magnetic bead was used to agitate the receptor medium at 200 rpm. At predefined time intervals (0.5, 1, 2, 3, 4, 5,6,7,8, and 24 h), 2 mL of the receptor medium was removed and replaced with an equivalent amount of fresh buffer. The quantity of MA was assessed using a ultraviolet spectroscopic technique at 289 nm, after the samples were filtered.[18,19]

Statistical analysis

The total quantity of MA that penetrated into the receptor *via* each unit area of the diffusion surface was determined and displayed as a function of time. Linear component of the permeation curve's slope was used to compute the steady state flux (mg/cm^2.h). The permeability coefficient (K_p, cm/h) of MA through the skin was calculated using equation 1:

$$K_p = \frac{Jss}{c_v} \quad \text{..... (equation 1)}$$

Where J_{ss} and C_v are the steady-state flux and initial concentration of MA in receptor compartment, respectively. Also, the lag time (T_{lag}) and clear diffusivity coefficient (D_{app}) parameters were calculated. Since h does not represent the actual length of the pathway, D calculated from this formula is also clear to D. The value of D_{app} is calculated from equation 2:

$$D_{app} = h^2/6T_{lag} \quad \text{..... (equation 2)}$$

Enhancement ratios (ER) were calculated from equation 3:[20,21]

$$ER = \frac{\text{permeability parameter after treatment}}{\text{permeability parameter before treatment}} \quad \text{..... (equation 3)}$$

Statistical comparison was made using One-Way ANOVA, and $p<0.05$ was considered statistically significant.

T_{lag} of the drug obtained from the skin along the line of equilibrium to the axis of time in the cumulative curve of the drug. The value of D is calculated from equation 2: $D = h^2/ 6 T_{lag}$. Since h does not represent the actual length of the pathway, D calculated from this formula is also clear to D. Seeing that all calculations are based on the steady-state region, the cumulative flow rate of the drug is determined, hence, the establishment of sink conditions is indispensable for the citation of these parameters. In this work, the maximum concentration established in the receptor phase was less than 10% of the saturation solubility of the drug in the receptor phase, and therefore, a steady concentration gradient was established during the experiments, and with these conditions, a steady state flux was computed.

The differential scanning calorimeter

Using a DSC (Mettler-Toledo DSC[1] system) equipped, the changes in the structure of the entire skin caused by permeation enhancers were investigated. The skin samples were submerged in each natural permeation enhancer for 4 h before being blotted clean. In hermetically sealed aluminum pans, about 6-10 mg of treated skin samples were deposited. Simultaneously, an empty pan served as a reference. Skin samples were regularly subjected to heat between 20 and 200˚C at a rate of 5 degrees *per* min. At least three times, each experiment was conducted. DSC analyzer was calibrated and verified using an indium standard to assure data accuracy and reproducibility.[12]

FTIR experiments

To eliminate evidence of the permeation enhancer, the excised rat skin samples were treated for 4 h with olive oil, corn oil, clove oil, menthol, and eucalyptus oil, then vacuum dried (650 mmHg, 25 ± 1˚C) for 30 minutes and kept in desiccators. An FTIR facility was used to scan the skin samples in the 4000 to 500 cm^{-1} range (Uker, Vertex70, and Germany).[12]

RESULT AND DISCUSSION

Effect of herbal penetration enhancers on MA permeability

Tables 1, 2, and Figures 1, 2 show the permeability parameters following skin pretreatment with natural enhancers for 2 and 4 h compared to control as well as the quantity of MA penetrated through the rat abdomen skin from different enhancers. Table 1 demonstrates the impact of natural enhancers' pretreatment for 2 h on MA permeability compared to control as ERflux (drug flux ratio after and before skin pretreatment with enhancer) and ERD (drug flux ratio after and before skin pretreatment with enhancer) (drug diffusion coefficient after and before skin pretreatment with enhancer).[12] According to the findings, eucalyptus oil, olive oil, corn oil, clove oil, and menthol substantially improved MA flux and diffusion coefficient, according to the findings. Clove oil increased MA flux the most after a 2 hour skin pretreatment, increasing it by up to 7.91 fold compared to control, followed by eucalyptus oil (3.32 fold), olive oil (2.6 fold), corn oil (1.119 fold), and menthol (1.13 fold). Except for corn oil ($p>0.05$), all of the natural penetration enhancers had a significant influence on the diffusion coefficient ($p<0.05$), with clove oil having the largest enhancement effect compared to control.

Table 2 illustrates the impact of natural penetration enhancers' pretreatment for 4 h on MA permeability as ERflux and ERD compared to control. According to the data, eucalyptus oil, olive oil, corn oil, clove oil, and menthol substantially enhance MA flux and diffusion coefficient. After a 4 hour skin pretreatment, clove oil increased MA flow the most, up to 18.65 fold, compared

Table 1. Permeability parameters after 2 hours pretreatment with permeation enhancers compared with control (mean ± SD, n: 3)

Enhancer	J_{ss} (mg/cm².h)	D_{app} (cm²/h)	*p* (cm/h)	T_{lag} (h)	ERflux	ERD	ERP
Control	0.0060 ± 0.00010	0.1090 ± 0.17000	0.0006 ± 0.00001	5.62 ± 0.10	-	-	-
Menthol	0.0067 ± 0.00010	0.0835 ± 0.00200	0.0007 ± 0.00010	4.20 ± 0.22	1.13 ± 0.28	1.12 ± 0.35	1.13 ± 0.28
Eucalyptus oil	0.0190 ± 0.00100	0.0550 ± 0.00600	0.0019 ± 0.00010	2.60 ± 0.62	3.32 ± 1.26	1.51 ± 1.03	3.31 ± 0.26
Olive oil	0.0145 ± 0.00100	0.1405 ± 0.00100	0.0014 ± 0.00020	3.85 ± 0.86	2.60 ± 1.57	3.91 ± 0.95	2.60 ± 0.57
Corn oil	0.0069 ± 0.00100	0.0826 ± 0.01100	0.0007 ± 0.00020	3.30 ± 0.60	1.199 ± 0.35	1.46 ± 0.70	1.20 ± 0.35
Clove oil	0.0460 ± 0.0003	0.1103 ± 0.00800	0.0046 ± 0.00030	1.93 ± 0.01	7.91 ± 0.80	6.24 ± 0.59	7.90 ± 0.06

J_{ss}: Steady-state flux, D_{app}: Diffusivity coefficient, T_{lag}: Lag time, SD: Standard deviation

to control, followed by eucalyptus oil (3.57 fold), olive oil (3.57 flod), corn oil (2.65 flod), and menthol (2.65 flod) (2.17 fold). Except for corn oil (p>0.05), all of the penetration enhancers had a significant impact on the diffusion coefficient, with clove oil having the biggest enhancing effect on the diffusion coefficient compared to the control.

1,8-Cineole makes up about 75% of eucalyptus oil. Cineole is a cyclic terpene that makes liquid pools in SC and changes SC's lipid structure. This makes it easier for polar and non-polar medicines to get through the membrane.[20]

Wang et al.[21] investigated the impact of corn oil, olive oil, and jojoba oil variations on the increase in skin permeability of aminophylline *via* the human skin. The data revealed that vegetable oils had a larger role in increasing drug permeability with jojoba oil having the most significant impact.[21] Salimi and Fouladi[22] looked at how different penetration enhancers affected meloxicam's skin permeability. Transcutol oil, eucalyptus oil, and oleic acid had the greatest impact on skin flux increase.[22] Salimi et al.[23] looked at how different penetration enhancers affected adapalene skin permeability. Clove oil and eucalyptus oil had the greatest impact on skin flux and partition coefficient increase.[23]

Differential scanning calorimetry

Thermotropic behavior of the treated skin was assessed using mean transition Tm and corresponding enthalpies (H). Transition Tm and enthalpies are shown in Table 3, Tm1 and Tm2 from hydrated rat skin were 67.5°C and 112°C, which means that the lipids in the skin had melted and the keratin in the skin had been broken down irreversibly. Any decrease in Tm might be the result of lipid breakdown in the bilayer and irreversible protein denaturation in the SC. While lipid fluidization in lipid bilayers and protein-lipid complexes is often linked to a decrease in enthalpy, this is not always the case.[16] In human dermal DSC graphs, Kaushik and Michniak-Kohn[15] found three endothermic transition peaks at Tm of 59-63°C (Tm1), 75-82°C (Tm2), and 99.5-120°C (Tm3). They proposed that Tm1 relates to the change of lipid forms from a lamellar to a disordered state, Tm2 to protein-lipid or the rupture of polar head groups of lipids, and Tm3 to irreversible denaturation of proteins, respectively.[15]

When compared to hydrate rat skin, the thermograms of skin treated with menthol show reduced Tm2 and H1 and H2. Tm1 was also eliminated by menthol. In this study, menthol was found to change the structure of SC layer in a number of ways, including making lipids more fluid in the intercellular area, breaking down lipids in the bilayer, and permanently breaking down proteins.

DSC findings from skin pretreatment with eucalyptus oil revealed reduced Tm1 and H1 as well as decreased H2 and Tm2. This means that eucalyptus oil may make the skin more permeable by causing lipids in the bilayer to break down and irreversible protein destabilization in SC layer.

Tm1 changed to lower melting points and Tm2 rose in skin

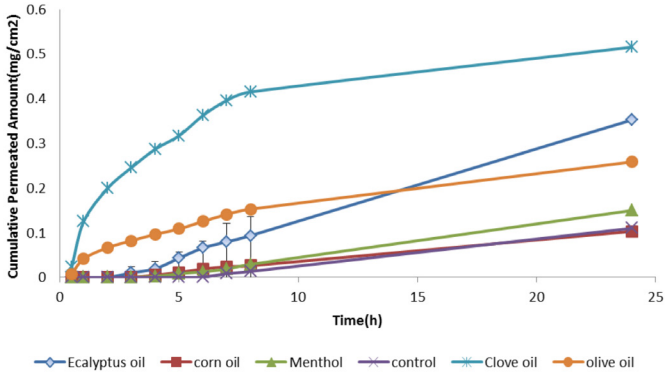

Figure 1. The amount of mefenamic acid permeated after 2 hours pretreatment rat skins with various herbal penetration enhancers

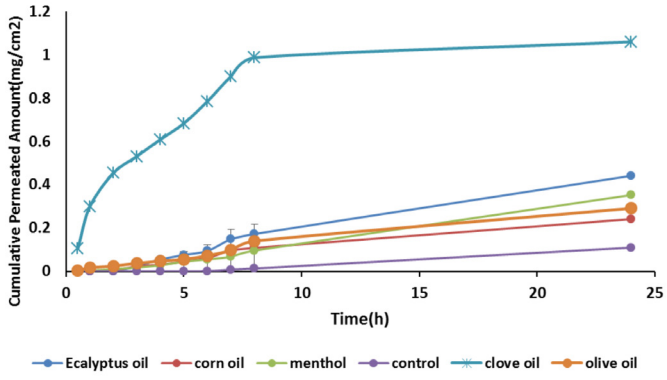

Figure 2. The amount of mefenamic acid permeated after 4 hours pretreatment rat skins with various herbal penetration enhancers

Table 2. Permeability parameters after 4 hours pretreatment with permeation enhancers compared with control (mean ± SD, n: 3)

Enhancer	J_{ss} (mg/cm².h)	D_{app} (cm²/h)	p (cm/h)	T_{lag} (h)	ERflux	ERD	ERP
Control	0.0060 ± 0.0001	0.1093 ± 0.017	0.0006 ± 0.00001	5.61 ± 0.10	-	-	-
Menthol	0.0126 ± 0.0001	0.4095 ± 0.002	0.0012 ± 0.00010	1.42 ± 0.50	2.17 ± 0.68	36.11 ± 0.68	2.17 ± 0.68
Eucalyptus oil	0.0208 ± 0.0010	0.1808 ± 0.002	0.0020 ± 0.00100	2.85 ± 0.70	3.57 ± 0.64	5.78 ± 0.06	3.57 ± 0.64
Olive oil	0.0206 ± 0.0020	0.4976 ± 0.030	0.0020 ± 0.000100	0.30 ± 0.03	3.63 ± 0.56	49.83 ± 0.64	3.63 ± 0.56
Corn oil	0.0158 ± 0.0010	0.0627 ± 0.004	0.0015 ± 0.00100	1.74 ± 0.60	2.65 ± 0.20	2.82 ± 0.66	2.65 ± 0.20
Clove oil	0.1098 ± 0.0500	0.0337 ± 0.003	0.0110 ± 0.00200	4.1 ± 0.90	18.35 ± 0.92	1.55 ± 0.05	18.35 ± 0.40

J_{ss}: Steady-state flux, D_{app}: Diffusivity coefficient, T_{lag}: Lag time, SD: Standard deviation

pretreated with olive oil thermograms, whereas H1 and H2 were reduced compared to controls. This means that olive oil may make the skin more permeable by causing lipids in the bilayer to break down and irreversible protein destabilization in SC layer.

When the skin was treated with corn oil, the melting points of Tm1 and Tm2 changed lower and higher, respectively, compared to the control. Additionally, compared to the control, H1 and H2 shifted to lower levels. This suggests that corn oil increase skin permeability by breaking down lipids in the bilayer and irreversibly destabilizing proteins in SC layer.

As the skin was treated with clove oil, the melting points of Tm1 and Tm2 changed lower and higher, respectively, when compared to the control. Additionally, as compared to the control, H1 and H2 shifted to lower levels. A study found that clove oil may make the skin more permeable because it breaks down lipids in the bilayer and permanently changes proteins in SC layer, which makes the skin more permeable.

FTIR spectroscopy

Tables 4-6 provide spectrum analysis of samples, showing peak position and intensity variations from 4000 cm^{-1} to 500 cm^{-1}. If the wave number increases (blue shift), it indicates that SC membrane (lipid bilayer) is becoming more fluid, making it simpler for drugs to enter the body through SC.[24] On the other hand, lipid groups reorient, changing a lower wave number (*e.g.*, red shift) and strengthening of subcutaneous-barrier qualities, resulting in a slowing down of permeant passage through the skin.[11]

The spectra of menthol-treated rat skin showed changes in peak height and wave numbers. Red shifts were noticed in the skin treated with menthol at wave numbers 2838.63cm^{-1} and 2747.53cm^{-1}. This shows that lipid groups have been altered, resulting in a stronger SC barrier. There was a relative red shift in 1728.58 cm^{-1} band was observed in the skin pretreated with menthol, indicating the formation of strong hydrogen bonds within the lipid structures. Pretreating skin rats with menthol had 75.17% reduction in the mean peak height of C-N stretching (amide I) absorbance, showing that it interacts mostly with proteins in SC layer.

Significant reductions in the height of peaks in the 2981.66, 2915.86, 1690.2, and 1642.65 cm^{-1} wave numbers were seen in the FTIR spectra of skin pretreated with clove oil. According to the findings, clove oil interacts mostly with lipids and proteins in SC layer. The findings of the permeability parameters after clove oil pretreatment correlated with FTIR and DSC measurements.

Changes in peak height and wave numbers are seen in the spectra of rat skin prepared with eucalyptus oil. At wave numbers 2848.59 cm^{-1} and 2741.57 cm^{-1}, a red shift was seen in the skin prepared with eucalyptus oil, suggesting lipid reorientation that causes SC barrier characteristics to be strengthened. The skin prepared with eucalyptus oil showed a red shift in which the peak number's height (1654.93 cm^{-1}) increased. The wave number (1791.51cm^{-1}) decreases in peak height, causing blue shifts.

Changes in peak height and wave numbers may be seen in the spectra of corn oil-treated rat skin. The skin treated with corn oil showed a blue shift in peak number heights (2981.64, 2919.9, 1733.58, and 1561.21 cm^{-1}), suggesting the denaturation of proteins and lipids in SC layer.

The spectra of rat skin pretreated with olive oil reveal changes in peak height and wave numbers. This implies that when olive oil was used to treat skin, the peak number shifted blue (2981.64, 1733.85 cm^{-1}). This shows that the olive oil broke down the proteins and lipids in SC layer.

CONCLUSION

According to the findings, the permeation enhancers used improved drug permeability through excised rat skin. The most plausible mechanisms for greater ERflux, ERD, and ERP ratios were lipid fluidization, disruption of the lipid structure, and intracellular keratin irreversible denaturation in the SC by eucalyptus oil, menthol, corn oil, olive oil, and clove oil.

Table 3. Effect of permeation enhancer on the thermal properties of excised rat skin (mean ± SD, n: 3)

Enhancer	Transition temperature (°C)		Transition enthalpy (mj/mg)	
	Tm1	Tm2	H1	H2
Water (control)	67.5 ± 2.1	112.0 ± 6.6	7.010 ± 0.4	552.4 ± 9.0
Menthol	0	124.0 ± 0.1	0	2.7 ± 0.3
Eucalyptus oil	31.0 ± 0.9	127.5 ± 1.1	2.672 ± 0.1	8.9 ± 0.8
Olive oil	37.7 ± 0.9	115.0 ± 0.9	5.844 ± 0.6	6.2 ± 0.2
Corn oil	0	118.1 ± 1.1	0	99.9 ± 2.1
Clove oil	36.0 ± 0.2	116.0 ± 0.5	0.900 ± 0.2	2.2 ± 0.1

Tm1: Mean transition temperature of lipids, SC Tm2: Mean transition temperature of irreversible denaturation of intracellular, SC keratin, H1: Transition enthalpy of lipid phase, SC H2: Transition enthalpy of keratin phase SC, SD: Standard deviation

Table 4. FTIR peak wave numbers (cm^{-1}) changes compared to control (untreated skin) and abdominal hydrated whole skin rat following treatment with different enhancers (mean SD, n: 3)

Enhancer	C-H stretching Asy	C-H stretching Sym	C=O stretching of lipid ester	Amide I	Amide II
Water	2981.77 ± 0.16	2856.34 ± 0.16	1731.68 ± 0.14	1667.04 ± 0.12	1547.67 ± 0.11
Menthol	2838.63 ± 0.15	2747.53 ± 0.13	1728.58 ± 0.11	1603.87 ± 0.16	1538.91 ± 0.20
Eucalyptus oil	2848.59 ± 0.12	2741.57 ± 0.15	1791.51 ± 0.13	1654.93 ± 0.18	1565.24 ± 0.12
Olive oil	2990.78 ± 0.12	2887.85 ± 0.14	1743.31 ± 0.18	1626.18 ± 0.18	1549.92 ± 0.15
Corn oil	2981.64 ± 0.21	2919.9 ± 0.14	1733.85 ± 0.19	1647.25 ± 0.13	1561.27 ± 0.14
Clove oil	2981.66 ± 0.15	2915.86 ± 0.11	-	1690.2 ± 0.21	1642.65 ± 0.17

SD: Standard deviation

Table 5. Decrease in mean peak height (± SD), compared with control (hydrated skin) of C=O stretching (amide I) and C-N stretching of keratin (amide II) absorbance of abdominal hydrated whole skin rat following treatment with different enhancers (mean ± SD, n: 3)

Enhancer	Asymmetric C-H stretching		Symmetric C-H stretching		C=O stretching of lipid ester	
	Peak height	%D	Peak height	%D	Peak height	%D
Water	1.8355 ± 0.008	-	1.95 ± 0.005	-	2.061 ± 0.001	-
Menthol	0.527 ± 0.050	71.29	0.512 ± 0.003	73.74	2 ± 0.01	2.96
Eucalyptus oil	0.517 ± 0.010	71.83	0.436 ± 0.008	77.64	0.775 ± 0.006	62.40
Olive oil	0.381 ± 0.001	79.24	0.207 ± 0.010	89.38	0.425 ± 0.002	79.38
Corn oil	2.272 ± 0.005	N.D	2.323 ± 0.007	N.D	2.079 ± 0.005	N.D
Clove oil	1.227 ± 0.004	33.15	0.464 ± 0.010	76.21	0	100.00

% Decrease in peak height (%D) = (peak height from untreated whole skin-peak height from solvent treated whole skin)/peak height from untreated whole skin x 100. N.D: No decrease in peak height, SD: Standard deviation

Table 6. Decrease in mean peak height (± SD), compared with control (hydrated skin) of C=O stretching (amide I) and C-N stretching of keratin (amide II) absorbance of abdominal hydrated whole skin rat following treatment with different enhancers (mean ± SD, n: 3)

Enhancer	Amide I stretching of keratin		Amide II stretching of keratin	
	Peak height	%D	Peak height	%D
Water	2.111 ± 0.006	-	2.151 ± 0.005	-
Menthol	1.2 ± 0.009	43.15	0.534 ± 0.009	75.17
Eucalyptus oil	0.727 ± 0.005	65.56	0.727 ± 0.007	66.20
Olive oil	0.479 ± 0.010	77.31	0.611 ± 0.010	71.59
Corn oil	2.1 ± 0.006	0.52	2.04 ± 0.011	5.16
Clove oil	1.889 ± 0.020	10.52	1.94 ± 0.006	9.81

SD: Standard deviation

Ethics

Ethics Committee Approval: Ahvaz Jundishapur University of Medical Sciences' Ethical Committee (IR.AJUMS.REC.1396.295).

Informed Consent: Not applicable.

Peer-review: Externally peer-reviewed.

Authorship Contributions

Concept: A.S., Design: A.S., Data Collection or Processing:S.S., Analysis or Interpretation: A.S., Literature Search: S.S., Writing: A.S.

Conflict of Interest: No conflict of interest was declared by the authors.

Financial Disclosure: The authors declared that this study received no financial support.

REFERENCES

1. Hadgraft J, Lane ME. Skin permeation: the years of enlightenment. Int J Pharm. 2005;305:2-12.

2. Ghosh TK, Banja AK. Methods of enhancement of transdermal drug delivery: part IIA, chemical permeation enhancers. Pharm Tech. 1993;18:62-90.

3. Sriamornsak P, Limmatvapirat S, Piriyaprasarth S, Mansukmanee P, Huang Z. A new self-emulsifying formulation of mefenamic acid with enhanced drug dissolution. Asian J Pharm Sci. 2015;10:121-127.

4. Sevgi F, Kaynarsoy B, Ertan G. An anti-inflammatory drug (mefenamic acid) incorporated in biodegradable alginate beads: development and optimization of the process using factorial design. Pharm Dev Technol. 2008;13:5-13.

5. Wen MM, Farid RM, Kassem AA. Nano-proniosomes enhancing the transdermal delivery of mefenamic acid. J Liposome Res. 2014;24:280-289.

6. Salimi A, Moghimipour E, Rahmani F. Effects of the various solvents on the *in vitro* permeability of indomethacin through whole abdominal rat skin. Annu Res Rev Biol. 2015;5:335-346.

7. Barry BW. Novel mechanisms and devices to enable successful transdermal drug delivery. Eur J Pharm Sci. 2001;14:101-114.

8. Samad A, Sultana Y, Aqil M. Liposomal drug delivery systems: an update review. Curr Drug Deliv. 2007;4:297-305.

9. Finnin BC, Morgan TM. Transdermal penetration enhancers: applications, limitations, and potential. J Pharm Sci. 1999;88:955-958.

10. Salimi A, Hedayatipour N, Moghimipour E. The effect of various vehicles on the naproxen permeability through rat skin: a mechanistic study by DSC and FT-IR techniques. Adv Pharm Bull. 2016;6:9-16.

11. Boncheva M, Damien F, Normand V. Molecular organization of the lipid matrix in intact *stratum corneum* using ATR-FTIR spectroscopy. Biochim Biophys Acta. 2008;1778:1344-1355.

12. Moghimipour E, Salimi A, Zadeh BSM. Effect of the various solvents on the *in vitro* permeability of vitamin B_{12} through excised rat skin. Trop J Pharm Res. 2013;12:671-677.

13. Kumar R, Philip A. Modified transdermal technologies: breaking the barriers of drug permeation *via* the skin. Trop J Pharm Res. 2007;6:663-644.

14. Salimi A, Zadeh BSA, Safavi G. Effect of formulation components on the *in vitro* skin permeation of microemulsion drug delivery system of piroxicam. Int Res J Pharm Appl Sci. 2013;3:152-160.

15. Kaushik D, Michniak-Kohn B. Percutaneous penetration modifiers and formulation effects: thermal and spectral analyses. AAPS PharmSciTech. 2010;11:1068-1083.

16. Obata Y, Utsumi S, Watanabe H, Suda M, Tokudome Y, Otsuka M, Takayama K. Infrared spectroscopic study of lipid interaction in *stratum corneum* treated with transdermal absorption enhancers. Int J Pharm. 2010;389:18-23.

17. Moghimipour E, Salimi A, Eftekhari S. Design and characterization of microemulsion systems for naproxen. Adv Pharm Bull. 2013;3:63-71.

18. 18. Zadeh BSA, Salimi A, Tolabi H. Preparation and characterization of minoxidil loaded niosome carrier for effective follicular delivery. Int J Curr Res Chem Pharma Sci. 2014;1:203-210.

19. Moser K, Kriwet K, Naik A, Kalia YN, Guy RH. Passive skin penetration enhancement and its quantification *in vitro*. Eur J Pharm Biopharm. 2001;52:103-112.

20. Vaddi HK, Ho PC, Chan SY. Terpenes in propylene glycol as skin-penetration enhancers: permeation and partition of haloperidol, fourier transform infrared spectroscopy, and differential scanning calorimetry. J Pharm Sci. 2002;91:1639-1651.

21. Wang LH, Wang CC, Kuo SC. Vehicle and enhancer effects on human skin penetration of aminophylline from cream formulations: evaluation *in vivo*. J Cosmet Sci. 2007;58:245-254.

22. Salimi A, Fouladi M. Effect of the various penetration enhancers on the *in vitro* skin permeation of meloxicam through whole rat skin. Eur J Biomed Pharm Sci. 2015;2:1282-1291.

23. Salimi A, Emam M, Mohammad Soleymani S. Increase adapalene delivery using chemical and herbal enhancers. J Cosmet Dermatol. 2021;20:3011-3017.

24. Songkro S. An overview of skin penetration enhancers: penetration enhancing activity, skin irritation potential and mechanism of action. Songklanakarin J Sci Technol. 2009;31:299-321.

Turk J Pharm Sci 2023;20(2):115-120
DOI: 10.4274/tjps.galenos.2022.95994

ORIGINAL ARTICLE

The Bioequivalence Study of Two Dexketoprofen 25 mg Film-Coated Tablet Formulations in Healthy Males Under Fasting Conditions

Fırat YERLİKAYA[1,2]*, Aslıhan ARSLAN[1], Hilal BAŞ[1], Onursal SAĞLAM[3], Sevim Peri AYTAÇ[3]

[1]Elixir Pharmaceutical Research and Development Corporation, Ankara, Türkiye
[2]Lokman Hekim University, Faculty of Pharmacy, Department of Pharmaceutical Technology, Ankara, Türkiye
[3]Novagenix Bioanalytical Drug R&D Centre, Ankara, Türkiye

ABSTRACT

Objectives: Dexketoprofen is a non-steroidal analgesic/anti-inflammatory drug and its trometamol salt is extensively preferred in mild or moderate pain due to its rapid onset of relief. A new formulation of 36.9 mg of dexketoprofen trometamol (equivalent to 25 mg dexketoprofen) tablet has been developed and its bioequivalence to the reference product was proven.

Materials and Methods: An open-label, single-dose, randomized, two-period, and cross-over bioequivalence study was conducted with healthy males under fasting conditions for two different tablet formulations of 25 mg dexketoprofen. To prove the bioequivalence of the test product with the reference product, a comparison study has been performed in compliance with regulations in force under Good Clinical Practice principles. A single-center clinical study was run and blood samples of the participants were withdrawn at specified time points, before and after dosing, to measure the plasma concentrations of dexketoprofen trometamol. A validated analytical method has been developed using an liquid chromatography with tandem mass spectrometry. Instrument to assess the plasma concentrations of the test and reference products.

Results: Forty-seven volunteers completed clinical phase of the study. For the test and reference products, the mean ± standard deviations (SD) of C_{max} were found 2543.82 ± 655.42 ng/mL and 2539.11 ± 662.57 ng/mL, and the mean ± SD of area under the curve (AUC) from time 0 to the last measurable concentration ($AUC_{0-tlast}$) were found 3483.49 ± 574.42 h.ng/mL and 3560.75 ± 661.83 h.ng/mL, respectively. The primary target variables data demonstrate the bioequivalence of test and reference products with regard to 90% confidence interval for C_{max} of 92.45-108.53% and for $AUC_{0-tlast}$ of 95.57-100.87%. The geometric mean ratios were found as 100.16% and 98.18% for C_{max} and $AUC_{0-tlast}$, respectively. There were no serious adverse events or adverse reactions reported throughout the study.

Conclusion: After statistical evaluation of the analytical results, the test and reference products were considered bioequivalent. Both products were well tolerated and considered as safe.

Key words: Bioequivalence, bioavailability, dexketoprofen trometamol

INTRODUCTION

Non-steroidal anti-inflammatory/analgesic drugs (NSAIDs) are widely prescribed medications for alleviating pain, fever, and inflammation.[1] A member of NSAIDs, ketoprofen is a chiral 2-arylpropionic acid derivative and a prostaglandin synthesis inhibitor, which is used for its analgesic, anti-inflammatory and antipyretic effects since 1973.[2] However, the strong prostaglandin synthesis inhibition was attributed to its (S)-(+)-enantiomer in the following years.[2] Currently, dexketoprofen is considered a member of first-line NSAIDs in the symptomatic treatment of mild or moderate pain.[3] To improve its benefit for treating acute pain, a derivative of more soluble dexketoprofen, has been trometamol, which leads to rapid efficacy.[4]

The rapid onset of action and proven efficacy of dexketoprofen trometamol draws attention of generic pharmaceutical companies whose function is fundamental in drug accessibility. However, a bioequivalence study is required for generic orally administered dexketoprofen trometamol products by European Medicines Agency (EMA).[5]

*Correspondence: firat.yerlikaya@elixirlabs.com.tr, Phone: +90 312 227 00 71, ORCID-ID: orcid.org/0000-0003-4648-3258
Received: 12.04.2022, Accepted: 15.06.2022

©Copyright 2023 by Turkish Pharmacists' Association / Turkish Journal of Pharmaceutical Sciences published by Galenos Publishing House.
Licenced by Creative Commons Attribution-NonCommercial-NoDerivatives 4.0 (CC BY-NC-ND)

A new generic formulation has been developed by Elixir Pharmaceutical Research and Development Corporation (Ankara, Türkiye) for Tebem İlaç (Ankara, Türkiye) as an alternative to the original brand and to be licensed by the authority, its' bioequivalence needs to be proven. Therefore, this study compares pharmacokinetic properties of a generic formulation to the reference product and to demonstrate bioequivalence of the products with respect to rate and extent of absorption of dexketoprofen trometamol in healthy male volunteers under fasting conditions.

MATERIALS AND METHODS

Study population

All volunteers were healthy adult males (aged 18-55 years) with a body mass index (BMI) within 18.5-30 kg/m^2. The volunteers who have atopic constitution or asthma and/or known allergy for dexketoprofen trometamol and/or other NSAIDs and/or any excipient of the products were excluded from the study. Volunteers who have any history or presence of clinical relevance of cardiovascular, neurological, musculoskeletal, hematological, hepatic, gastrointestinal, renal, pulmonary, endocrinological, and metabolism disorders were also excluded. History of malabsorption or other conditions that might affect pharmacokinetics of the study drugs, blood donation more than 400 mL within the last two months before the first drug administration, being included in another clinical trial, intake of depot injectable solutions within 6 months and/or intake of enzyme-inducing, organotoxic or long half-life drugs within 4 weeks before the start of the study were among the other exclusion criteria. Regular consuming of beverages or food containing methylxanthines (*e.g.* coffee, tea, cola, caffeine, chocolate, and sodas) equivalent to or more than 500 mg methylxanthines daily, taking any grapefruit or grapefruit juice during 7 days before drug administration, during the study or during the washout periods, having a history of drug or alcohol abuse and/or having positive alcohol breath test results were counted as exclusion criteria, as well. The inclusion and exclusion criteria were established clearly together with the reasons for withdrawal from the study. The volunteers who were willing to participate in the clinical trial signed a written informed consent form on their own freewill and understood that they could withdraw from the study anytime without specifying any reason.

Study design

A single-center, open-label, randomized, single oral dose, cross-over, two-sequence, two-period study was conducted in 48 healthy, Caucasian adult males under fasting conditions. This study was reviewed and approved by Erciyes University Ethical Committee of Bioequivalence/Bioavailability Studies (2019/03; 16.01.2019) and Turkish Medicines and Medical Devices Agency (20.02.2019) and was held in Türkiye according to the regulations run by the Ministry of Health of the Republic of Türkiye, which comply with Declaration of Helsinki and Good Clinical Principles (GCP).[6]

This study was conducted at FARMAGEN Good Clinical Practice and Research Center (Gaziantep, Türkiye) before the coronavirus disease-2019 era. The clinical study spanned a period of approximately 4 weeks, including pre-study screening (day 14 to 1), wash-out period (7 days), and final examination (2-8 days after the last blood sampling). The standard clinical screening and laboratory examinations in blood and urine were performed and the volunteers were checked for the presence of HBsAg, HCV-Ab, and HIV-Ab in serum. They were requested to provide a urine sample for a drug screening, which includes "amphetamines, cannabinoids, benzodiazepines, cocaine, opioids, and barbiturates" and an alcohol breath test on entry visit and hospitalization days of both periods. The standard clinical screening was included demographic data, brief anamnestic data, physical examination, determination of body temperature, weight and height, standard electrocardiogram (12 lead), measurements of blood pressure, and pulse rate. All laboratory tests were carried out in a certified local laboratory.

A total of 48 volunteers was randomized, and 47 volunteers completed the clinical study. They were admitted to the clinic on the day before dosing day, and after staying 24 h fasted, they received their study drugs. Volunteers were not allowed to drink water from 1 hour before until 1 h after the administration of study products, except while dosing and they remained fasted until 4 h after administration. Immediately after pre-dose sampling, 1 tablet of the test drug or 1 tablet of the reference drug (25 mg dexketoprofen each case), were taken by the volunteers with 240 mL water at ambient temperature. After the washout period (approximately 7 days); in period II, the volunteers were administered the other drug they did not take in the period I. The same procedures were applied in each period.

Investigational medicinal products

The test drug used was dexketoprofen 25 mg film-coated tablet (Tebem İlaç, Türkiye) (batch no: 1809002; expiration date: 09.2020); the reference drug used was Arveles® 25 mg film-coated tablet, UFSA, Türkiye) (batch no: 18180; expiration date: 09.2020).

Blood sampling and study assessment

The samples were drawn by a short intravenous catheter at pre-dose and after ingestion of study products at following points: 0.17, 0.33, 0.50, 0.67, 0.83, 1.00, 1.33, 1.66, 2.00, 2.33, 2.66, 3.00, 4.00, 6.00, 8.00, 10.00, 12.00, 14.00 h in each clinical study period, and they were collected into polypropylene tubes using K_2EDTA as an anti-coagulating agent.

An evening meal was provided at hospitalization days (total caloric value of approximately 1200 kcal) in each period. On medication days, a standard lunch (total caloric value is approximately 1200 kcal) was provided 4 h after dosing, and a standard dinner (total caloric value is approximately 1200 kcal) was provided 10 h after dosing in each period.

After sampling, the samples were immediately refrigerated at approximately +4°C not more than 30 min. Following the centrifugation (3000 rpm, 4-6°C, 10 min), the separated plasma

from each sample was transferred into two 3 mL transparent, polypropylene tubes, then, transferred to a deep-freeze and stored at -70˚C until they were transported to the bioanalytical center.

Determination of plasma concentrations of dexketoprofen

Bioanalytical phase of the study was run using a validated chromatographic method at Novagenix Bioanalytical R&D Center (Ankara, Türkiye). To avoid any bias, the analytical studies were operated as analytically blinded.

Analytical reference standard of dexketoprofen trometamol was supplied from Saurav Chemicals Ltd. (India) and internal standard; (S)-ketoprofen D3 (IS), was supplied from Toronto Research Chemicals, Inc. (Canada). Solvents used including methanol, acetonitrile, and formic acid were supplied from Merck (Germany). Ultrapure (type 1) water was supplied through Millipore MilliQ Water Purification System; K_2EDTA blank human plasma was supplied from Gaziantep University, Farmagen GCP Centre (Türkiye).

A liquid chromatography with tandem mass spectrometry (LC-MS/MS, Waters Acquity) system with a TQ detector was used. An Atlantis HILIC silica 3 µm (4.6 x 100 mm) chromatographic column was chosen with a mobile phase consisting of 0.1% formic acid and acetonitrile (35/65, v/v) with a column oven temperature maintained at 40˚C. The flow rate was 0.7 mL/min. Electrospray ionization was performed in Multiple reaction monitoring (MRMI mode and positive ion, selective ion monitoring mode was used to detect m/z 255.2 › 209.15 (dexketoprofen) and *m/z* 258.2 › 212.3 [(*S*)-ketoprofen D3] ions, simultaneously. Total run time for the method was 3.5 min.

Stock standard solutions of dexketoprofen were prepared in methanol at a concentration of 5 mg/mL. Working solutions in the concentration range of 0.4-240 µg/mL were prepared by diluting stock standard solutions with methanol. The working IS was prepared in methanol at a concentration of 0.2 mg/mL. Stock solutions of dexketoprofen and IS were stored at -20˚C. Calibration standards were prepared by spiking the appropriate amounts of standard solutions into blank plasma to obtain final concentration levels between 20-12.000 ng/mL. The quality control samples were prepared similarly at concentrations between 20-9.600 ng/mL. The lower limit of quantification (LLOQ), using 100 µL of human plasma, was 20 ng/mL. Calibration standards and Quality Control (QC) samples were stored at -70˚C freezer until the analyses.

For sample preparation, protein precipitation method was preferred to extract dexketoprofen and the samples were prepared according to the bioanalytical center's sample preparation Standard Operating Procedures (SOP).

The method validation was performed with K_2EDTA human plasma according to EMA Guideline on Bioanalytical Method Validation.[7] The method was validated for selectivity, specificity, carry-over, linearity, precision and accuracy, recovery, dilution integrity, influence of hemolyzed and hyperlipidemic plasma, drug-drug interaction, matrix effect, and stabilities.

The analytical curves were constructed from a blank sample (plasma sample processed without IS), a zero sample (plasma processed with IS) and 8 concentrations of dexketoprofen, including LLOQ, ranging from 20 to 12.000 ng/mL. The concentrations were calculated using peak area ratios and the linearity of the calibration curve was determined using least squares regression analysis employing a weighted ($1/x$) linear (y: $mx + b$) for dexketoprofen. The acceptance criterion for each calculated standard concentration was not more than 15% deviation from the nominal value, except for LLOQ, which was set at 20%. The within-batch precision and accuracy were evaluated by analyzing QC samples at five different concentration levels (LLOQ, QC low, QC medium, QC high, ULLOQ) between 20-9.600 ng/mL with 6 replicates in a batch. The between-batch precision and accuracy were determined by analyzing 3 different batches. The within-batch and between-batch values did not exceed 15% for QC samples, expected for LLOQ, which did not exceed 20%.

The selectivity was studied by checking the chromatograms obtained from 10 different sources of human plasma including one hemolytic and one lipemic plasma. By comparing the chromatograms of those plasma samples spiked with dexketoprofen and IS with the chromatograms of the blank plasma samples, no peak was found at the retention time of dexketoprofen and IS in 10 of the blank plasma samples. The recoveries were estimated by comparing the peak areas of dexketoprofen in 3 replicates of QC samples with those of post-extraction blank matrix extracts at the corresponding concentrations. The matrix effects of dexketoprofen were evaluated by comparing the peak areas of post-extraction blank plasma that were spiked at certain concentrations of QC samples with the areas obtained by the direct injection of the corresponding standard solutions. The stability of dexketoprofen in the plasma samples was determined from three QC levels with 6 replicates each under the following conditions; long-term stability at -70˚C for 27 days, short-term stability at room temperature (RT) for 6 h, using processed samples in autosampler vials for 52 h, and after four freeze/thaw cycles (-70˚C to RT).

In-house high performance LC-MS/MS detector method was developed and validated to quantify dexketoprofen in plasma.

The plasma samples were maintained at -70˚C during the assay. Thawed samples (0.1 mL) at RT were transferred in a polypropylene tube and were prepared for analysis using protein precipitation according to SOPs of bioanalytical center.

Pharmacokinetic and statistical analyses

To demonstrate bioequivalence with a power of 80% and a test/reference parameter ratio between 0.95 and 1.05, 48 volunteers were included in the study to obtain at least 44 completed volunteers.

C_{max} and area under the curve from time 0 to the last measurable concentration ($AUC_{0\text{-}tlast}$) were considered the primary target variables; area under the curve from time 0 to the infinite time ($AUC_{0\text{-}\infty}$), time to reach the peak concentration (t_{max}), terminal half-life ($t_{½}$), terminal disposition rate constant (λ_z) and mean

residence time (MRT) were declared as the secondary target variables in this bioequivalence study.

C_{max} and t_{max} for dexketoprofen were obtained directly by plasma concentration-time curves. $AUC_{0\text{-}tlast}$ was calculated using the trapezoidal rule. $AUC_{0\text{-}\infty}$ was calculated by summing $AUC_{0\text{-}tlast}$ and extrapolated area. The latter was determined by dividing the last measured concentration by λ_z, which was estimated by regression of the terminal log-linear plasma concentration time points.

C_{max} and $AUC_{0\text{-}tlast}$ were tested for statistically significant differences by using Analysis of Variance (ANOVA) test procedure after logarithmic transformation (ln). The effects of ANOVA were treatment, period, and volunteer within the sequence and tested at 5% level of significance.

In the assessment of bioequivalence, the confidence intervals (CI) approach was used. Two one-sided hypothesis at the 5% level of significance was tested by constructing the 90% CIs for the geometric mean ratios of test/reference products. Two formulations were considered as bioequivalent, if the 90% CIs were within 80.00-125.00% for C_{max} and $AUC_{0\text{-}tlast}$. The difference in t_{max} was evaluated non-parametrically.

All statistical analyzes were performed using Phoenix WinNonlin (version 8.1, Certara L.P.).

Also, ANOVA and determination of 90% CIs were applied to non-logarithmic transformed data of t_{max}, $t_{1/2}$, λ_z, and MRT and to ln transformed data of $AUC_{0\text{-}\infty}$.

RESULTS

Sixty-nine volunteers were screened, while 48 volunteers were randomized and included in the study. The volunteers were divided into two groups according to the randomization table. There was one drop-out from the study, who did not want to continue the trial by his freewill before dosing in period II. As a result, 47 volunteers completed the clinical phase of the study. All the volunteers were Caucasian. The mean ± standard deviation (SD) age of volunteers was 26.72 ± 7.85 years and the mean ± SD BMI was 24.86 ± 2.74. The demographic data for volunteers are presented in Table 1. There was no protocol deviation through the clinical period. The actual time of sampling was used in the estimation of the pharmacokinetic parameters. In Period II, there was no pre-dose drug concentrations observed, which indicated that the washout period of 7 days was sufficient.

The pharmacokinetic parameters for test and reference products are summarized in Table 2 and the geometric least square means, ratios, and 90% CIs are summarized in Table 3. Average plasma concentration-time curves and average ln plasma concentration-time curves of test and reference products for a single dose of dexketoprofen are displayed in Figures 1 and 2, respectively.

Table 1. Demographic data of the volunteers

n: 47	Age	Weight (kg)	Height (cm)	BMI
Mean	26.72	78.49	177.72	24.86
SD	7.85	9.12	5.97	2.74
Minimum	19	60	170	18.83
Maximum	53	95	195	29.75

SD: Standard deviation, BMI: Body mass index

For the test and reference products, the mean ± SD of C_{max} was found 2543.82 ± 655.42 ng/mL and 2539.11 ± 662.57 ng/mL, and the mean ± SD of $AUC_{0\text{-}tlast}$ was found 3483.49 ± 574.42 h.ng/mL and 3560.75 ± 661.83 h.ng/mL, respectively (Table 2).

The primary target variables data demonstrate bioequivalence of test and reference products regarding 90% CI for C_{max} of 92.45-108.53 and for $AUC_{0\text{-}tlast}$ of 95.57-100.87, which are within acceptance limits (80.00-125.00%).[4] The geometric mean ratios were found as 100.16% and 98.18% for C_{max} and $AUC_{0\text{-}tlast}$, respectively (Table 3).

For the secondary endpoint data, the median of t_{max} for both the test and reference products were found 0.5 h and ranged from 0.33 h to 1.33 h for the test product, and 0.33-1.66 h for the reference product. Besides, the mean ± SD of $t_{1/2}$ for the test and reference products was found 1.88 ± 1.09 h (ranged from 1.16 h to 7.08 h) and 1.94 ± 1.24 h (ranged from 1.69 h to 9.09 h), respectively. The mean ± SD of λ_z for the test and reference product was 0.42 ± 0.11 1/h (ranged from 0.1 1/h to 0.6 1/h) and 0.42 ± 0.12 1/h (ranged from 0.08 1/h to 0.63 1/h), respectively (Table 2).

Safety and tolerability

There were 3 possible and 4 unlikely associated drug-related adverse events occurred in all two periods. Five of 7 adverse events were fully recovered. One volunteer received concomitant medication (paracetamol) due to a headache complaint. The severity and seriousness of adverse events and

Table 2. The arithmetic mean ± SD of pharmacokinetic parameters of single oral dose of 25 mg dexketoprofen in the test drug (dexketoprofen 25 mg film-coated tablet, Tebem İlaç, Türkiye); the reference drug used was (Arveles® 25 mg film-coated tablet, UFSA, Türkiye) in healthy adult male volunteers under fasting conditions (arithmetic mean ± SD, n: 47)

Parameters (units)	Test (T)	Reference (R)
C_{max} (ng/mL)	2543.82 ± 655.42	2539.11 ± 662.57
$AUC_{0\text{-}tlast}$ (ng.h/mL)	3483.49 ± 574.42	3560.75 ± 661.83
$AUC_{0\text{-}\infty}$ (ng.h/mL)	3562.44 ± 587.99	3640.81 ± 694.17
t_{max} (h)*	0.61 ± 0.28 (0.33-1.33)	0.66 ± 0.32 (0.33-1.66)
$t_{½}$ (h)	1.88 ± 1.09	1.94 ± 1.24
λ_z (1/h)	0.42 ± 0.11	0.42 ± 0.12
MRT (h)	2.03 ± 0.50	2.05 ± 0.63

*t_{max} values are presented as median with range (minimum - maximum) in parentheses. SD: Standard deviation, $AUC_{0\text{-}tlast}$: Area under the curve from time 0 to the last measurable concentration, $AUC_{0\text{-}\infty}$: Area under the curve from time 0 to the infinite time, t_{max}: Time to reach the peak concentration, $t_{½}$: Terminal half-life, λ_z: Terminal disposition rate constant, MRT: Mean residence time

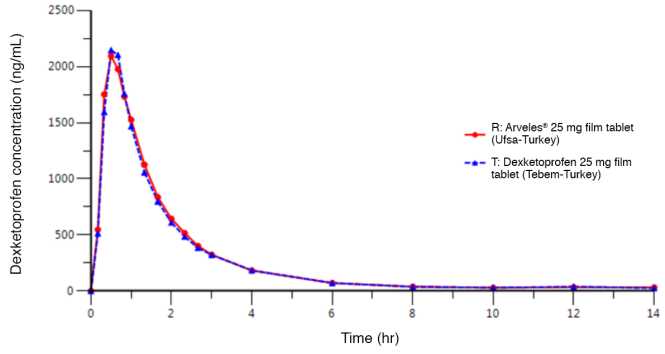

Figure 1. Mean plasma concentration-time curves of dexketoprofen after a single dose of the test drug (dexketoprofen 25 mg film tablet, Tebem İlaç, Türkiye) and the reference drug (Arveles® 25 mg film-coated tablet, UFSA, Türkiye) of oral dexketoprofen in healthy adult male volunteers under fasting conditions (n: 47)

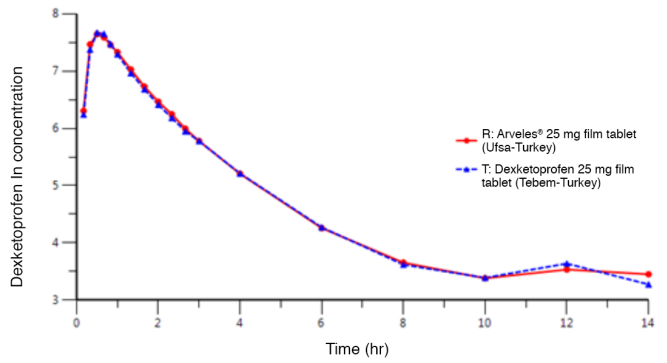

Figure 2. Average ln plasma concentration curves of dexketoprofen after a single dose of the test drug (dexketoprofen 25 mg film-coated tablet, Tebem İlaç, Türkiye) and the reference drug (Arveles® 25 mg film-coated tablet, UFSA, Türkiye) of oral dexketoprofen in healthy adult male volunteers under fasting conditions (n: 47)

Table 3. Geometric least square means, ratio, and 90% confidence intervals of the test drug (dexketoprofen 25 mg film-coated tablet, Tebem İlaç, Türkiye) and the reference drug (Arveles® 25 mg film-coated tablet, UFSA, Türkiye) in healthy adult male volunteers under fasting conditions

Parameter	Difference	DiffSE	TESTLSM	REFLSM	Ratio%	90% CI	ISCV%
ln (C_{max})	0.0016	0.0477	7.8022	7.8005	1.0016	0.9245 – 1.0853	23.45
ln ($AUC_{0-tlast}$)	-0.0183	0.0161	8.1419	8.1602	0.9818	0.9557 – 1.0087	7.81
ln ($AUC_{0-\infty}$)	-0.0174	0.0161	8.1643	8.1817	0.9827	0.9566 – 1.0096	7.79
t_{max} (h)	-0.0512	0.0474	0.6095	0.6607	0.9225	0.8019 – 1.0431	
$t_{½}$ (h)	-0.0639	0.0915	1.8753	1.9391	0.9671	0.8878 – 1.0463	
λ_z (1/h)	0.0033	0.0141	0.4202	0.4169	1.0078	0.9512 – 1.0645	

$AUC_{0-tlast}$: Area under the curve from time 0 to the last measurable concentration, $AUC_{0-\infty}$: Area under the curve from time 0 to the infinite time, t_{max}: Time to reach the peak concentration, $t_{½}$: Terminal half-life, λ_z: Terminal disposition rate constant, CI: Confidence interval, DiffSE: Standard error of the difference in least square mean, TESTLSM: Test least square mean, REFLSM: Reference least square mean, ISCV: Intra-subject coefficient of variation

the overall tolerability of the products were considered as mild. There were no serious adverse events or adverse reactions reported throughout the study.

DISCUSSION

Dexketoprofen trometamol is a widely prescribed molecule in symptomatic treatment of mild or moderate pain and its place in the NSAID market, especially in the pharmaceutical industry specialized on generic drugs is remarkable. A novel formulation of dexketoprofen trometamol, which is aimed to be licensed and presented to the pharmaceutical market, was developed and according to the current regulations, where the pharmacokinetic properties were assessed in a bioequivalence study.

ANOVA results exhibited that treatment, sequence, period, and volunteer within sequence had no statistically significant effects on C_{max} and $AUC_{0-tlast}$ (except volunteer within sequence effect for only $AUC_{0-tlast}$). Since the sequence or carry-over effect was not significant, ANOVA was valid.

Besides, ISCVs were found as 23.45% and 7.81% and the geometric mean ratios were found as 100.16% and 98.18% for C_{max} and $AUC_{0-tlast}$, respectively.

Study limitations

To acquire a standardized environment and reach an optimum sample size, only male populations were selected in this study. Therefore, the pharmacokinetic parameters of dexketoprofen be different among females.

CONCLUSION

Since the 90% CIs for the test/reference geometric mean ratios for C_{max} and $AUC_{0-tlast}$ of dexketoprofen are contained within the acceptance limits, 80.00-125.00%, according to the applied bioequivalence study, it is concluded that test and reference dexketoprofen trometamol products are bioequivalent under fasting conditions. Therefore, newly formulated generic dexketoprofen 25 mg tablets can be licensed under the requirements of regulatory authorities. Moreover, both study drugs were well-tolerated and considered safe.

ACNOWLEDGMENTS

This study was sponsored by Tebem İlaç (Ankara, Türkiye). The test drug product was developed by Elixir Pharmaceutical Research and Development Corporation (Ankara, Türkiye) and the biobatch of the test drug product was manufactured by

Gen İlaç ve Sağlık Ürünleri San. ve Tic. A.Ş. (Ankara, Türkiye) under current Good Manufacturing Practices (GMP). The bioequivalence study was conducted by FARMAGEN Good Clinical Practice and Research Center (Gaziantep, Türkiye) and the bioequivalence analysis was carried out by Novagenix Bioanalytical Drugs R&D Centre (Ankara, Türkiye).

Ethics

Ethics Committee Approval: This study was reviewed and approved by the Erciyes University Ethical Committee of Bioequivalence/Bioavailability Studies (2019/03; 16.01.2019) and Turkish Medicines and Medical Devices Agency (20.02.2019).

Informed Consent: Written informed consent obtained.

Peer-review: Externally peer-reviewed.

Authorship Contributions

Surgical and Medical Practices: O.S., S.P.A., Concept: F.Y., O.S., S.P.A., Design: F.Y., O.S., S.P.A., A.A., H.B., Data Collection or Processing: F.Y., O.S., Analysis or Interpretation: F.Y., O.S., Literature Search: F.Y., A.A., H.B., Writing: F.Y., S.P.A.

Conflict of Interest: No conflict of interest was declared by the authors.

Financial Disclosure: The authors declared that this study received no financial support.

REFERENCES

1. Bacchi S, Palumbo P, Sponta A, Coppolino MF. Clinical pharmacology of non-steroidal anti-inflammatory drugs: a review. Antiinflamm Antiallergy Agents Med Chem. 2012;11:52-64.
2. Barbanoj MJ, Antonijoan RM, Gich I. Clinical pharmacokinetics of dexketoprofen. Clin Pharmacokinet. 2001;40:245-262.
3. Carne X, Rios J, Torres F. Postmarketing cohort study to assess the safety profile of oral dexketoprofen trometamol for mild to moderate acute pain treatment in primary care. Methods Find Exp Clin Pharmacol. 2009;31:533-540.
4. Sweetman BJ. Development and use of the quick acting chiral NSAID dexketoprofen trometamol (Keral). Acute Pain. 2003;4:109-115.
5. Bermejo M, Kuminek G, Al-Gousous J, Ruiz-Picazo A, Tsume Y, Garcia-Arieta A, González-Alvarez I, Hens B, Amidon GE, Rodriguez-Hornedo N, Amidon GL, Mudie D. Exploring bioequivalence of dexketoprofen trometamol drug products with the gastrointestinal simulator (GIS) and precipitation pathways analyses. Pharmaceutics. 2019;11:122.
6. The Guidance for GCP, published by the Ministry of Health of Türkiye. Circular. 13.11.2015.
7. Guideline on Bioanalytical Method Validation, EMEA/CHMP/EWP/192217/2009 Rev.1 Corr.2, London, 21 July 2011.

Turk J Pharm Sci 2023;20(2):121-125
DOI: 10.4274/tjps.galenos.2022.69922

REVIEW

The Role of Pro-Inflammatory Mediator Interleukin-32 in Osteoclast Differentiation

Taha NAZIR[1]*, Nida TAHA[1], Azharul ISLAM[2], Ishtiaq RABBI[3], Pervaiz Akhter SHAH[4]

[1]Advanced Multiple Incorporation, Microbiology and Molecular Biology Research Group, Mississauga, Canada
[2]University of Texas Medical Branch, Department of Internal Medicine, Texas, USA
[3]Consultant Pharmacist, Dubai Production City, Dubai, UAE
[4]University of the Punjab, University College of Pharmacy, Lahore, Pakistan

ABSTRACT

The recently explained cytokine, which is produced after the stimulation of interferon (IFN)-c, interleukin (IL)-2, and IL-18 is IL-32, has pro-inflammatory IFN-c, IL-2 and IL-18 are IL-32 mediator's properties that are generally entailed in many diseases, including infections, cancer, and chronic inflammation. After the initial statement in 2005, it promoted the osteoclast precursor's differentiation into TRAcP plus VNR plus multinucleated cells that express explicit osteoclast indicators. Furthermore, the loss of bone resorption might be accredited because of the collapse of the multinucleated cells, which are produced of the reaction to IL-32 to direct factoring that is ultimately essential for attaching the cells for bone resorption. Thus, in conclusion, IL-32, the pro-inflammatory mediator, has an important and indirect role in regulating osteoclast differentiation. In bone disorder's pathophysiology, critical role of IL-32 needs more scientific evidence to develop a rational treatment protocol. IL-32 can become a potent mediator of active osteoclast generation in the presence of receptor activator of NF-κB ligand (RANKL). This novel cytokine can introduce more favorable conditions for osteoclastogenesis in the rheumatic arthritis by increasing the RANKL and osteoprotegerin ratio in fibroblast-like synoviocytes.

Key words: Interleukin-32, cytokines, osteoclast, pro-inflammatory

INTRODUCTION

In 1992, the focused molecule in this review was first reported, where there is a protein which was called NK4, which is extremely articulated in activated-T and NK cells. This protein was rapidly up-regulated after the stimulation by phytohaemaglutinin a lectin that is primary for activation of T-cells in human peripheral blood mononuclear cells (PBMCs). In 2005, NK4 was found to be one of the most up-regulated genes using microarray expertise and interleukin (IL)-18 receptive cell unit.[1] After that, two other innovative integrins of IL-32 were established in IL-32 mRNA transcript and IL-32ζ, but IL-32β appears superabundant.[2] IL-32 different isoforms are produced by splicing of isoform IL-32γ pre-mRNA. Many reports have explained that IL-32 different transcripts present both *in vitro*[3] and *in vivo*.[4] Its remnants that, by which means, IL-32γ mRNA copies are replicated and incomplete body cells process is the same. Keeping in mind the cell stimulation and cell demise, IL-32γ is the utmost leading IL-32 isoform, which explains why IL-32γ explodes into less injurious IL-32 isoforms, such as IL-32β and α.[4] IL-32 isoform differential potency was explained in many reports, however, basis of potency differences between the isoforms remain unknown. In the explanation of this process, the variance between the extent of the integrins from 14.9 kDa (IL-32α) to 26.7 kDa (IL-32γ), so that the isoform's tertian assembly can be explained.[5]

Expression and regulation of osteoclast

Inlacunarily, bone resorption is the specific function of multinucleated osteoclasts cells that originate from the hematopoietic lineage (colony forming unit-granulocyte–macrophage; CFU-GM).[6] The presence of KB ligand nuclear factor by receptor activator and colony-stimulating factor of macrophages is compulsory for the discrepancy of osteoclasts by circulating hematopoietic predecessors.[7] The site triggers

*Correspondence: taha@advancedmultiple.ca, Phone: +1 647 526 0885, ORCID-ID: orcid.org/0000-0002-5308-6798
Received: 26.10.2021, Accepted: 31.03.2022

©Copyright 2023 by Turkish Pharmacists' Association / Turkish Journal of Pharmaceutical Sciences published by Galenos Publishing House.
Licenced by Creative Commons Attribution-NonCommercial-NoDerivatives 4.0 (CC BY-NC-ND)

for nuclear feature κB ligand (RANKL) is part of tumor necrosis factor (TNF), which is present on T-cells, osteoblasts, and binds with its receptor, a receptor activator for nuclear factor-κB (RANK), which are articulated on precursors of osteoclast.[8] Activation of different intracellular pathways such as mitogen-activated protein kinase, nuclear factor activated T-cells (NFATc1), Akt, and nuclear factor-κB (NF-κB) pathways has been described as a result of RANK binding with RANKL. Osteoprotegerin (OPG), which acts like RANKL decoy receptor, causes the stimulation of resorbing activity by osteoclasts and blocks the differentiation of osteoclast-mediated by RANKL.[9,10] Although RANKL is one of the critical factors for osteoclastogenesis, several pro-inflammatory cytokines such as IL-8, TNF-α, and LIGHT proves the RANKL independent mechanisms.[11]

Multiple cell interaction evolute of rheumatoid arthritis (RA)

Approximately 0.5% adult population is affected by rheumatoid arthritis (RA) worldwide, which is the main reason for disability. RA can be defined as an enduring inflammatory disease, in which advanced joint annihilation occur including articular cartilage damage, which is caused by inflammatory cells that are chondrocytes and activated synovial fibroblasts. The factors that produced in the affected joints and a broad array of cytokines control the arthritis evolution. The anti-inflammatory cytokines *i.e.* IL-10 and transforming growth factor-beta (TGF-β) are exceeded by pro-inflammatory molecules level, particularly monokines TNF-α and IL-1b.[12] The importance of macrophages and cytokine production in RA is clearly explained by biological therapies that were directing TNF-α, targeting IL-1 and IL-6.[13] However, these treatments, when given repeatedly, achieve only brief clinical responses. Furthermore, approximately 40% of patients with 50% response reach American College of Rheumatology.[14]

Fibroblast-like synoviocytes (FLS) cultures

In sub confluence (70%), FLS were grown which contained complete medium *i.e.* 10% fetal calf serum in addition to RPMI 1640, 500 units/mL of penicillin, and 100 lg/mL streptomycin in a culture flask. From 3rd passage, all the experiments were performed using FLS. At this time, there were 0-2% contaminating macrophages, natural killer cells, and lymphocytes.[15]

RNA preparation

To eliminate genomic DNA contamination, DNase I are treated with entire RNA, which is obtained after culturing cells in RLT® RNA extraction buffer (Rneasy, Qiagen kit). By using RNA kit 6000 Lab Chip (Agilent Technologies) and a Bio-analyzer 2100, the unity and clarity of the entire RNA, and cRNA, were analyzed. The ratio of total RNA with 28S/18S >1.7 was only used. Through NanoDrop (Nanodrop Technologies) concentrations of cRNA were calculated.[16]

cRNA production and probe range hybridization

As *per* the producer's protocol (GeneChip® Expression Analysis Technical Manual, Rev.5, Affymetrix Inc., 2004) through the GeneChip Expression 3' Amplification One-Cycle Target Tagging and Controlling Components, cRNA preparation was carried out with 3 lg of entire RNA, then combine with the human genetic material U133 plus 2.0. Briefly, in an initial-strand cDNA composite reaction using a T7-Oligo(dT) protagonist primer, the entire RNA was initially inverse transcribed. Then, the double-stranded cDNA was washed in second-strand cDNA synthesis that is facilitated by RNase H and is active as a prototype in the *in vitro* transcript reaction (IVT).[17] In the presence of a biotinylated nucleotide analog and T7 RNA polymerase, an IVT reaction was performed. Then, biotinylated cRNA marks were washed up, broken into pieces, and hybridized with GeneChip expression arrays. Then, using Affymetrix Fluidics Station 450 (Affymetrix, Inc.), it was washed and stained and then the reviewed ranges were perused into the Affymetrix GeneChip Scanner 3000.

FLS gene express model

Using GeneChip Human Genome U133A plus 2.0 (Affymetrix, Santa Clara, CA, USA), microarrays evaluated the genetic appearance profiles. Gene expression was evaluated by cultivated FLS obtained of 8 and 9 patients with RA and OA, respectively. For further analysis, outcomes from 241 investigations on behalf of 171 different cytokines and their particular receptors. The selected genes, whose appearance were diverse and approximately 1.6 times among the FLS of two disorders, had a *p* value of up to 0.05.[18]

Microarray scrutiny

In gene spring, the stated raw details were computed with the GC-RMA File preprocessor. Specific probe data stored in Affymetrix CEL files were used using the GC-RMA algorithm. With Genespring 7.2, raw data processing, data analysis, and normalization were performed. The value of each gene was set to 1 in different conditions and it was ensured using GeneSpring normalization ("*per* gene: normalize the median"). This means that those genes that do not alter in different conditions have a value of 1 for normalization expression that allow easy detection of distinctive expressed genes visually.

The absence of sRANKL IL-32 inspires the discrepancy of supporter PBMCs into multinucleated TRAcP + and VNR + cells

Now it is thought that M-CSF and RANKL are two crucial aspects that are supplied by osteoclasts, which are vital for the maturation and discrepancy of precursors of osteoclasts.[19-22] However, the mice defective by M-CSF (op/op) exhibit an osteopetrotic appearance that could be voluntarily converse with time and suggest that there is a substitute osteoclastic trail that exists.[22]

Lacking M-CSF, vascular endothelial growth factor, hepatocyte growth factor, and Flt3 ligand all have revealed support to osteoclast creation.[21] Moreover, the mice demonstrate an osteopetrotic appearance triggered by a whole loss of osteoclast in their bones having a deficiency of either RANKL or its receptor RANK.[22] If there are no osteoclasts detected in the bones of the mice that are flawed in RANKL or RANK, it might not happen due to the total disaster of osteoclastogenesis. RANKL as a significant and endurance aspect for modified osteoclasts[23]

and in the mice deficient with RANKL or RANK, the observed phenotype can be explained by the idea that differentiation is diminished osteoclast superimposed on the summarized lifecycle.[24] As such, in the existence of a large amount of OPG that is an inhibitor of interactions of RANKL-RANK, it has been reported that a substitute RANKL-independent pathway (*e.g.* LIGHT, TGF-β and TNF-α) supports osteoclastogenesis.[25] The ground aspect of the osteoimmunology explained that T-cells, which are activated straight regulate bone resorption and osteoclastogenesis,[26] and T-cell products *i.e.*, IL-17, TWEAK, GM-CSF, and IFN-c, which can modulate the establishment of osteoclasts.[27] This existing study pursued to determine a part of IL-32, having the representation of pro-inflammatory cytokine and participating in an assortment of inflammatory syndromes by osteoclast activation and differentiation (Figures 1, 2).

TNF and osteoclast activation

It has been described that TNF receptor-associated factor-6 (TRAF-6) is imperative for osteoclast stimulation, *i.e.*, lacunar bone resorption and there is a composite part of IFN-c in osteoclastogenesis. They show that strong reluctance of RANKL-induced activation occurs due to fast degradation of TRAF-6 by IFN-c. Therefore, we hypothesized that due to TRAF-6 degradation, the IL-32 single or in combination with soluble RANKL showed inhibitory outcome. However, we found and were surprised that TRAF6 is not destroyed but is overexposed, when treated with IL-32 related to RANKL. Recently, Yao et al.[28] have shown IFN-c shows a "direct" anti-resorptive outcome by reducing the distinction of osteoclasts. Therefore, by stimulating T-cells IFN-c can act "indirectly" as a pro-resorptive feature to direct RANKL and TNF-α.[29] In this current study, we use PBMCs as a basis of pioneers of osteoclasts and significantly cells were cleansed completely to abolish non-adherent cells (B & T-cells), it is reasonable that few T-cells might be existing in the culture and donated to osteoclastogenesis.[30] This supposition is also strengthened by indication, which explains that the decrease in size and number of multinucleated cells newly-synthesised due to excessive accumulation of OPG in the IL-32-treated cultures.

Therapeutic techniques or process

Osteoclast differentiation was induced by IL-32 is somewhat autonomous of the RANK/RANKL pathway. Although the freeing of pro-inflammatory mediators that were increased by IL-32 have a positive influence on osteoclastogenesis, it had a straight inhibitor consequence *in vitro* osteoclast instigation and it cannot induce these recently-prepared multinucleated cells activation into bone-resorbing osteoclasts.[31-33] It is important to notice that IL-32 has a straight influence over further cell types *i.e.*, epithelial cells, natural killer cells, T-cells, and monocytes. Downstream pathways are not fully interpreted that involved in osteoclasts in return to IL-32. NF-κB and JNK trail activation are severely increased by PBMC handling of M-CSF/RANKL or M-CSF/IL-32 compared to cultures that are treated with M-CSF. However, Akt pathway activation appeared more complex. Akt pathways are strongly activated by M-CSF/IL-32 or M-CSF treatments compared with M-CSF/RANKL.

CONCLUSION

In conclusion, IL-32, the pro-inflammatory mediator, has an important and indirect role in regulating osteoclast differentiation. In bone disorder's pathophysiology, critical role of IL-32 needs more scientific evidence to develop a rational

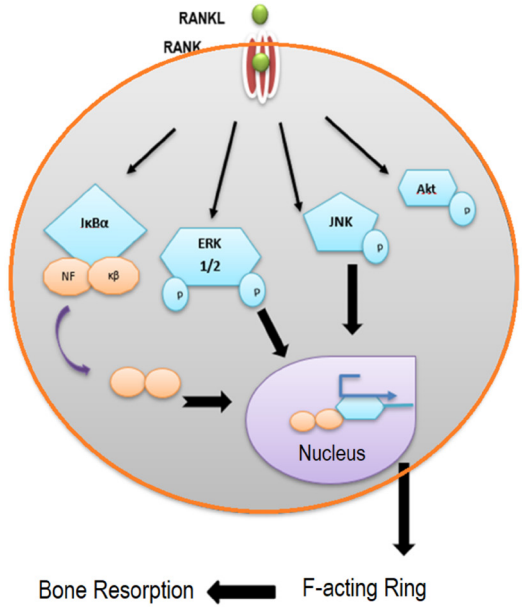

Figure 1. The graphic illustration of downriver trails triggered by receptor activator of NF-κB ligand (RANKL). Inconsistency detected in RANKL signaling trails; increased ERK1/2 activation may lead to the activation of downriver goals, which, in fact, can subsidize the incapacity of cells to expose the F-actin ring

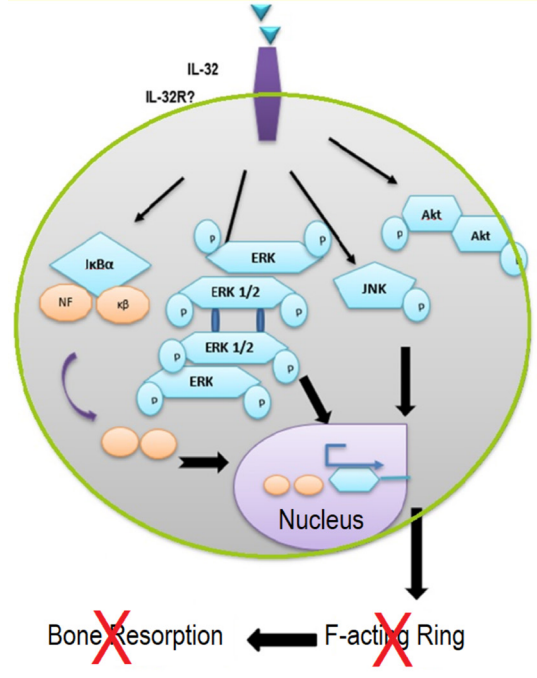

Figure 2. The graphic illustration of downriver trails triggered by IL-32. The inconsistency detected among IL-32; Akt activation by IL-32 may lead to the activation of downriver goals, which, in fact, can subsidize the incapacity of cells to expose F-actin ring and resorb in reaction to IL-32

treatment protocol. IL-32 can become a potent mediator of active osteoclast generation in the presence of RANKL. This novel cytokine can introduce more favorable conditions for osteoclastogenesis in the rheumatic arthritis by increasing the RANKL and OPG ratio in fibroblast-like synoviocytes.

Ethics

Peer-review: Externally peer-reviewed.

Authorship Contributions

Concept: T.N., N.T., Design: T.N., N.T., Data Collection or Processing: A.I., I.R., Analysis or Interpretation: T.N., N.T., A.I., I.R., Literature Search: T.N., N.T., A.I., I.R. P.A.S., Writing: T.N., N.T., A.I., I.R., P.A.S.

Conflict of Interest: No conflict of interest was declared by the authors.

Financial Disclosure: The authors declared that this study received no financial support.

REFERENCES

1. Dahl CA, Schall RP, He HL, Cairns JS. Identification of a novel gene expressed in activated natural killer cells and T cells. J Immunol. 1992;148:597-603.
2. Kim SH, Han SY, Azam T, Yoon DY, Dinarello CA. Interleukin-32: a cytokine and inducer of TNFalpha. Immunity. 2005;22:131-142.
3. Goda C, Kanaji T, Kanaji S, Tanaka G, Arima K, Ohno S, Izuhara K. Involvement of IL-32 in activation-induced cell death in T cells. Int Immunol. 2006;18:233-240.
4. Heinhuis B, Koenders MI, van de Loo FA, Netea MG, van den Berg WB, Joosten LA. Inflammation-dependent secretion and splicing of IL-32{gamma} in rheumatoid arthritis. Proc Natl Acad Sci USA. 2011;108:4962-4967.
5. Heinhuis B, Netea MG, van den Berg WB, Dinarello CA, Joosten LA. Interleukin-32: a predominantly intracellular proinflammatory mediator that controls cell activation and cell death. Cytokine. 2012;60:321-327.
6. Heinhuis B, Koenders MI, van den Berg WB, Netea MG, Dinarello CA, Joosten LA. Interleukin 32 (IL-32) contains a typical α-helix bundle structure that resembles focal adhesion targeting region of focal adhesion kinase-1. J Biol Chem. 2012;287:5733-5743.
7. Choi JD, Bae SY, Hong JW, Azam T, Dinarello CA, Her E, Choi WS, Kim BK, Lee CK, Yoon DY, Kim SJ, Kim SH. Identification of the most active interleukin-32 isoform. Immunology. 2009;126:535-542.
8. Boyle WJ, Simonet WS, Lacey DL. Osteoclast differentiation and activation. Nature. 2003;423:337-342.
9. Udagawa N, Takahashi N, Akatsu T, Tanaka H, Sasaki T, Nishihara T, Koga T, Martin TJ, Suda T. Origin of osteoclasts: mature monocytes and macrophages are capable of differentiating into osteoclasts under a suitable microenvironment prepared by bone marrow-derived stromal cells. Proc Natl Acad Sci USA. 1990;87:7260-7264.
10. Fujikawa Y, Quinn JM, Sabokbar A, McGee JO, Athanasou NA. The human osteoclast precursor circulates in the monocyte fraction. Endocrinology. 1996;137:4058-4060.
11. Hofbauer LC, Khosla S, Dunstan CR, Lacey DL, Boyle WJ, Riggs BL. The roles of osteoprotegerin and osteoprotegerin ligand in the paracrine regulation of bone resorption. J Bone Miner Res. 2000;15:2-12.
12. Lacey DL, Timms E, Tan HL, Kelley MJ, Dunstan CR, Burgess T, Elliott R, Colombero A, Elliott G, Scully S, Hsu H, Sullivan J, Hawkins N, Davy E, Capparelli C, Eli A, Qian YX, Kaufman S, Sarosi I, Shalhoub V, Senaldi G, Guo J, Delaney J, Boyle WJ. Osteoprotegerin ligand is a cytokine that regulates osteoclast differentiation and activation. Cell. 1998;93:165-176.
13. Quinn JM, Elliott J, Gillespie MT, Martin TJ. A combination of osteoclast differentiation factor and macrophage-colony stimulating factor is sufficient for both human and mouse osteoclast formation *in vitro*. Endocrinology. 1998;139:4424-4427.
14. Hsu H, Lacey DL, Dunstan CR, Solovyev I, Colombero A, Timms E, Tan HL, Elliott G, Kelley MJ, Sarosi I, Wang L, Xia XZ, Elliott R, Chiu L, Black T, Scully S, Capparelli C, Morony S, Shimamoto G, Bass MB, Boyle WJ. Tumor necrosis factor receptor family member RANK mediates osteoclast differentiation and activation induced by osteoprotegerin ligand. Proc Natl Acad Sci USA. 1999;96:3540-3545.
15. Nakagawa N, Kinosaki M, Yamaguchi K, Shima N, Yasuda H, Yano K, Morinaga T, Higashio K. RANK is the essential signaling receptor for osteoclast differentiation factor in osteoclastogenesis. Biochem Biophys Res Commun. 1998;253:395-400.
16. Yasuda H, Shima N, Nakagawa N, Yamaguchi K, Kinosaki M, Mochizuki S, Tomoyasu A, Yano K, Goto M, Murakami A, Tsuda E, Morinaga T, Higashio K, Udagawa N, Takahashi N, Suda T. Osteoclast differentiation factor is a ligand for osteoprotegerin/osteoclastogenesis-inhibitory factor and is identical to TRANCE/RANKL. Proc Natl Acad Sci USA. 1998;95:3597-3602.
17. Simonet WS, Lacey DL, Dunstan CR, Kelley M, Chang MS, Lüthy R, Nguyen HQ, Wooden S, Bennett L, Boone T, Shimamoto G, DeRose M, Elliott R, Colombero A, Tan HL, Trail G, Sullivan J, Davy E, Bucay N, Renshaw-Gegg L, Hughes TM, Hill D, Pattison W, Campbell P, Sander S, Van G, Tarpley J, Derby P, Lee R, Boyle WJ. Osteoprotegerin: a novel secreted protein involved in the regulation of bone density. Cell. 1997;89:309-319.
18. Yasuda H, Shima N, Nakagawa N, Mochizuki SI, Yano K, Fujise N, Sato Y, Goto M, Yamaguchi K, Kuriyama M, Kanno T, Murakami A, Tsuda E, Morinaga T, Higashio K. Identity of osteoclastogenesis inhibitory factor (OCIF) and osteoprotegerin (OPG): a mechanism by which OPG/OCIF inhibits osteoclastogenesis *in vitro*. Endocrinology. 1998;139:1329-1337.
19. Bendre MS, Montague DC, Peery T, Akel NS, Gaddy D, Suva LJ. Interleukin-8 stimulation of osteoclastogenesis and bone resorption is a mechanism for the increased osteolysis of metastatic bone disease. Bone. 2003;33:28-37.
20. Edwards JR, Sun SG, Locklin R, Shipman CM, Adamopoulos IE, Athanasou NA, Sabokbar A. LIGHT (TNFSF14), a novel mediator of bone resorption, is elevated in rheumatoid arthritis. Arthritis Rheum. 2006;54:1451-1462.
21. Vervoordeldonk MJ, Tak PP. Cytokines in rheumatoid arthritis. Curr Rheumatol Rep. 2002;4:208-217.
22. Arend WP, Dayer JM. Cytokines and cytokine inhibitors or antagonists in rheumatoid arthritis. Arthritis Rheum. 1990;33:305-315.
23. Arend WP, Dayer JM. Inhibition of the production and effects of interleukin-1 and tumor necrosis factor alpha in rheumatoid arthritis. Arthritis Rheum. 1995;38:151-160.
24. Elliott MJ, Maini RN, Feldmann M, Kalden JR, Antoni C, Smolen JS, Leeb B, Breedveld FC, Macfarlane JD, Bijl H, Woody JN. Randomised double-blind comparison of chimeric monoclonal antibody to tumour necrosis factor alpha (cA2) *versus* placebo in rheumatoid arthritis. Lancet. 1994;34:1105-1110.
25. Lard LR, Visser H, Speyer I, vander Horst-Bruinsma IE, Zwinderman AH, Breedveld FC, Hazes JM. Early *versus* delayed treatment in patients

with recent-onset rheumatoid arthritis: comparison of two cohorts who received different treatment strategies. Am J Med. 2001;111:446-451.

26. Goekoop YP, Allaart CF, Breedveld FC, Dijkmans BA. Combination therapy in rheumatoid arthritis. Curr Opin Rheumatol. 2001;13:177-183.
27. Neumann E, Gay RE, Gay S, Müller-Ladner U. Functional genomics of fibroblasts. Curr Opin Rheumatol. 2004;16:238-245.
28. Yao Z, Getting SJ, Locke IC. Regulation of TNF-induced osteoclast differentiation. Cells. 2021;11:132.
29. Begg SK, Radley JM, Pollard JW, Chisholm OT, Stanley ER, Bertoncello I. Delayed hematopoietic development in osteopetrotic (op/op) mice. J Exp Med. 1993;177:237-242.
30. Mabilleau G, Sabokbar A. Interleukin-32 promotes osteoclast differentiation but not osteoclast activation. PLoS One. 2009;4:e4173.
31. Felix R, Cecchini MG, Fleisch H. Macrophage colony stimulating factor restores *in vivo* bone resorption in the op/op osteopetrotic mouse. Endocrinology. 1990;127:2592-2594.
32. Hasanzadeh A, Alamdaran M, Ahmadi S, Nourizadeh H, Bagherzadeh MA, Mofazzal Jahromi MA, Simon P, Karimi M, Hamblin MR. Nanotechnology against COVID-19: immunization, diagnostic and therapeutic studies. J Control Release. 2021;336:354-374.
33. Safiabadi Tali SH, LeBlanc JJ, Sadiq Z, Oyewunmi OD, Camargo C, Nikpour B, Armanfard N, Sagan SM, Jahanshahi-Anbuhi S. Tools and techniques for severe acute respiratory syndrome Coronavirus 2 (SARS-CoV-2)/COVID-19 detection. Clin Microbiol Rev. 2021;34:e00228-20.

Turk J Pharm Sci 2023;20(2):126
DOI: 10.4274/tjps.galenos.2023.48961.e001

ERRATUM

Kahlous Y, Palanirajan VK, Starlin M, Negi JS, Cheah SC. Preparation and Characterization of Chitosan and Inclusive Compound-Layered Gold Nanocarrier to Improve the Antiproliferation Effect of Tamoxifen Citrate in Colorectal Adenocarcinoma (Caco-2) and Breast Cancer (MCF-7) Cells. Turk J Pharm Sci. 2022;19:391-399.

The mistake have been made inadvertently by the author.

The captions of Figures 7 and 8 in the article have been swapped with each other as follows.

*The subtitle of Figure 7 on page 397 of the relevant article has been changed.

- Incorrect subtitle; **Figure 7.** Rhodamine incorporated Tam-β-CD-HA-Chi-Au nanocomposite uptake by MCF-7 cells was analysed by fluorescence microscopy after 0 h, 1 h, and 2 h of incubation with Tam-β-CD-HA-Chi-Au nanocomposite. The red-light intensity due to rhodamine incorporated Tam-β-CD-HA-Chi-Au nanocomposite represents the cellular uptake of the developed formulation at 0 h, 1 h, and 2 h

β-CD: β-Cyclodextrin, Tam: Tamoxifen, HA: Hyaluronic acid, Chi: Chitosan, Au: Gold

- Corrected subtitle; **Figure 7.** The cytotoxicity of Tam-β-CD-HA-Chi-Au nanocomposite on Caco-2 cells is shown by the RTCA DP instrument (8A). Cells were seeded and incubated with DMEM media (1A), 23.69 µM of Tam-β-CD-HA-Chi-Au nanocomposite (2A), 35.62 µM of Tam-β-CD-HA-Chi-Au nanocomposite (3A), 47.55 µM of Tam-β-CD-HA-Chi-Au nanocomposite (4A). The cytotoxicity of Tam-β-CD-HA-Chi-Au nanocomposite on MCF-7 cells is shown by the RTCA DP instrument (8B). Cells were seeded incubated with DMEM medium (pink), 2.15 µg of Tam-β-CD-HA-Chi-Au nanocomposite (red), 3.23 µg of Tam-β-CD-HA-Chi-Au nanocomposite (green), 4.31 µg of Tam-β-CD-HA-Chi-Au nanocomposite (dark blue), cells incubated with DMSO (light blue)

β-CD: β-Cyclodextrin, Tam: Tamoxifen, HA: Hyaluronic acid, Chi: Chitosan, Au: Gold, RTCA: Real-time cellular analysis xCELLigence, DMEM: Dulbecco's Modified Eagle's Medium, DMSO: Dimethyl sulfoxide

*The subtitle of Figure 8 on page 398 of the relevant article has been changed.

- Incorrect subtitle; **Figure 8.** The cytotoxicity of Tam-β-CD-HA-Chi-Au nanocomposite on Caco-2 cells is shown by the RTCA DP instrument (8A). Cells were seeded and incubated with DMEM media (1A), 23.69 µM of Tam-β-CD-HA-Chi-Au nanocomposite (2A), 35.62 µM of Tam-β-CD-HA-Chi-Au nanocomposite (3A), 47.55 µM of Tam-β-CD-HA-Chi-Au nanocomposite (4A). The cytotoxicity of Tam-β-CD-HA-Chi-Au nanocomposite on MCF-7 cells is shown by the RTCA DP instrument (8B). Cells were seeded incubated with DMEM medium (pink), 2.15 µg of Tam-β-CD-HA-Chi-Au nanocomposite (red), 3.23 µg of Tam-β-CD-HA-Chi-Au nanocomposite (green), 4.31 µg of Tam-β-CD-HA-Chi-Au nanocomposite (dark blue), cells incubated with DMSO (light blue)

β-CD: β-Cyclodextrin, Tam: Tamoxifen, HA: Hyaluronic acid, Chi: Chitosan, Au: Gold, RTCA: Real-time cellular analysis xCELLigence, DMEM: Dulbecco's Modified Eagle's Medium, DMSO: Dimethyl sulfoxide

- Corrected subtitle; **Figure 8.** Rhodamine incorporated Tam-β-CD-HA-Chi-Au nanocomposite uptake by MCF-7 cells was analysed by fluorescence microscopy after 0 h, 1 h, and 2 h of incubation with Tam-β-CD-HA-Chi-Au nanocomposite. The red-light intensity due to rhodamine incorporated Tam-β-CD-HA-Chi-Au nanocomposite represents the cellular uptake of the developed formulation at 0 h, 1 h, and 2 h

β-CD: β-Cyclodextrin, Tam: Tamoxifen, HA: Hyaluronic acid, Chi: Chitosan, Au: Gold